Chemical Papers (2020) 74:1–54
https://doi.org/10.1007/s11696-019-00982-9

REVIEW

Interaction of conducting polymers, polyaniline and polypyrrole, with organic dyes: polymer morphology control, dye adsorption and photocatalytic decomposition

Jaroslav Stejskal[1]

Received: 11 September 2019 / Accepted: 25 October 2019 / Published online: 16 November 2019

Abstract
Conducting polymers, such as polyaniline and polypyrrole, have frequently been discussed in the literature due to ease of preparation and high application potential. These polymers have been observed to interact with organic dyes because of the similarity in the conjugated molecular structure of both moieties. The interaction manifests itself in three fundamental directions that have been so far treated separately. The first is represented by the conductivity enhancement and morphology control when using organic dyes as templates in polypyrrole preparation. The adsorption of dyes on conducting polymers is the second field oriented at the water pollution treatment. Finally, the photocatalytic decomposition of organic dyes aims at the similar environmental target. The last two applications do not require the presence of conductivity which, on the other hand, is a key parameter of conducting polymers. The future design of advanced adsorbents, however, has to exploit both the conductivity and electroactivity in the control of pollutant adsorption or degradation. For this reason, all these interactions and their practical impact are considered in the present review.

Keywords Adsorption · Conducting polymer · Nanotubes · Organic dyes · Photocatalytic decomposition · Water pollution treatment

Contents

✉ Jaroslav Stejskal
stejskal@imc.cas.cz

[1] Institute of Macromolecular Chemistry, Academy of Sciences of the Czech Republic, 162 06 Prague 6, Czech Republic

Concluding remarks on perspectives of conducting polymers
Conclusions

Preamble

The oxidation of aniline as early as in 1834 afforded a green product called polyaniline in present terminology (Rasmussen 2018). This is an example of probably the first man-made polymer. Its conductivity, however, was revealed only much later (MacDiarmid 2001). The first commercial synthetic dye, mauveine, was discovered serendipitously by William Henry Perkin in 1856 also by the oxidation of aniline (Sousa et al. 2008). Other aniline dyes soon followed: fuchsin, safranin and induline. Many synthetic organic dyes have since been prepared. Conducting polymers, such as polyaniline, and dyes thus have a common origin and related history. It is proposed that they may have also a promising joint future.

Introduction

The present review is based on the assumption that conducting polymers and organic dyes interact due to the similar features of their molecular structure. Such interactions manifest themselves in three directions: (1) by the effects of dyes on the preparation of conducting polymers, (2) in the adsorption of dyes on conducting polymers and (3) by the photocatalytic degradation of dyes using conducting polymers. It thus connects three seemingly unrelated research directions and points out to their common roots. Among conducting polymers, polyaniline and polypyrrole have been selected as the main objects of concern due to the simplicity and similarity of their preparation and large number of studies that have already appeared in the literature. They both include aromatic structure and nitrogen atoms in the constitutional units, which are likely to play role in their interactions with dyes.

It is not the purpose of this review to enumerate quantitatively the results presented in the literature but rather to organize them according to the type of experiments done and the dyes involved in them. The review is thus meant to provide the guidance to the researchers interested in concrete systems by listing the studies that have already been done on them and to point out the directions that are still a challenge to future research.

Conducting polymers

The design of conducting organic systems, represented here by polyaniline (Stejskal et al. 2010, 2015), polypyrrole (Sapurina et al. 2017; Stejskal and Trchová 2018) and their composites, is highly desirable for new applications (Bhadra et al. 2009; Inzelt 2017) in energy-conversion and energy-storage devices (Meng et al. 2017), analytical sciences (Jain et al. 2017), corrosion protection of metals (Yang et al. 2015; Ates 2016), in biomedicine (Humpolíček et al. 2018; Nair et al. 2019; Runsewe et al. 2019) and in environmental issues (Nasar and Mashkoor 2019). The last uses of conducting polymers, such as water pollution treatment, have recently come to the forefront (Zare et al. 2018a) despite the fact that the conductivity, the key parameter of conducting polymers, has no impact on this type of applications.

Conducting polymers represent unique class of semiconducting, electroactive and responsive materials with a benefit of easy and economic preparation. Due to the limited processability, conducting polymers have often been used in the composites with organic and inorganic materials that improved the processing and utility properties (Khatoon and Ahmad 2017). Especially one-dimensional conducting-polymer nanofibers

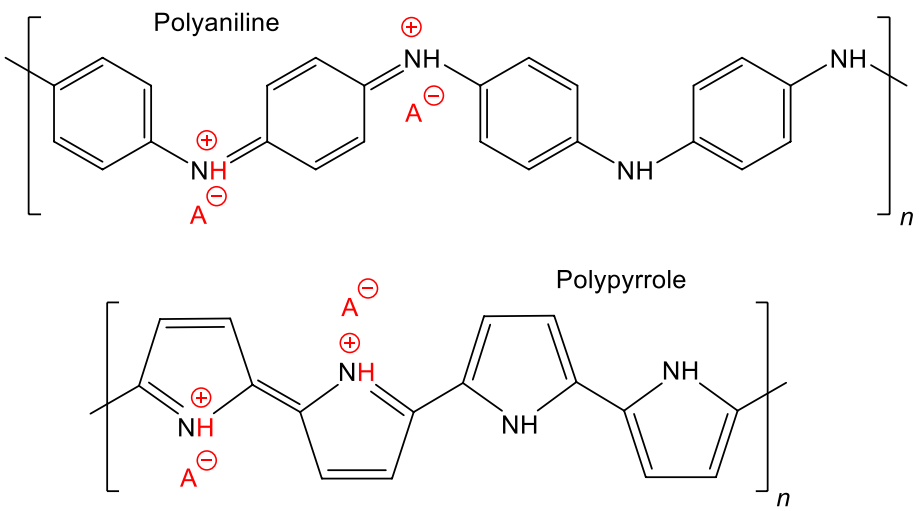

Fig. 1 Polyaniline (emeraldine form) and polypyrrole are prepared as salts with various acids, HA (depicted in red)

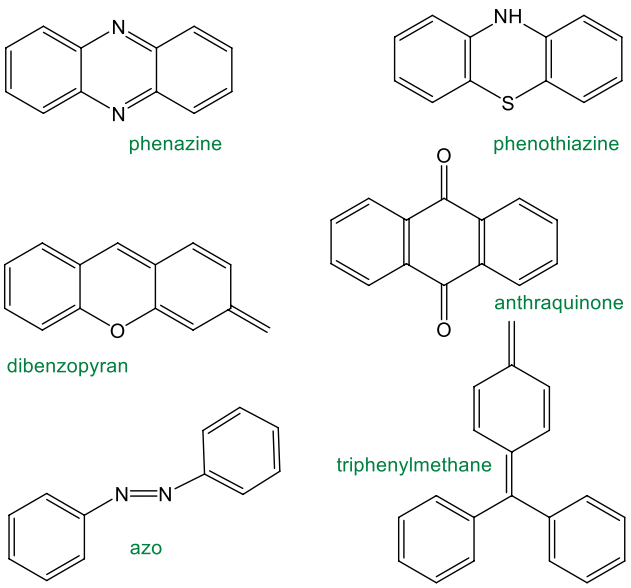

Fig. 2 Typical chromogenic segments that appear in organic dyes: phenazine (phz), phenothiazine (ptz), dibenzopyran (dbp), anthraquinone (anq), azo, and triphenylmethane (tpm)

and nanotubes has received attention in the field of nanotechnologies (Long et al. 2011; Baker et al. 2017; Huang et al. 2017) as demonstrated by the number of papers published on polypyrrole nanotubes (Stejskal and Trchová 2018). Polyaniline and polypyrrole (Fig. 1), are easily prepared by the chemical oxidation of respective monomers in acidic aqueous medium. Ammonium peroxydisulfate is favoured oxidant of aniline while iron(III) chloride is the typical oxidant of pyrrole. Conducting polymers are received as polymer salts. It should be kept in mind that the properties of these polymers substantially vary for different counter-ions A^- afforded by protonating acids (Stejskal et al. 2004a, 2008a, 2016), sometimes called as "dopants".

Conducting polymers and organic dyes have one feature in common. They are coloured due to the presence of conjugated double bonds in the molecular structure and consequent selective absorption of light in visible region. While the former group has a polymer character including polarons as charge carriers responsible for the conductivity, the dyes are low-molecular-weight compounds rated as electric insulators.

Fig. 3 Examples of cationic dyes (safranin, methylene blue, rhodamine B, crystal violet) and anionic dyes (Acid Blue 25, methyl orange)

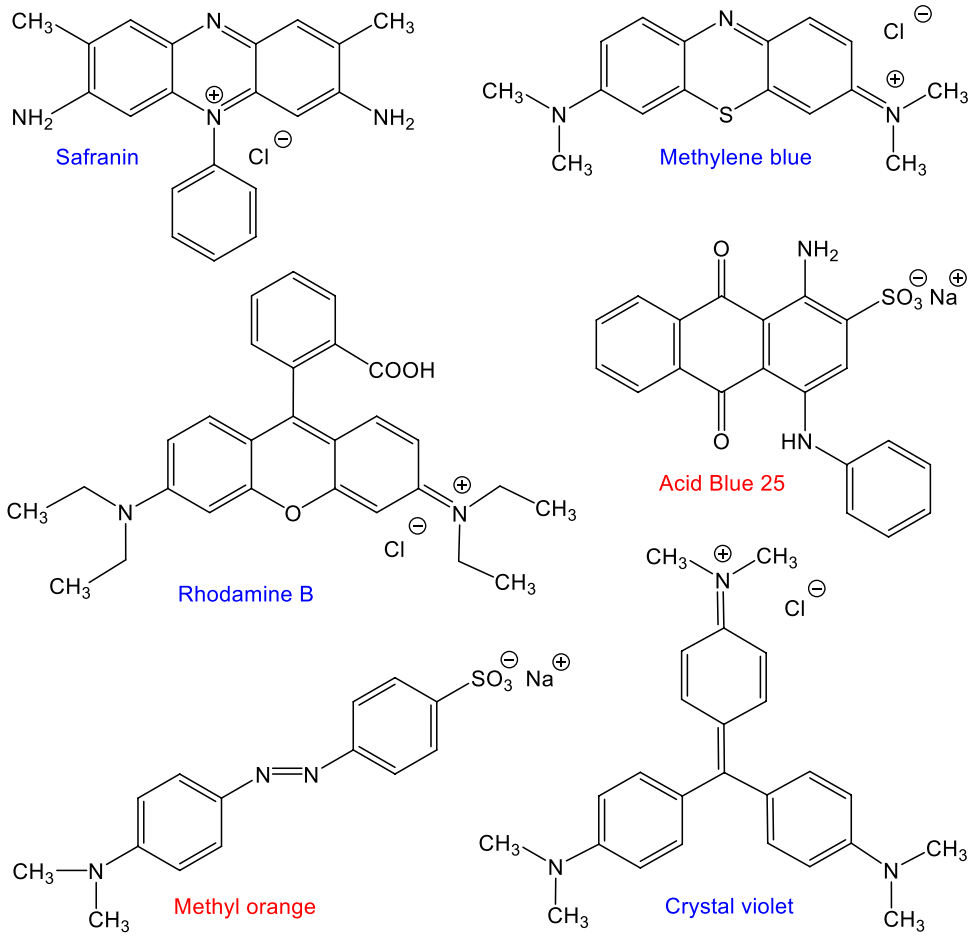

Organic dyes

Organic dyes are by definition used in dyeing of various substrates. Similarly to conducting polymers, their molecular structure is based on the system of conjugated double-bonds afforded by chromogenic groups (Fig. 2). Many other organic compounds are also coloured while they are not regarded as dyes in the technological sense. They are represented by various drugs (cytostatics, antibiotics, antibacterial agents, etc.), herbicides and pesticides, acidobasic or redox indicators, and they appear in natural products, such as in fruits or vegetables, etc. From the point of molecular structure, they also have a conjugated system of bonds responsible for the light absorption even though they are not regarded as dyes. For that reason they are also marginally considered in this review.

Dyes are intensely coloured organic substances which impart colour to a substrate by selective absorption of light. They are usually well soluble in aqueous media. The use of synonyma and commercial trademarks for the dye names somewhat complicates the survey of the literature. For example, Congo red is also known as Congo Red 4B, Cosmos Red, Cotton Red B, Cotton Red C, Direct Red R, Direct Red Y, etc. For that reason the Colour Index (https://www.colour-index.com) generic name, here Direct Red 28, has been introduced and used in this review when available. Generic name identifies a commercial product by its usage class, its colour shade and a number reflecting the chronological order of the registration with the Colour Index. The examples of dye classes are: Acid, Basic, Direct, Disperse, Food, Mordant and Reactive, but others have also been in use. The colour shades are Black, Blue, Green, Orange, Red, Violet and Yellow.

The dyes can be divided in two basic groups. *Anionic dyes* carry one or more negatively charged groups (Fig. 3), typically sulfonate or carboxyl ones that promote the dye solubility in aqueous media. They are usually delivered as sodium salts. Methyl orange (Fig. 3) is probably the most important member of this family when it comes to the morphology control of polypyrrole. There is a large variety especially of azo dyes that have been investigated for their interaction with conducting polymers in adsorption experiments. *Cationic dyes* include a positive charge, usually localized on nitrogen atom, which is balanced by a counter-ion. Among cationic dyes, methylene blue, a photosensitizer used to produce singlet oxygen when exposed to both light and oxygen, and rhodamine B (Fig. 3) have been the dyes of choice in photocatalytic degradation. Safranin also is an important example of a cationic dye.

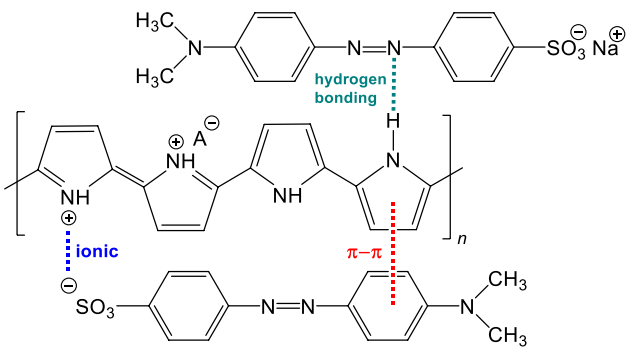

Fig. 4 Illustration of π–π, ionic, and hydrogen bonding interactions between conducting polymer, polypyrrole, and organic dye, methyl orange

Dyes have frequently been observed to interact with conducting polymers. Two classes of experiments have to be distinguished. In the first, the dyes are present during the preparation of conducting polymers and, as a rule, they affect both their morphology or conductivity or both. The second group reports the preparation of conducting polymers followed by the interaction with organic dyes. This is illustrated by numerous studies on adsorption of dyes on conducting polymers or by photocatalytic decomposition of dyes. The present contribution reviews the relevant papers in order to elucidate nature of the interaction and ways of its exploitation.

Principles of interaction

There are four fundamental ways how conducting polymers and dyes interact:

1. The *π–π interaction* between the aromatic rings is based on sharing the π-electrons by individual molecules and constitutional polymer units, which is favourable from the energy point of view. As the conducting polymers and dyes share the common features of molecular structure, the *π–π* interaction between their constitutional units and dyes is possible and probably dominating (Fig. 4). The charge-transfer complexes between chemisorbed dyes and the chains of conducting polymers are expected to exist in analogy with phenosafranin dye and carbon nanotubes (Curran et al. 2004). The formation of one-dimensional liquid-crystalline J-aggregates produced by organic dyes themselves is based on the similar principle (Harrison et al. 1996; Collings et al. 2010; Würthner et al. 2011; Gospodinova and Tomšík 2015).
2. The electrostatic *ionic interactions* have also to be considered (Fig. 4). Conducting polymers discussed here are polycations (Fig. 1) and their ionic coupling with sulfo groups in anionic dyes is anticipated (Stejskal et al. 2008a; Wang et al. 2019a; Yang et al. 2019), i.e. they may constitute, in principle, the mutual salts. This concerns especially the cases when polyaniline or polypyrrole bases would interact with anionic dyes in acid form

and not with sodium salts. The experimental support of this type of interaction is still scarce (Mahanta et al. 2008; Janaki et al. 2012a), but was proposed (Prasad and Joseph 2017), e.g., to manifest itself by cross-linking with dyes carrying multiple sulfo groups (Yang et al. 2019).

3. The *hydrogen bonding* is represented by interactions of hydrogen atoms with nitrogen atoms in conducting polymers and nitrogen- or oxygen-containing groups in dyes (Fig. 4) (Li et al. 2017a; Sarkar et al. 2018). The intermolecular hydrogen bonding between amino –NH– and imine –N = nitrogens, which was well established by FTIR spectroscopy (Trchová and Stejskal 2011), is probably the reason for the insolubility of conducting polymers in aqueous media. Such interaction is likely to constitute the basis of dye adsorption on conducting polymers. We can speculate that the nitrogen atoms in dyes would be involved in similar manner.
4. The *hydrophobic interactions* may also take place (Ren et al. 2018). It is important to realize that the dyes resemble surfactants (Shi et al. 2017; Bai et al. 2018). They similarly have a hydrophilic ionic group that promotes the solubility in water and large hydrophobic part (Fig. 3). The latter part has a tendency to self-assemble to micellar objects or to interact with hydrophobic parts of conducting-polymer chains. In the contrast to classical surfactants, where the hydrophobic part is represented by flexible chains and promotes the formation of micelles, the stiff part in dyes favours the formation of one-dimensional self-assembled aggregates. The list of interactions may be extended to dipole–dipole interactions, dispersion forces and other weak interactions of van der Waals type.

The possibility of *covalent bonding* was exceptionally proposed in the literature (Jangid et al. 2014) but the chemical reaction between conducting polymers and dyes is hardly expected to occur spontaneously. The synthetic procedure aimed at the covalent attachment of pendant Rhodamine 6G and Azure B to polyaniline chain, however, has been reported (Jangid et al. 2015). From the formal point of view the copolymerization of aniline with some dyes bearing amino groups might fall into this category, too. Such situation might appear when polyaniline is prepared in the presence of organic dyes.

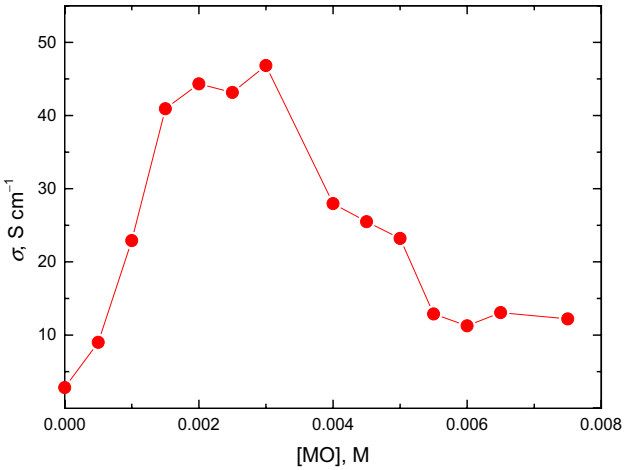

Fig. 6 Conductivity of polypyrrole in dependence on methyl orange concentration in the reaction mixture (adapted from Sapurina et al. 2017)

As mentioned above, the interaction between conducting polymers and dyes manifests itself in four ways:

1. *Control of polymer morphology.* The morphology of polyaniline prepared by the oxidative polymerization of aniline depends on the reaction conditions; globules, nanotubes and nanofibres being the most common forms (Sapurina and Stejskal 2008; Stejskal et al. 2008b, 2010). Polypyrrole is typically produced also in globular form (Fig. 5a). Only after introduction of some dyes, such as methyl orange, its morphology converts to nano-

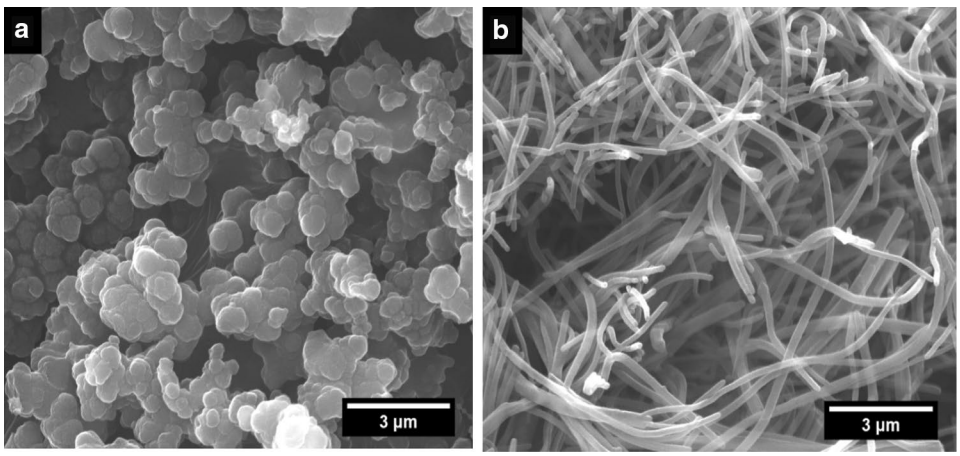

Fig. 5 **a** Globular polypyrrole and **b** polypyrrole nanotubes produced in the presence of methyl orange (Stejskal et al. 2016)

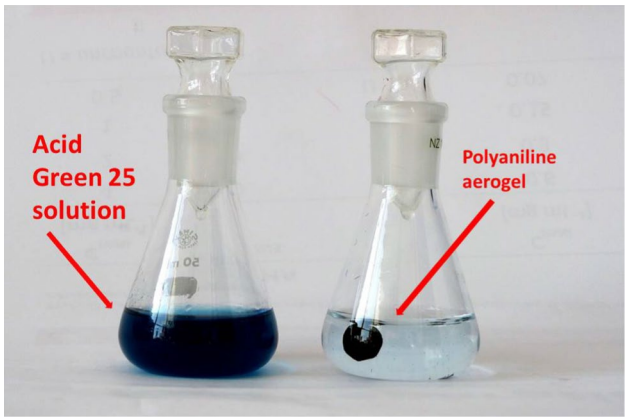

Fig. 7 Conducting polyaniline/poly(vinyl alcohol) aerogel adsorbs methylene blue from aqueous solution (Islam Minisy, unpublished results)

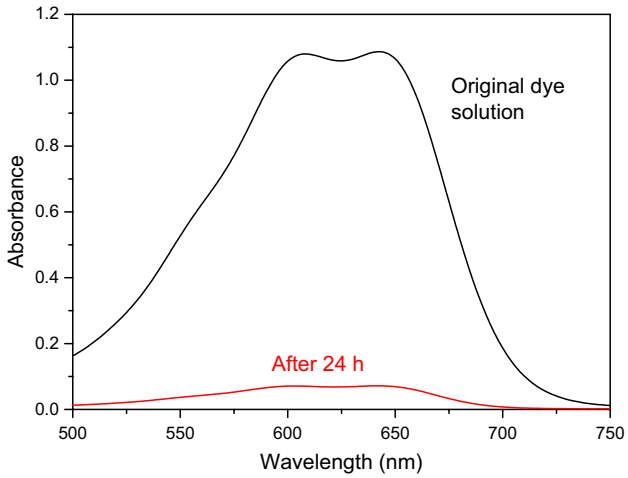

Fig. 8 The experiment shown in Fig. 7 can be followed by decrease in optical absorption (Islam Minisy, unpublished results)

tubes (Fig. 5b). The search for the dyes that guide one-dimensional growth is of importance (Sapurina et al. 2017). One-dimensional objects are better suited for the preparation of conducting composites because the percolation threshold can be reached at considerably lower volume fraction compared to three-dimensional globular objects (Li et al. 2009). Nanotubes have also higher specific surface areas than globules (Zeng et al. 2013; Stejskal and Trchová 2018). One-dimensional polymer structures are also more suitable to act as adsorbents (Stejskal and Trchová 2018). The polymer nanotubes and nanofibers are preferred morphologies in biomedical applications (Nair et al. 2019).

2. *Conductivity enhancement.* When the dyes participate in the preparation of conducting polymers, they significantly affect the resulting conductivity both in negative or positive manner (Sapurina et al. 2017). For instance, methyl orange increased the conductivity of polypyrrole at low concentrations but the conductivity dropped when the dye concentration became high (Fig. 6). The conductivity increase was often substantial, from 1 S cm^{-1} to 100 S cm^{-1} for polypyrrole nanotubes (Li et al. 2017b). The link between morphology and conductivity, however, is definitely not straightforward. It is tempting to assume that dyes assist in intermolecular charge transport between polymer chains due to their conjugated molecular structure, but convincing support of such hypothesis has not yet been provided in the literature. In addition, it has recently been observed that dyes alone display low, but non-negligible conductivity, up to 10^{-7} S cm^{-1}. The interaction of two different semiconductors thus may provide materials with new physical properties.
3. *Dye adsorption.* The interaction between dyes and conducting polymers manifests itself in adsorption phenomena (Fig. 7). There are numerous papers reporting the role of conducting polymers as dyes adsorbents applicable in water-pollution treatment (Ayad et al. 2018a) as reviewed below. The dye removal is conveniently followed by the decrease in the optical adsorption of solutions (Fig. 8). The process has usually been described in terms of adsorption isotherms in detail, but the understanding of the adsorption nature is still open to discussion. In the contrast to classical adsorbents, controlled adsorption and release on conducting polymers could be achieved by pH control and possibly also by exploiting electrochemical activity of conducting polymers.
4. *Photocatalytic dye degradation.* The deposition of conducting polymers on various inorganic photocatalysts,

Table 1 Preparation of polyaniline in the presence of dyes

Colour index	Dye	Type	Polymer	Reference
Anionic dyes				
Acid Green 25	Green GS	anq	Nanotubes	Amer et al. (2018)
Acid Orange 52	Methyl orange	azo	Nanotubes	Amer et al. (2019a)
Food Yellow 3	Sunset Yellow FCF	azo	Coral-like	Shi et al. (2017)
Acid Red 27	Amaranth	azo	Coral-like	Shi et al. (2018)

azo azo, *anq* anthraquinone

such as metal oxides, has led to the improved photocatalytic degradation dyes. The literature on above four directions is reviewed below in more detail.

Dyes in the preparation of conducting polymers

The organic dye used in the preparation of conducting polymers can fulfil several roles, the generation of the template for deposition of polyaniline or polypyrrole being the most currently met. In addition, the dyes that include primary amino group in their molecular structure may polymerize alone or copolymerize with aniline or pyrrole.

Polyaniline

Influence of the organic dyes on the morphology of polyaniline produced in their presence has not been systematically studied (Table 1). The "standard" polymerization of aniline hydrochloride (Stejskal and Gilbert 2002) yields globular morphology of polyaniline (Stejskal et al. 2008b). Such polymerization proceeds under strongly acidic conditions at pH < 2.5 (Sapurina and Stejskal 2008). On the contrary, it is known that the oxidation of liquid aniline in water, i.e. under mild acidity conditions, yields polyaniline nanotubes (Trchová et al. 2006; Stejskal et al. 2008b; Trchová and Stejskal 2011). The same applies to the polymerization of aniline in the solutions of weak organic acids (acetic, citric, succinic, etc.) (Stejskal et al. 2008b; Trchová and Stejskal 2011; Jeong et al. 2014; Mondal et al. 2019a). This was explained by the in-situ formation of aniline oligomers, resembling safranin dye (Fig. 3), that serve as a template for the nanotubular growth.

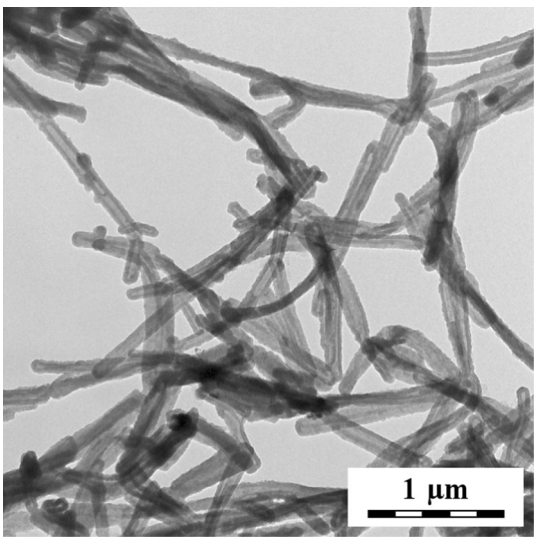

Fig. 9 Transmission electron micrograph of polypyrrole nanotubes (Sapurina et al. 2017)

The similar polymerizations carried out under low acidity in the presence of Acid Green 25 (Amer et al. 2018) or methyl orange (Amer et al. 2019a) have also yielded the nanotubes (Table 1), but these would be most probably obtained even in the dye absence (Trchová et al. 2006; Rakić et al. 2011). When the oxidation of aniline was carried out in the presence of methyl orange in the solution of hydrochloric acid, nanotubes were observed only when the acid concentration was reduced below 0.034 M (Ren et al. 2009), i.e. again at relatively low acidity. The assignment of the template role to these dyes under low acidity conditions is, therefore, ambiguous. The syntheses of polyaniline were limited to anioninic dyes, no cationic dyes have been tested.

When the polymerization of aniline took place under acidic conditions, coral-like morphology of polyaniline was produced in the presence of Sunset Yellow FCF (Shi et al. 2017) or amaranth dye (Acid Red 27) (Shi et al. 2018). The formation of one-dimensional morphology, however, could be a result of high dilution of reactants used by the authors, which is a method how to prepare polyaniline nanofibers (Chiou and Epstein 2005; Rakić et al. 2011). Preliminary experiments in the author's group indeed suggest that the influence of the dyes on the morphology and conductivity of polyaniline is marginal, in the dramatic contrast to polypyrrole.

Polypyrrole

The present review was also motivated by the observation that the presence of dyes during the preparation of polypyrrole affects both its morphology and conductivity (Stejskal 2018; Stejskal and Trchová 2018). In the classical synthesis, pyrrole is oxidized with iron(III) chloride, and polypyrrole is obtained as globules (Fig. 5a). The growth of polypyrrole nanotubes (Figs. 5b, 9) supported by methyl orange in the reaction mixture is probably the best known way how to prepare one-dimensional polymer morphology (Ćirić-Marjanović et al. 2014, Kopecká et al. 2014; Stejskal et al. 2016; Kopecký et al. 2017; Li et al. 2017b; Varga et al. 2017; Sapurina et al. 2017).

Methyl orange has routinely been used in the preparation of nanotubes since 2004 (Hu et al. 2004; Yang et al. 2005) in many follow-up papers. Examples of such synthesis, called the method of "self-degraded template", can also be found in recent literature, when polypyrrole nanotubes have been prepared as a powder or deposited on a suitable support (Škodová et al. 2013; Park et al. 2014; Alekseeva et al. 2015; Bober et al. 2015; Rudajevová et al. 2015; Stejskal et al. 2015; Varga et al. 2015; Wei et al. 2015; Xu et al. 2015; Kang et al. 2019; Kopecká et al. 2016; Sapurina et al. 2016; Babayan et al. 2017; Chen et al. 2017a; Galář

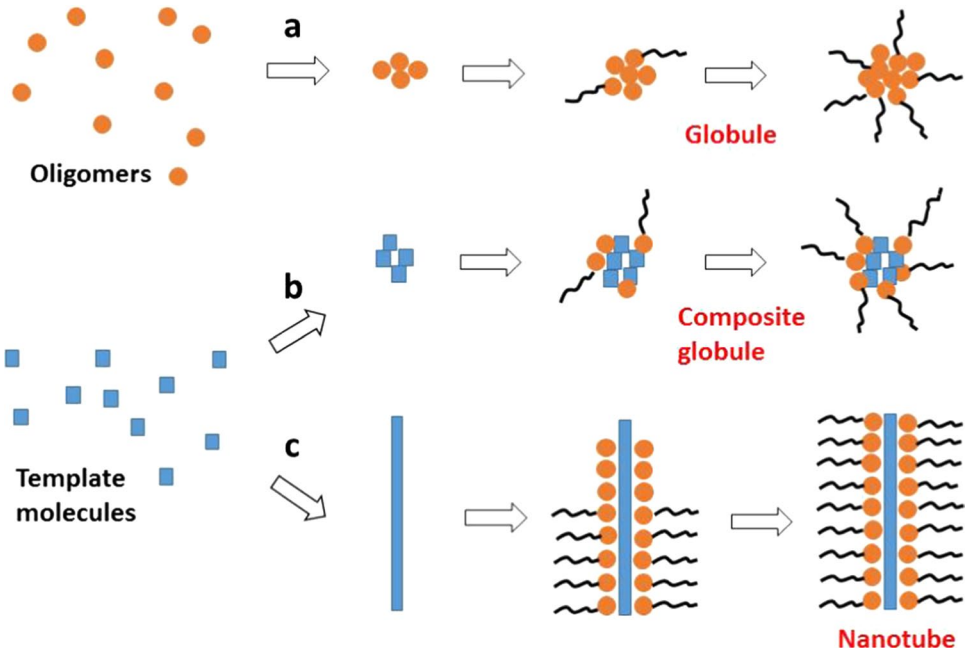

Fig. 10 The formation of polypyrrole **a** globules, **b** composite globules, and **c** nanotubes by aggregation of pyrrole oligomers (orange circles) and template dye molecules (blue squares) followed by the growth of polypyrrole chains (black curves). Reprinted from (Stejskal 2018)

et al. 2017; Ivanova et al. 2017; Xin et al. 2017; Zhang et al. 2017; Bober et al. 2018a; Lee et al. 2018; Li et al. 2018a; Lin et al. 2018; Pei et al. 2018; Stejskal 2018; Trchová and Stejskal 2018; Tuo et al. 2018; Xiao et al. 2018; Xin et al. 2018; Wang et al. 2018a; Wei et al. 2018; Wu et al. 2018; de Lazzari et al. 2019; Dong et al. 2019a; Dubal et al. 2019; Hryniewicz et al. 2019; Le et al. 2019; Mao et al. 2019; Pei et al. 2019; Prokeš et al. 2019; Yang and Chen 2019; Yashas et al. 2019; Zhang et al. 2019a, 2019b). For older papers reporting the use of methyl orange in polypyrrole synthesis the readers are referred to relevant review article (Stejskal and Trchová 2018). Methyl orange became incorporated in polypyrrole (Alekseeva et al. 2015; Li et al. 2017b) and this was the case also with other dyes, such as methylene blue (Phan et al. 2017). The conductivity of polypyrrole prepared in the presence of methyl orange increased several times at the same time (Fig. 6).

Various models of the nanotubular growth in polypyrrole have recently been proposed (Yang et al. 2005; Kopecká et al. 2014; Joulazadeh and Navarchian 2015). One of them (Stejskal 2018) (Fig. 10) assumes that the aggregation of pyrrole oligomers is followed by the growth of polypyrrole chains (black curves) to produce *globules*. When the template molecules are present (blue squares), they randomly aggregate at the same time and serve as loci for adsorption of pyrrole oligomers; *composite globules* are obtained. Nanotubes are formed if the template molecules order to one-dimensional aggregates and become coated by polypyrrole. It should be stressed that nanotubes were prepared also by electrochemical oxidation (Hryniewicz et al. 2019) and the chemical nature of oxidant in chemical oxidation thus cannot be decisive. *Nanofibers*, which can be regarded as a special case of nanotubes when the internal cavity is not discernible, have also been synthesized (Feng et al. 2014; Bober et al. 2018a). Among experimental studies, especially Raman spectroscopy proved to be powerful tool in the assessment of nanotubular structure (Trchová and Stejskal 2018). By using various excitation laser wavelengths, the beam penetration depth can be varied and detailed information about the nanotube profile may be obtained.

Other organic dyes had generally an influence on the morphology and conductivity of polypyrrole but their effect on the formation of polypyrrole is hardly predictable (Table 2). Some dyes had also promoted the formation of one-dimensional morphology despite of different molecular structure compared with methyl orange. This concerned especially anionic dyes, such as Acid Red 1 (Yan and Han 2007; Valtera et al. 2017), Acid Blue 25 (Wang et al. 2011; Bober et al. 2018a; Stejskal 2018), Acid Red 249 (Feng et al. 2009), Direct Blue 2 (Yang et al. 2019), Direct Blue 14 (Yang et al. 2019) and indigo carmine (Li et al. 2016; Hu et al. 2018), which all supported the growth of nanofibers or nanorods. Among cationic dyes, the formation of one-dimensional nanostructures was observed with rhodamine B (Xue et al. 2010), methylene blue/heparin (Wei et al. 2010), methylene green (Bonfin et al. 2019) phenosafranin (Minisy et al. 2019a), safranin (Stejskal 2018; Minisy et al. 2019a) (Fig. 11a) and acriflavine (Fig. 11b). Last three dyes are closely related chemicals of phenazine type, methylene blue and methylene green of phenothiazine type. The morphology of polypyrrole was also affected by the presence of acid fuchsin (Dong et al. 2019b). We conclude that both the morphology and conductivity are strongly influenced by the presence of dyes during polymer preparation, in contrast to

Table 2 Preparation of polypyrrole in the presence of dyes

Colour index	Dye	Type	Polymer[a]	References
Anionic dyes				
Acid Blue 25	Acid Fast Blue RB	anq	Nanofibres	Wang et al. (2011) and Bober et al. (2018a)
Acid Blue 74	Indigo Carmine	ind	Nanorods	Girotto et al. (2002), Sapurina et al. (2017), Hu et al. (2018), Li et al. (2016) and Loguercio et al. (2016)
Acid Blue 129	Atanyl Blue PRL	anq	Globules	Bober et al. (2018a)
Acid Blue 324	Telon Blue K-BRLL	anq	Globules	Wang et al. (2013a)
Acid Green 25	Green GS	anq	Nanoparticles	Sapurina et al. (2017)
Acid Orange 10	Orange G	azo	Globules	Valtera et al. (2017)
Acid Orange 52	Methyl orange	azo	Nanotubes	Li et al. (2017b), Sapurina et al. (2017), Stejskal and Trchová (2018) and many others[b]
Acid Red 1	Amido Naphthol Red G	azo	Nanofibres	Valtera et al. (2017)
Acid Red 18	Ponceau 4R	azo	Globules	Chen et al. (2019b)
Acid Red 249	Polar Brilliant Red B	azo	Nanofibres	Feng et al. (2009)
Acid Yellow 23	tartrazine	azo	Globules	Wang et al. (2019a)
Direct Blue 2	Direct Blue BH	azo	Nanofibers	Yang et al. (2019)
Direct Blue 14	Trypan blue	azo	Nanofibres	Yang et al. (2019)
Direct Red 28	Congo red	azo	Small globules	Stejskal (2018)
Direct Violet 1	Direct Violet 4RB	azo	Globules	Yang et al. (2019)
Food Yellow 3	Sunset Yellow FCF	azo	Nanobarrels	Valtera et al. (2017)
Mordant Red 3	Alizarin red S	anq	Globules	Zang et al. (2018)
Reactive Black 5	Remazol Black B	azo	Spheres	Sapurina et al. (2017)
–	Thymol blue	tpm	Hollow spheres	Sapurina et al. (2017)
–	Ethyl orange	azo	Globules	Li et al. (2017b), Sapurina et al. (2017) and Stejskal (2018)
–	Cresol red	tpm	Spheres	Sapurina et al. (2017)
–	Bromophenol blue	tpm	Globules/rods	Eslami and Alizadeh (2019)
Cationic dyes				
Basic Blue 9	Methylene blue	ptz	Nanoparticles, tubes, rods	Wei et al. (2010), Phan et al. (2017) and Sapurina et al. (2017)
Basic Red 2	Safranin	phz	Nanorods	Stejskal (2018), Stejskal and Trchová (2018) and Minisy et al. (2019a)
Basic Violet 10	Rhodamine B	dbp	Nanotubes	Xue et al. (2010)
–	Phenosafranin	phz	Globules/nanotubes	Minisy et al. (2019a)

azo azo, *anq* anthraquinone, *dbp* dibenzopyran, *ind* indigoid, *phz* phenazine, *poz* phenoxazine, *ptz* phenothiazine, *tpm* triphenylmethane dye types in Tables 2–9. Cf. also Figure 2

Only one chromophore is listed but more may be present in the dye structure

[a]Polymer morphology may vary depending on dye concentration

[b]There are many other papers employing methyl orange for the preparation of nanotubes

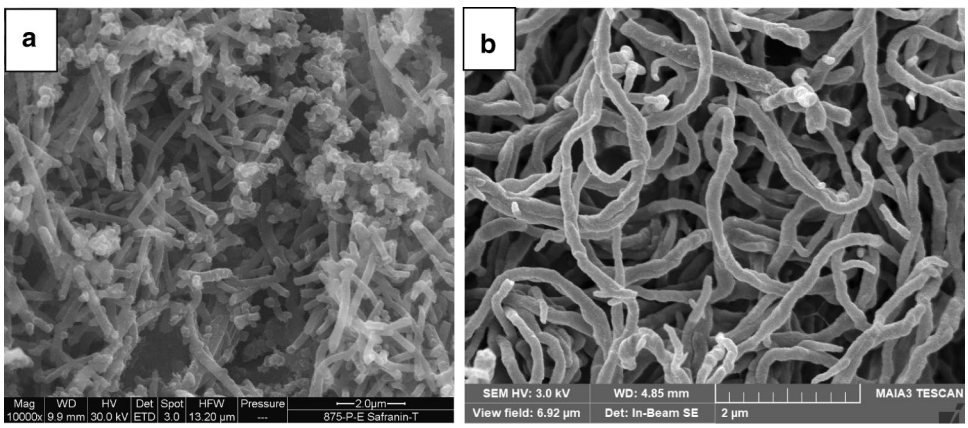

Fig. 11 Polypyrrole nanorods/nanofibers prepared in the presence of **a** safranin and **b** acriflavine (unpublished results)

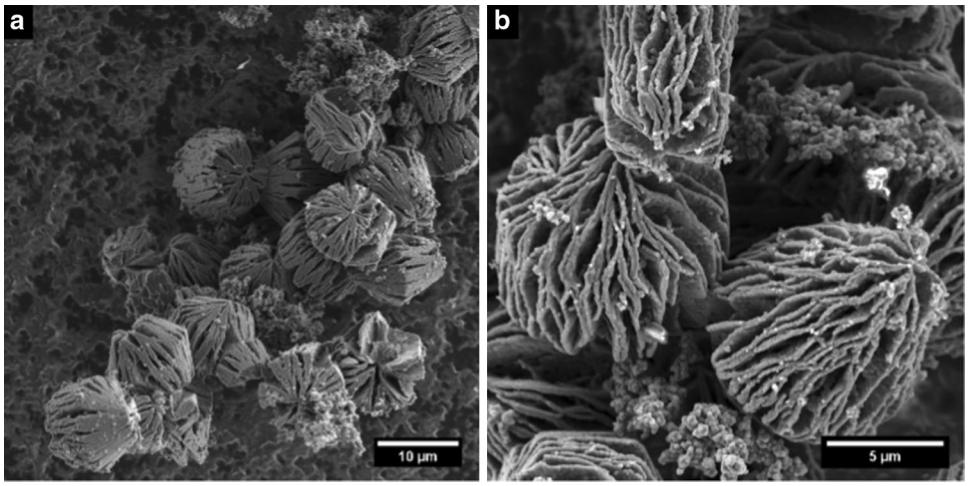

Fig. 12 Polypyrrole prepared in the presence of Sunset Yellow FCF dye (two magnifications). Reprinted from (Valtera et al. 2017)

polyaniline. It also seems that the electrostatic interactions between polypyrrole and dyes are not operational.

The presence of other dyes produced polypyrrole globules of various sizes. These were Acid Blue 324 (Wang et al. 2013a), Acid Blue 129 (Bober et al. 2018a), Acid Green 25 (Sapurina et al. 2017), alizarin red S (Zang et al. 2018), cresol red (Sapurina et al. 2017), Direct Violet 1 (Yang et al. 2019), ethyl orange (Li et al. 2017b), indigo carmine (Sapurina et al. 2017), Orange G (Valtera et al. 2017), methylene blue (Phan et al. 2017), Reactive Black 5 (Sapurina et al. 2017), tartrazine (Wang et al. 2019b) and thymol blue (Sapurina et al. 2017). Sunset Yellow FCF yielded exceptional hierarchical polypyrrole microbarrels (Valtera et al. 2017) (Fig. 12), and methylene blue promoted the formation of hollow spheres (Sapurina et al. 2017).

A group of papers reports the electrochemical oxidation of pyrrole to polypyrrole in the solutions of various organic dyes. Polypyrrole prepared along with methyl orange was used as a pH sensor base on Raman spectroscopy (Czaja et al. 2019). The presence of indigo carmine displayed improved photocurrent density under polychromatic illumination (Girotto et al. 2002) or the potential to be applied as counter electrode in dye-sensitized solar cells (Loguercio et al. 2016). The same system including indigo carmine was also used for the reduction of tetrachloroauric acid to gold nanoparticles (Luguercio et al. 2015). The dye was proposed to increase the ordering degree and to provide better electronic charge transfer in the bulk. Polypyrrole was also prepared in the presence of malachite green, which was expected to produce molecularly imprinted composite film on the electrode (Xu et al. 2019a). The electrochemical synthesis of polypyrrole in the presence of bromophenol blue led to globules or rods applicable in the sensing of explosives (Eslami and Alizadeh 2019). When polypyrrole was prepared electrochemically in the presence of Eriochrome cyanine R, the dye was incorporated in the polymer film (Tavoli and Alizadeh 2014). The electrochromic properties were enhanced compared with the film prepared in the dye absence. The presence of alizarin red reduced the electropolymerization potential in the preparation of polypyrrole and affected the morphology of films (Chen and Zhitomirsky 2013; Rounaghi et al. 2015). The presence of a dye in the electropolymerization of pyrrole thus has influence on the properties of polypyrrole films. It has to be stressed that the film morphology depends also on the concentrations of reactants, their proportions, acidity conditions and other factors.

Dyes as monomers

It was proposed that the oxidation of some dyes carrying primary amino groups could be a novel approach to the synthesis of conducting polymers (Jiang et al. 2018). This is a reasonable expectation because the conjugated molecular structure of dyes extended to polymer chain could indeed to have such result. While the polymerization might have indeed taken place, the convincing illustration of reasonable conductivity has not been reported.

The chance to obtain a conducting polymer might be expected after the oxidation of dyes containing primary amino group(s) on benzenoid ring (Gouveia-Caridade et al. 2013), in analogy of aniline oxidation to polyaniline. The *chemical oxidation* of safranin (Basic Red 2), however, led to non-conducting oligomeric rather than conducting polymeric products (Ćirić-Marjanović et al. 2007). The chemical oxidation of 1,5-diaminoanthraquinone produced the electroactive polymer in nanotubular form (Liu and Liu 2019), but the conductivity was not determined. The chemical oxidation of azulene with iron(III)chloride yielded electroactive polyazulene (Gradzka et al. 2018), but its conductivity has not again been reported. In contrast to current dyes, azulene is a bicyclic hydrocarbon that does not contain any nitrogen atoms. Similarly, the joint oxidation of aniline and thymol blue, where the dye was expected to be a comonomer, was claimed to yield a corresponding copolymer (Ponprapakaran et al. 2017). The

dye, however, does not again contain any amino group and the formation of a copolymer is thus unlikely.

The *electrochemical oxidation* of safranin produced a non-conducting polymer (Pauliukaite et al. 2009; Lavanya et al. 2015; Yang 2016), similarly like neutral red (Gouveia-Caridade et al. 2013; Broncová et al. 2004, 2008, 2016; Pauliukaite and Brett 2008). The phenoxazine dyes, such as Brilliant Cresyl Blue or Nile blue A, have also been reported to produce polymer upon the electrooxidation (Gouveia-Caridade et al. 2013) similarly like phenothiazine dye, Azure B (Stoikov et al. 2019). The electrochemical oxidation of alizarin, which does not contain any amino group, yielded the corresponding polymer (Jiang et al. 2018). Glassy carbon electrode was modified by poly(methyl orange) (Chiwunze et al. 2019) or poly(phenol red) (Karabiberoglu and Dursun 2017) by the electropolymerization of corresponding dyes. These dyes also do not contain primary amino groups, which would account for the formation of a polymer. The insolubility of the product has often been regarded as a proof of polymerization in electrochemistry but this need not be convincing for a polymer chemist.

Another strategy consists in the *attachment of a polymerizable group* to a dye. For example, methyl red was covalently bonded to nitrogen atom in pyrrole, which was subsequently electropolymerized (Almeida et al. 2017). The Disperse Red 1 was similarly functionalized with an acrylic group followed by its polymerization (Spiridon et al. 2018). In such cases, the dye is a pendant moiety and does not produce the main chain.

Conducting polymers as adsorbents of dyes

Basic principles

The uses of conducting polymers in highly topical environmental uses, such as removal of organic dyes and heavy-metal ions from wastewater, have recently been reviewed (Zare et al. 2018a). It should be observed that this important application does not exploit the most important property, the conductivity, even though the contribution of the ionic conductivity might affect the kinetics of adsorption. In typical studies, the effects of dye concentration, the adsorbent dosage, adsorption kinetics, temperature and pH have been investigated for conducting polymers or their composites and dyes. Due to the plethora of existing dyes, many reports have been published and still will appear in the literature. Adsorption of the dyes is easily followed spectrophotometrically by the decrease in the colouration of dye solution after addition of adsorbent (Figs. 7, 8).

The adsorption of dyes on conducting polymers is routinely assessed by the series of experiments (Ayad et al. 2012; Salem et al. 2016; Tayebi et al. 2016; Tanzifi et al. 2017; Zhou et al. 2017; Kaushal et al. 2018; Kumar et al. 2018; Lyu et al. 2018; Maruthapandi et al. 2018; Shahriman et al. 2018; Amer et al. 2019a; Bagheri and Mardani 2019). The relative dye *removal efficiency* in % or absolute *adsorption capacity* (adsorptivity) in mg g^{-1} is the fundamental characteristics reported in the literature. Adsorption isotherms, i.e. the dependences of the adsorbed amount on the adsorbate concentration at fixed temperature, have been used in the literature to describe the *adsorption mechanism.* Langmuir, Dubinin-Raduskievich, Freundlich, Halsey and Temkin isotherms are the best known types and the reader is referred to a review article (Huang et al. 2014) for their survey. Time dependence of adsorption, i.e. the *adsorption kinetics*, has usually been rated as the pseudo-first order or pseudo-second order type, or discussed in terms of Elovich and intraparticle-diffusion models (Huang et al. 2014). Temperature dependence of adsorption parameters and of equilibrium concentrations of adsorbates allows for the determination of *adsorption thermodynamics* expressed in quantities, such as free energy or enthalpy. Adsorption experiments are usually performed in water close to neutral conditions but the dependence of adsorption parameters on pH is of importance for the recovery of adsorbents.

The quantitative parameters of adsorption isotherms, kinetics or thermodynamics have often been extensively reported in the literature. Especially for the composites, however, they are difficult to compare for several reasons: (1) Components of the composite may adsorb dyes independently and the contribution conducting polymers alone has not been specified, (2) the composite composition is often unknown, (3) it was not specified if the adsorption capacity concerns the whole composite or any part only, (4) the experimental conditions, especially adsorbent content and dye concentrations ranges, differ and (5) other parameters, especially pH or temperature, also vary in individual studies. Especially the studies of conducting polymers alone are scarce. The conducting polymer deposition was usually reported to improve the adsorption of the current adsorbent.

Adsorbent forms and properties

The use of composites dominates the adsorption studies for practical reasons. Conducting polymers have been as a

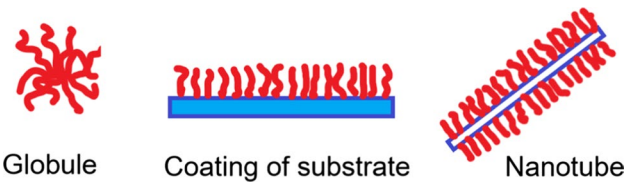

Fig. 13 Random chains in globular conducting polymer, and ordered chains in coatings deposited on the substrates or in nanotubes

rule deposited at the surface of substrates by in-situ *polymerization* (Stejskal et al. 1999; Fedorova and Stejskal 2002; Omastová and Mičušík 2012), sometimes referred to as *surface polymerization*, i.e. when the substrates were immersed in the aqueous reaction mixture used for the preparation of conducting polymers. It has to be stressed that this approach results indeed in the coating of substrates rather than in a mere mixture of a substrate and conducting polymer. It has been established that any interface immersed in the reaction mixture used for the oxidative polymerization of aniline or pyrrole becomes coated with a thin film of conducting polymer (Stejskal et al. 2010). The oligomers produced at early stage of monomer oxidation are adsorbed at available interfaces at first and stimulate the following growth of conducting-polymer chains. The typical thickness of the coating is 100–200 nm (Stejskal and Sapurina 2005). The film thickness is reduced when the water-soluble polymers (Riede et al. 2002) or surfactants (Castillo-Reyes et al. 2015) are present in the reaction mixture. The experiments suggest the brush-like ordering of polymer chains and enhanced conductivity in the coatings due to improved inter-chain charge-transfer compared with common globular morphology (Fig. 13). For that reason, the composites composed of surface-coated substrates, may have higher conductivity than globular conducting polymer or the substrate alone (Acharya et al. 2018) and may perform better in other respects, e.g., in adsorption. The dye adsorption is likely to be little dependent on the substrate nature and will be dominated by the conducting polymer coating including its specific surface area. The role of the material used for the polymer deposition, however, would be of importance in photocatalysis, because the polymer coating is penetrated by UV–visible light and the catalytic performance of the substrate alone may be exploited.

Various organic and inorganic substrates coated with conducting polymers proved to be better adsorbents or photocatalysts than the individual components (Mukhta et al. 2007; Zhang et al. 2014; Elsayed and Gobara 2016; An et al. 2018; Mohamed et al. 2018; Nerkar et al. 2018; Chatterjee et al. 2019; Chen et al. 2019a, 2019b). The often-mentioned synergistic effect can be explained by the improved brush-like ordering of the polymer chains deposited at the substrate surface (Sapurina et al. 2001, 2002; Stejskal et al. 2019), although some authors suggest the interfacial heterojunctions to be responsible for this effect (Megha et al. 2019). In addition to enhanced dye adsorption or photodegradation, such ordering manifests itself similarly in the synergistic conductivity increase (Acharya et al. 2018; Megha et al. 2019). Please note that the formation of nanotubes can be regarded as the surface coating of the template afforded, e.g., by dyes (Figs. 10, 13) and, for that reason, the nanotubes may also have higher conductivity (Li et al. 2017b) or dye adsorptivity (Ayad and Abu El-Nasr 2010) compared with classical globular polymers.

Among non-conventional approaches, plasma deposition technique has been used for surface modification of titanium dioxide (Subramaniam et al. 2019). In this case, the coating is suspected to consist rather of aniline oligomers than polyaniline. The solution of polyaniline base in *N*-methylpyrrolidone was used for the surface modification of graphene/wolframate composite (Biswas et al. 2019). The opposite strategy when the surface of a conducting polymer instead of the substrate was altered has been mentioned only rarely. For example, polyaniline was used as a reductant of silver ions to silver nanoparticles (Stejskal 2013) and the resulting composite was used as an adsorbent of brilliant green (Salem et al. 2016).

When it comes to the individual application forms, *powders* have been most frequently investigated. Although they are best suited for the academic studies, other material forms have been sought for the practice. In the composites, one of the components is often used to provide the mechanical properties and integrity. For example, conducting polymers were deposited on *fibrillar materials* of organic nature, such as, cotton textile (Fan et al. 2017; Ayad et al. 2018a, b; Gamal and Attia 2019), electrospun mats (Qi et al. 2016; Gorza et al. 2018), chitosan (Sananmuang et al. 2017) and kapok fibres (Zheng et al. 2012; Mu et al. 2015), paper (Liu et al. 2015), polyamide (Li et al. 2019a) and polyamide nanofibres (Li et al. 2015; Zarrini et al. 2017), polyimide (Ding et al. 2019) or polyester fabric (Ghaemi and Safari 2018; Gamal and Attia 2019). The inorganic nanofibers have been used rarely and they are represented by carbon nanotubes (Zeng et al. 2013) or silicon carbide nanofibres (Koysuren 2019). Titanium dioxide membranes (Li et al. 2018b) and stainless-steel mash (Yihan et al. 2018) similarly served as substrates for in-situ polymer deposition.

Composite *hydrogels* (Yan et al. 2015; Stejskal 2017; Stejskal and Bober 2018; Yao et al. 2018; Song et al. 2019; Xing et al. 2019) or macroporous cryogels based on conducting polymers (Stejskal et al. 2017) represent three-dimensional forms worth of investigation. When the conducting polymers have been prepared in the solutions of water-soluble polymers, *colloidal dispersions* with conducting polymer core and supporting polymer shell are produced as a rule (Stejskal 2001; Stejskal and Sapurina 2005; Stejskal and Bober 2018; Song et al. 2019). The composite material obtained after their precipitation and drying has only exceptionally been used in dye-adsorption studies (Abbasian et al. 2017). Such materials have been regarded not quite precisely as graft copolymers with conducting polymer backbone.

The *simple mixtures* of substrates with separately prepared conducting polymers have been used exceptionally. Polyaniline combined with zirconium dioxide adsorbed methylene blue (Agarwal et al. 2016), polyaniline mixture with strontium stannate photocatalysed the decomposition

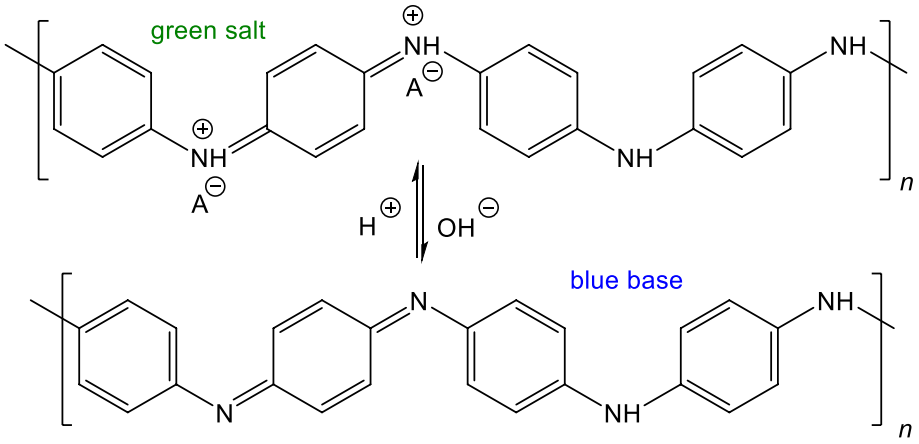

Fig. 14 Green conducting polyaniline salt converts to blue non-conducting polyaniline base in alkaline media

of the same dye (Faisal et al. 2019). Polyaniline mixture with poly(vinyl chloride) was similarly applied to the decolorization of methyl orange (Bahrudin et al. 2018a). The combination of titanium dioxide with polyaniline colloid was tested in the photocatalytic decomposition of rhodamine B (Zhou et al. 2019) or methyl orange (Bahrudin et al. 2018b, 2019). The blend of polyaniline with custom-made orange dye was exploited in impedance humidity sensor (Chani et al. 2013). Polyaniline solution in tetrahydrofuran was used to modify zinc oxide particles (Poorarjmand et al. 2019). The reasoning of such approach instead of an in-situ coating method has to be still justified.

Specific surface area is a key parameter in the adsorption experiments. It is relatively low for polyaniline, 3.6 m^2g^{-1} (Xu et al. 2019c), 8 m^2g^{-1} (Tanzifi et al. 2018a), 9.1 m^2g^{-1} (Vidya and Balamurugan 2019a), 18 m^2g^{-1} (Hasan et al. 2019) or 20 m^2g^{-1} (Ayad and Zaghlol 2012). It increased to 17–31 m^2g^{-1} when polyaniline was prepared in the presence of surfactants (Ahmed et al. 2016) that reduced the size of globules. The annealing of polyaniline base at 180 °C associated with cross-linking led to the increase in specific surface area to 349 m^2g^{-1} (Ayad and Zaghlol 2012). Analogous values have been reported for polypyrrole, 6.9 m^2g^{-1} (Chen et al. 2019b), 10 m^2g^{-1} (Kopecký et al. 2017) or 26 m^2g^{-1} (Acharya et al. 2018). The specific surface area may be increased by the control of morphology (Meng et al. 2014). Polypyrrole nanotubes have about one order of magnitude higher surface area than polypyrrole globules (Li et al. 2017b; Kopecký et al. 2017; Stejskal and Trchová 2018) and the behaviour of both morphologies with respect to dye adsorption may differ. Polyaniline nanoparticles have been more efficient adsorbents of methylene blue than the conventional globular polyaniline (Ayad et al. 2013). When two-dimensional substrates with a high specific surface area, such as graphene of molybdenum disulfide, are coated with conducting polymers, such composites may become promising adsorbents. On the other hand, when the substrates are porous, the micropores may be filled with conducting polymers during their deposition, and the specific surface area would be reduced (Jia et al. 2012).

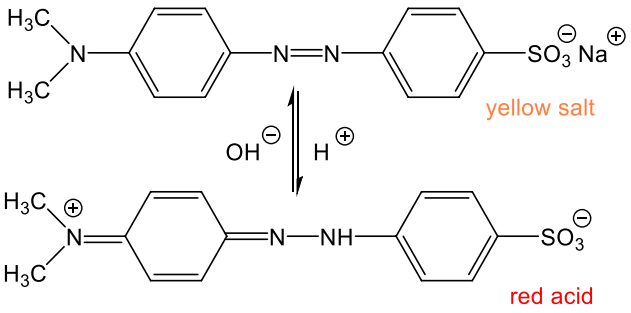

Fig. 15 Methyl orange salt, sodium 4-((4-dimethylamino)phenyldiazenyl)benzene-1-sulfonate, converts to a corresponding acid below pH 3.5 (Sapurina et al. 2017)

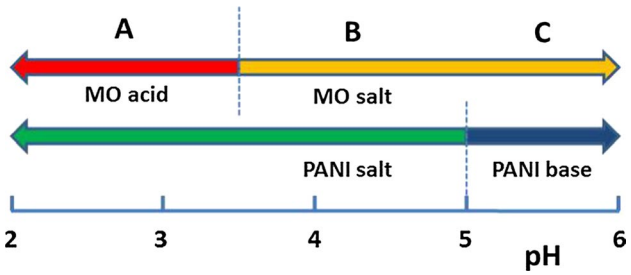

Fig. 16 **a** Red methyl orange acid interacts with green polyaniline salt at pH < 3.5, **b** yellow methyl orange salt interacts still with polyaniline salt within 3.5 > pH < 5 range and **c** MO salt interacts with blue polyaniline base at pH > 5. The transitions are gradual in the reality

The role of pH

The pH in adsorption experiments is important and adsorption parameters were found to depend on pH (Baseri et al. 2013; Ovando-Medina et al. 2015a; Gorza et al. 2018; Ma

et al. 2018; Ayad et al. 2018b; Chen et al. 2019b). In practice the adsorption from aqueous solutions takes place at neutral conditions but the change in pH may be of importance for the adsorbent regeneration or recovery (Ayad et al. 2018a; Zare et al. 2018b). Depending on pH, polyaniline exists under acidic conditions as a conducting salt and above ca pH 4–6 it converts to a corresponding non-conducting base (Fig. 14). The base is less hydrophilic than the salt (Stejskal et al. 2008a) and it is thus better suited to interact with hydrophobic part of a dye by hydrophobic interactions. This explains the enhanced dye adsorption observed often at high pH. The similar salt–base transition is found also in polypyrrole (Stejskal et al. 2016) but generally polypyrrole is less sensitive to pH than polyaniline.

Many dyes also exist in two forms depending on pH, typically as acids and salts, acidobasic indicators being the best examples. For instance, methyl orange is present as a red hydrophobic acid of limited solubility in water below pH 3.5 and above this pH as well-soluble yellow salt (Ren et al. 2009; Li et al. 2017b) (Fig. 15). The adsorption of the dye thus would be affected by the acidity of the medium. For example, the adsorption efficiency of methyl orange on polyaniline at pH 6 was 90% and decreased to 64.5% at pH 2 (Tanzifi et al. 2017). Up to three combinations of polymer and dye forms may interact depending on pH (Fig. 16).

For example, adsorption of methylene blue on polypyrrole increased three times when the pH 3.5 was changed to 10.5 (Ayad et al. 2018a; Wang et al. 2018b). The better adsorption on polyaniline composite under alkaline conditions was reported for methylene blue, neutral red and crystal violet (all cationic dyes) while opposite trend was found for Eriochrome Black T (anionic dye) (Kaushal et al. 2018). Both the conducting polymers and cationic dyes

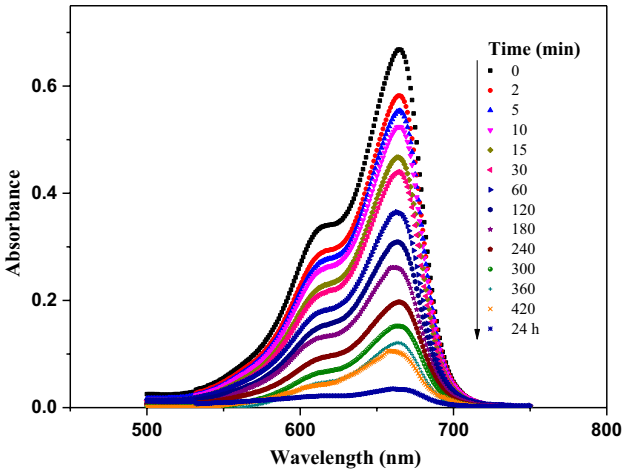

Fig. 18 Time dependence of absorption spectra of methylene blue (3.9 mg L^{-1}) with 50 mg cotton textile coated with polypyrrole. Reprinted from Ayad et al. 2018a

are not protonated under alkaline condition, their hydrophobicity is enhanced and hydrophobic interactions thus seem to be driving or supporting forces in the adsorption. Improved adsorption of anionic dyes on polymer bases was indeed better compared to protonated forms (Aliabad and Mahmoodi 2018). Optimum adsorption on polyaniline nanotubes was at pH 9 for cationic dye and pH 5 for anionic one (Amer et al. 2018), i.e. when the dissociation of dyes was limited.

Recycling of the adsorbents is of importance. Treatment based on the variation of acidic/basic pH is the most commonly used to remove sorbates (Fig. 17) and to recover the adsorbent (Li et al. 2012; Zheng et al. 2012; Kumar

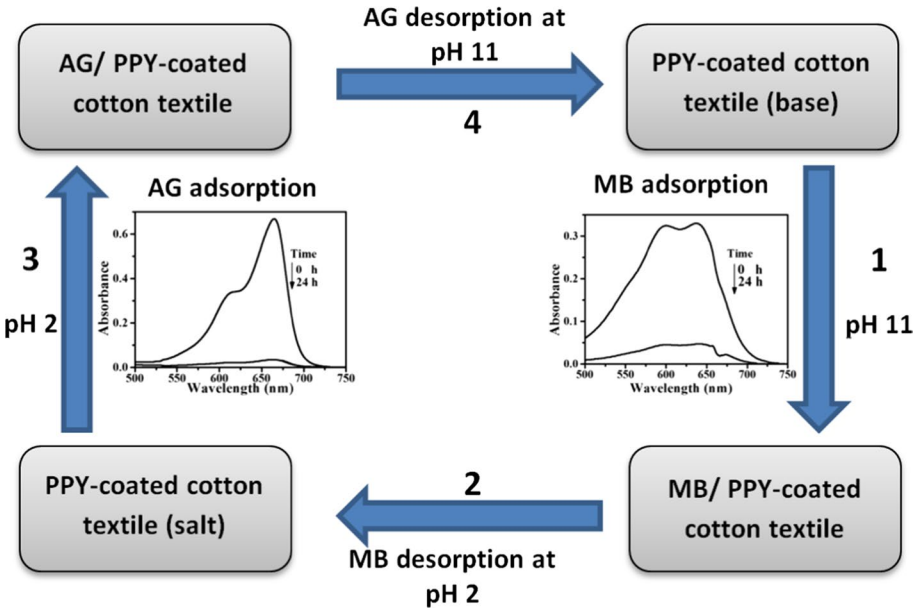

Fig. 17 Illustration of the reusability of cotton textile coated with polypyrrole in adsorptive removal of cationic dye, methylene blue (MB), and anionic dye, Acid Green 25 (AG), using changes in acidity of the medium. For details cf. (Ayad et al. 2018a)

et al. 2016; Ayad et al. 2018a; Lyu et al. 2018). One has to keep in mind that the deprotonation/reprotonation cycles introduce the changes in hydrogen bonding in the conducting polymer that manifest themselves in incomplete reversibility of conductivity (Prokeš et al. 2019) with expected impact also on other polymer properties. The extraction with organic solvent served for the recycling, too (Shanehsaz et al. 2015; Aliabad and Mahmoodi 2018; Shahriman et al. 2018).

Experimental methods in dye adsorption

The absorption of light in visible region is the inherent property of dyes. The monitoring of the decrease in the optical absorbance of the dye solution is the most easy and convenient method how to follow the course and extent of dye adsorption (Fig. 18) (Ayad et al. 2012, 2018a; Kumar et al. 2016; Kaushal et al. 2018; Maruthapandi et al. 2018; Amer et al. 2019a; Chatterjee et al. 2019; Yuan et al. 2019). The experimental simplicity is the reason for the large number of studies in this area.

The quartz microbalance seems to be a suitable method for the testing of dye adsorption on conducting polymer films and its kinetics. This has been demonstrated for methylene blue adsorption on polyaniline film deposited on quartz crystal (Ayad and Abu El-Nasr 2010). Despite its simplicity, the method has not been routinely used. Liquid chromatography combined with mass spectrometry has frequently been applied as an additional method, especially in the photodegradation of dyes when the fate of the decomposition products had to be identified.

Table 3 Dye adsorption on polyaniline

Colour index	Dye	Type[a]	References
Anionic dyes			
Acid Blue 40	Acid Brilliant Blue RAW	anq	Muhammad et al. (2019b)
Acid Blue 74	Indigo carmine	ind	Chafai et al. (2017b) and Mondal et al. (2019a)
Acid Blue 83	Coomassie Brilliant Blue R-250	tpm	Mahanta et al. (2008)
Acid Green 25	Alizarine cyanine green	anq	Mahanta et al. (2008), Amer et al. (2018) and Minisy et al. (2019b)
Acid Orange 10	Orange G	azo	Mahanta et al. (2008)
Acid Orange 52	Methyl orange	azo	Ai et al. (2010), Guo et al. (2011), Sharma et al. (2016), Tanzifi et al. (2017), Karri et al. (2018), Nerkar et al. (2018), Duhan and Kaur (2019), Mondal et al. (2019a) and Vidya et al. (2019)
Acid Red 1	Acid red G	azo	Lyu et al. (2019)
Acid Red 14	Acid Red 4B	azo	Ahmed et al. (2016)
Acid Red 94	Rose bengal	dbp	Shen et al. (2018) and Xu et al. (2019c)
Acid Violet 90	Bordeaux MB	azo	Akti and Okur (2018)
Direct Blue 78	Direct Sky Blue	azo	Salem (2010)
Direct Red 28	Congo red	azo	Chafai et al. (2017a), Chafai et al. (2017b), Aliabadi and Mahmoodi (2018) and Mondal et al. (2019a)
Food Yellow 3	Sunset Yellow FCF	azo	Aliabadi and Mahmoodi (2018)
Mordant Black 11	Eriochrome Black T	azo	Mondal et al. (2019a)
Reactive Black 5	Remazol Black B	azo	Bhaumik et al. (2016)
Reactive Blue 19	Remazol Brilliant Blue R	anq	Mahanta et al. (2008)
Reactive Blue 39	Cibacron Navy P-2R-01	azo	Bingöl et al. (2012)
Reactive Red 120	Reactive Brilliant Red KE-4B	azo	Maqbool et al. (2019)
Cationic dyes			
Acid Red 87	Eosin Y	dbp	Majumdar et al. (2019)
Basic Blue 9	Methylene blue	ptz	Mahanta et al. (2008), Ayad and Abu El-Nasr (2010), Ayad and Zaghlol (2012), Ayad et al. (2013), Agarwal et al. (2016), Rafiqi and Majid (2017), Amer et al. (2018), Maruthapandi et al. (2018), Shen et al. (2018), Amer et al. (2019a), Minisy et al. (2019b), Sahu et al. (2019) and Mondal et al. (2019a)
Basic Green 4	Malachite green	tpm	Zeng et al. (2013)
Basic Violet 10	Rhodamine B	dbp	Mahanta et al. 2008
Basic Violet 3	Crystal violet	tpm	Sharma et al. (2016) and Mondal et al. (2019a)

[a]Cf. Figure 2 for the definition

Adsorption of dyes on conducting polymers

This section lists various combinations of conducting polymers, substrates and dyes reported in the literature trying to organize them as a guide for future adsorption studies. While the entries in tables are sorted by the organic dyes, the type of the composite adsorbents has been used in the text. No quantitative comparison has been attempted except for quoting occasionally maximum adsorption capacities. These can be rated as relatively poor below 10 mg g^{-1}, fair for 10–100 mg g^{-1}, good above 100 mg g^{-1} and exceptional above 1000 mg g^{-1}. Several tendencies can be traced in the design of new adsorbents: (1) The surface modification of various *natural, often waste materials* with conducting polymers, (2) the analogous deposition of conducting polymers on inorganic *substrates with high specific surface area*, (3) the use of *substrates active also as photocatalysts* and (4) incorporation of component that allows the *easy separation*, e.g., ferromagnetic one (iron, iron oxides, magnetite, ferrites) by magnetic field.

The papers devoted to the adsorption of dyes on neat conducting polymers are rare (Majumdar et al. 2019). Some studies reporting the dye adsorption on conducting polymer composites include also the behaviour of its components. They demonstrate that conducting polymers alone perform as adsorbents of organic dyes. The vast majority of papers concerns the surface modification of various substrates with conducting polymers and reports the improvement of adsorption capacities; the conducting polymers alone, however, have not usually been considered.

Polyaniline

For the adsorption of various organic dyes on polyaniline and its composites, the reader is referred to a recent review (Nasar and Mashkoor 2019). *Anionic dyes* have been represented especially by *methyl orange* (Table 3). The maximum capacity of methyl orange adsorption was 76 mg g^{-1} (Tanzifi et al. 2017). Polyaniline nanofibres prepared by the interfacial polymerization method adsorbed up to 25 mg g^{-1} of this dye (Duhan and Kaur 2019). Polyaniline prepared in the presence of sodium dodecylbenzenesulfonate had 76 mg g^{-1} capacity for methyl orange adsorption (Karri et al. 2018). High adsorption of methyl orange, 385 mg g^{-1}, was found on polyaniline microspheres (Guo et al. 2011) but, considering the preparation protocol, they were composed most likely rather by aniline oligomers (Stejskal et al. 2008a).

Other anionic dyes have also been well adsorbed. For example, Acid Violet 90 complex with chromium(III) was separated by polyaniline from aqueous solutions, the adsorption capacity being 153 mg g^{-1} (Akti and Okur 2018). Polyaniline was a good adsorbent of Congo red from wastewaters (Chafai et al. 2017a, b). Polyaniline treated with copper(II) chloride adsorbed reactive azo dye Cibacron Navy P-2R-01 (Bingöl et al. 2012). Finally, adsorption capacities reached 300 mg g^{-1} for indigo carmine (Mondal et al. 2019a), 310 mg g^{-1} for Acid Orange G (Lyu et al. 2019) and even 435 mg g^{-1} for Reactive Black 5 (Bhaumik et al. 2016). Adsorption up to 5950 mg g^{-1} has also been observed with Acid Red 94 (Xu et al. 2019c) but needs independent confirmation.

Relatively little attention has been paid to the adsorption of *cationic dyes*. Methylene blue has been the most popular representative of this group (Table 3) but the experimental results differ due to varying conditions. The adsorption was spontaneous and the capacity was 19 mg g^{-1} (Maruthapandi et al. 2018) or 192 mg g^{-1} (Agarwal et al. 2016) but reached even above 413 mg g^{-1} (Rafiqi and Majid 2017). Both the Langmuir and Freundlich isotherms fitted the data well (Ayad and Abu El-Nasr 2010; Ayad et al. 2012; Ayad and Zaghlol 2012; Chafai et al. 2017a; Rafiqi and Majid 2017; Amer et al. 2018, 2019a; Kaushal et al. 2018; Maruthapandi et al. 2018). Polyaniline adsorbed up to 48 mg g^{-1} of Basic Blue 3 (Muhammad et al. 2019a), 265 mg g^{-1} of Acid Blue 40 (Muhammad et al. 2019b) or 335 mg g^{-1} of Eosin Y (Majumdar et al. 2019).

Several papers have compared the performance of both dye types. They generally agree that the type does not play a significant role, i.e. the adsorption is not controlled by the ionic interactions. For example, adsorption capacity 467 mg g^{-1} was found for cationic methylene blue and 440 mg g^{-1} for anionic rose bengal dye (Shen et al. 2018). A chemically modified polyaniline adsorbed a cationic dye, crystal violet and an anionic dye, methyl orange, also with comparable capacity, 245 and 220 mg g^{-1}, respectively (Sharma et al. 2016). Polyaniline nanotubes also adsorbed both anionic and cationic dyes, Acid Green 25 (Amer et al. 2018) and methylene blue (Amer et al. 2019a), to similar extent. It can be concluded that the ionic interactions do not play a decisive role in the adsorption on conducting polymers.

Polyaniline base was more efficient in adsorption of anionic dyes than the corresponding protonated form, polyaniline salt (Tanzifi et al. 2017; Aliabad and Mahmoodi 2018). This is associated with higher hydrophobicity of polyaniline base compared with the corresponding salt (Stejskal et al. 2008a). Also various polyaniline salts substantially differ in hydrophobicity depending on the counter-ions (Stejskal et al. 2008a) and, consequently, also in adsorption capacity (Salem 2010).

Polyaniline composites

Polyaniline composites have been often used instead of neat polyaniline in the search of various application forms

Table 4 Dye adsorption on polyaniline composites

Colour index	Dye	Type	Composite component	References
Anionic dyes				
Acid Black 1	Amido Black 10B	azo	Silica	Tanzifi et al. (2018a)
Acid Blue 40	Acid Brilliant Blue RAW	anq	Magnetite	Muhammad et al. (2019b)
Acid Blue 62	Acid Blue 2BR	azo	Alumina	Javadian et al. (2014)
			Silicate MCM-41	Torabinejad et al. (2017) and Binaeian et al. (2018)
Acid Blue 83	Coomassie Brilliant Blue	tpm	Cellulose	Liu et al. (2015)
			Chitosan	Janaki et al. (2012d)
Acid Blue 93	Methyl blue	tpm	Carbon nanotubes/ferrite	Li et al. (2017b)
Acid Green 25	Green GS	azo	Sawdust	Ansari et al. (2011)
Acid Orange 7	Orange II	azo	Aluminium potassium sulfate	Patra and Majhi (2015)
			Kapok fibres	Zheng et al. (2012)
			Rice bran	Bagheri and Mardani (2019)
Acid Orange 10	Orange G	azo	Kapok fibres	Zheng et al. (2012)
Acid Orange 52	Methyl orange	azo	Activated carbon	Hasan et al. (2019)
			Bismuth vanadate	Vidya et al. (2019)
			Carbon nanotubes/ferrite	Li et al. (2017b)
			Cellulose	Bhowmik et al. (2018)
			Graphene oxide	Wang et al. (2018b)
			Copper ferrite	Kharazi et al. (2019)
			Iron/attapulgite	Xu et al. (2019b)
			Iron oxide	Xie et al. (2017)
			Kapok fibres	Herrera et al. (2018)
			Magnetite/carbon nanotubes	Zhao et al. (2013a)
			Magnetite/silica	Mahto et al. (2015)
			Nylon 6	Zarrini et al. (2017)
			Poly(*N*-vinylpyrrolidone)	Prasad and Joseph (2017)
			Pulp waste	Li et al. (2017a)
			Sawdust	Ansari and Mosayebzadeh (2011)
			Titanium dioxide/carbon dots	Feizpoor et al. (2018)
			Zinc oxide	Nerkar et al. (2018)
Acid Red 1	Acid Red G	azo	Sawdust	Lyu et al. (2018)
Acid Red 2	Methyl red	azo	Iron/attapulgite	Xu et al. (2019b)
Acid Red 4	Acid Eosin G	azo	Chitosan	Abbasian et al. (2017b)
			Cellulose	Abbasian et al. (2017a)
Acid Red 14	Acid Red 4B	azo	Yiest	Ahmed et al. (2016)
Acid Red 18	Acid Brilliant Red 4R	azo	Cotton textile	Gamal and Attia (2019)
			Rice husk	Shabandokht et al. (2016)
Acid Red 52	Sulforhodamine B	dbp	Poly(*N*-vinylpyrrolidone)	Gouthaman et al. (2018)
			Poly(*N*-vinylpyrrolidone)/zinc oxide	Gouthaman et al. (2018)
Acid Red 87	Eosin yellow	dbp	Cellulose	Bhowmik et al. (2018)
			Lignocellulose	Debnath et al. (2015b)
Acid Red 94	Rose bengal	dbp	Lignocellulose	Xu et al. (2019c)
Acid Violet 19	Acid fuchsin	tpm	Carbon nanotubes/ferrite	Li et al. (2017b)
			Carboxymethylcellulose/gelatin	Xing et al. (2019)
Acid Violet 90	Bordeaux MB	azo	Clinoptilolite	Akti and Okur (2018)
Acid Yellow 23	Tartrazine	azo	Titanium dioxide	Elsayed and Gobara (2016)
Acid Yellow 23	Tartrazine	azo	Zn-Fe layered double hydroxide	Sahnoun et al. (2018)
Basic Green 1	Brilliant green	tpm	Poly(ethylene oxide)/zinc oxide/silver	Gouthaman et al. (2019)

Table 4 (continued)

Colour index	Dye	Type	Composite component	References
Basic Green 4	Malachite green	tpm	Carbon nanotubes	Zeng et al. (2013)
			Magnetite	Mahto et al. (2014)
			Reduced graphene oxide	Ghahramani et al. (2019)
Basic Orange 2	Basic Orange II	azo	Polyamide	Li et al. (2015)
Direct Blue 199	Direct Blue FBL	ptc	Alumina	Javadian et al. (2014)
Direct Red 23	Direct Red B	azo	Activated carbon	Gopal et al. (2014)
			Cellulose	Abbasian et al. (2017a)
			Chitosan	Abbasian et al. (2017b)
Direct Red 28	Congo red	azo	Carbon nanotubes	Aliabadi and Mahmoodi (2018)
			Chitosan	Janaki et al. (2012d)
			Graphene oxide/carbon nanotubes	Ansari et al. (2017)
			Graphene/poly(vinyl chloride)	Kumar et al. (2015)
			Iron	Bhaumik et al. (2014, 2015)
			Kapok fibres	Zheng et al. (2012)
			Lignocellulose	Debnath et al. (2015a)
			Magnetite/attapulgite	Mu and Wang (2015)
			Magnetite/carbon nanotubes	Zhao et al. (2013a)
			Magnetite/clay	Mu et al. (2016)
			Magnetite/graphene	Mu et al. (2017)
			Molybdenum disulfide	Kumar et al. (2018)
			Molybdenum trioxide	Dhanavel et al. (2016)
			Polystyrene	Gorza et al. (2018)
			Titanium dioxide	Tanzifi et al. (2016)
			Titanium dioxide/carboxymethylcellulose	Tanzifi et al. (2018b)
Food Yellow 3	Sunset Yellow FCF	azo	Carbon nanotubes	Aliabad and Mahmoodi (2018)
Mordant Black 11	Eriochrome Black T	azo	Zirconium(IV) phosphoborate	Kaushal et al. (2018)
			Iron/attapulgite	Xu et al. (2019b)
Mordant Orange 1	Alizarin Yellow R	azo	Iron/attapulgite	Xu et al. (2019b)
Mordant Yellow 10	Acid Chrome Yellow H	azo	Aluminium potassium sulfate	Patra and Majhi (2015)
Reactive Black 5	Remazol Black B	azo	Cellulose	Janaki et al. (2013)
			Lignocellulose	Ballav et al. (2015)
			Magnetite	Hamzehloo et al. (2019)
Reactive Blue 19	Remazol Brilliant Blue R	anq	Bacterial polysaccharide	Janaki et al. (2012a, b)
			Cellulose	Janaki et al. (2013)
			Chitosan	Janaki et al. (2012d)
Reactive Blue 194	Reactive Blue M-2GE	azo	Montmorillonite/starch	Olad et al. (2014)
Reactive Blue 222	Reactive Blue FBN	azo	Chitosan	Sananmuang et al. (2017)
Reactive Orange 4	Reactive Orange M2R	azo	Sawdust	Baseri et al. (2013)
Reactive Orange 16	Remazol Brilliant Orange 3R	azo	Bacterial polysaccharide	Janaki et al. (2012a)
			Cellulose	Janaki et al. (2013)
			Chitosan/zinc oxide	Pandiselvi and Thambidurai (2013) and Kannusamy and Sivalingam (2013)
			Mesoporous silica	Aghajani and Tayebi (2017)
Reactive Red 2	Reactive Brilliant Red X-3B	azo	Bentonite	Tie et al. (2017)
			Petaline/NiO	Zhong et al. (2018)
Reactive Red 194	Reactive Brilliant Red M-2BE	azo	Alumina	Javadian et al. (2014)
Reactive Red 195	Reactive Red 3BS	azo	Chitosan	Sananmuang et al. (2017)
Reactive Red 198	Reactive red RB	azo	Magnetite	Tayebi et al. (2016)

Table 4 (continued)

Colour index	Dye	Type	Composite component	References
Reactive Violet 5	Remazol Brilliant Violet 5R	azo	Cellulose	Janaki et al. (2013)
Reactive Yellow 145	Reactive Yellow 3RS	azo	Chitosan	Sananmuang et al. (2017)
Cationic dyes				
Basic Blue 3	Cationic Blue SD-GB	poz	Magnetite	Muhammad et al. (2019a)
Basic Blue 9	Methylene blue	thz	Aluminium potassium sulfate	Patra and Majhi (2015)
			Carbon nitride	Zhang et al. (2014)
			Chitosan	Janaki et al. (2012d)
			Cotton	Fan et al. (2017)
			Graphene oxide	Wang et al. (2018b)
			Iron/attapulgite	Xu et al. (2019b)
			Kapok fibres	Mu et al. (2015)
			La/Cd bimetal	Sharma et al. (2015)
			Magnetite/attapulgite	Mu and Wang (2015)
			Magnetite/clay	Mu et al. (2016)
			Nickel ferrite	Patil and Shrivastava (2016) and Singh et al. (2019)
			Phytic acid	Yan et al. (2015)
			Poly(*N*-vinylpyrrolidone)	Prasad and Joseph (2017)
			Silica	Ayad et al. (2012)
			Sodium nitroprusside	Rafiqi and Majid (2017)
			Titanium dioxide/graphene	Kumar et al. (2016)
			Xanthan gum	Tanzifi et al. (2019)
			Zinc oxide/seaweed	Pandimurugan and Thambidurai (2016)
			Zirconium dioxide	Agarwal et al. (2016)
			Zirconium(IV) phosphoborate	Kaushal et al. (2018)
			Zirconium(IV) silicophosphate	Gupta et al. (2014)
Basic Green 1	Brilliant green	tpm	Magnetite/clay	Mu et al. (2016)
			Magnetite/graphene	Mu et al. (2017)
			Plant leaves	Kanwal et al. (2018)
			Silver	Salem et al. (2016)
Basic Red 5	Neutral red	phz	Zirconium(IV) phosphoborate	Kaushal et al. (2018)
Basic Violet 3	Crystal violet	tpm	Peanut hull	Tahir et al. (2017)
			Zirconium(IV) phosphoborate	Kaushal et al. (2018)
Basic Violet 10	Rhodamine B	dbp	Activated carbon	Gopal et al. (2016)
			Aluminium potassium sulfate	Patra and Majhi 2015
			Iron	Guo et al. (2016)
			Iron/attapulgite	Xu et al. (2019b)
			Iron oxide	Xie et al. (2017)
			Magnetite/ionic liquid	Shahriman et al. (2018)
			Molybdenum trioxide	Dhanavel et al. (2016)

(Table 4). Table 4 is ordered by the adsorbed dyes, the following text by the type of adsorbents. The composites contained up to three components as a rule: (1) a conducting polymer, (2) a polymer providing the processability or mechanical support and (3) an inorganic part, which had independent adsorption ability or another value-added property, such as magnetic one. Comparison of the reported data is possible only on the relative basis because the adsorption on the individual composite components had often been missing, as well as the composition of composites.

The composites are classified by the type of a non-conducting component as follows:

Ag Polyaniline decorated with silver nanoparticles using the reductive properties of this conducting polymer on silver

Fig. 19 Illustration of a conducting polymer cryogel containing ferrite particles (left). Magnetic aerogel obtained after freeze-drying is attracted to a magnet (right) (Islam Minisy, unpublished results)

ions was applied for the adsorption of brilliant green (Salem et al. 2016; Gouthaman et al. 2019). The presence of silver hardly affected the adsorption behaviour but should have other, e.g., antibacterial value-added properties.

Al Polyaniline/aluminium potassium sulfate adsorbed the anionic dyes with a preference compared with cationic ones (Patra and Majhi 2015). Polyaniline/alumina composite was tested for adsorption of various anionic dyes (Javadian et al. 2014).

Bi Bismuth vanadate particles coated with polyaniline were reported to be an efficient adsorbent of methyl orange (Vidya and Balamurugan 2019b; Vidya et al. 2019). The composite performed better than polyaniline alone.

C Carbon in various forms was often present in the composites. The deposition of polyaniline on activated carbon provided the adsorbent of methyl orange with the maximum capacity 285 mg g^{-1}. The coating of carbon nanotubes with polyaniline improved the adsorption of malachite green compared with neat polyaniline (Zeng et al. 2013). Here, the nanotubes afforded the high specific surface area. Polyaniline/graphene oxide efficiently adsorbed cationic methylene blue at 962 mg g^{-1} capacity as well as anionic methyl orange, 885 mg g^{-1}, the high specific surface area being again of benefit (Wang et al. 2018b). The fact that both cationic and anionic dyes were adsorbed in comparable amounts again suggests the limited role of the electrostatic interactions over, e.g., π–π ones. Polyaniline/graphene oxide composite adsorbed cationic dyes, malachite green and rhodamine G, or anionic dye, Congo red, practically completely within tens of minutes (Mitra et al. 2019). Polyaniline-coated graphene oxide/multiwall carbon nanotubes composite adsorbed Congo red and simultaneously reduced Cr(VI) ions (Ansari et al. 2017). Finally, polyaniline/reduced graphene oxide afforded maximum adsorption capacity of 667 mg g^{-1} for a cationic dye, malachite green (Ghahramani et al. 2019).

Fe The incorporation of magnetic component, such as iron, iron oxides, magnetite or ferrites, may be conveniently used in the separation of adsorbent by magnetic field (Fig. 19). Polyaniline/iron composite was tested in the removal of Congo red (Bhaumik et al. 2014, 2015) and rhodamine B (Guo et al. 2016) from aqueous medium. Polyaniline/iron/attapulgite composite adsorbed preferentially azo dyes than non-azo type (Xu et al. 2019b). Polyaniline/iron oxide adsorbed both anionic and cationic dyes, methyl orange and rhodamine B (Xie et al. 2017). Magnetite coated with polyaniline was used for the removal of Acid Blue 40 (Muhammad et al. 2019b), Basic Blue 3 (Muhammad et al. 2019a), brilliant green (Mu et al. 2016, 2017), malachite green (Mahto et al. 2014), methylene blue (Zhao et al. 2013a; Mu and Wang 2015; Mu et al. 2016, 2017), methyl orange (Zhao et al. 2013a; Mahto et al. 2015), Reactive Red 198 (Tayebi et al. 2016), Reactive Black 5 (Hamzehloo et al. 2019) and rhodamine B (Shahriman et al. 2018). Adsorption capacities up to 400 mg g^{-1} were reported (Zhao et al. 2013a). A similar composite with copper ferrite adsorbed up to 346 mg g^{-1} of methyl orange (Kharazi et al. 2019). The adsorption of methylene blue on polyaniline/nickel ferrite, however, was reported to be only 6.6 mg g^{-1} (Patil and Shrivastava 2016; Singh et al. 2019). The composite with sodium nitroprusside also falls into the category of iron compounds (Rafiqi and Majid 2017) and was used for the removal of methylene blue.

Mo Polyaniline/molybdenum disulfide removed Congo red from the aqueous medium (Kumar et al. 2018) with adsorption capacity reaching 71 mg g^{-1}. The composite with molybdenum trioxide adsorbed up to 36 mg g^{-1} of cationic rhodamine B and 76 mg g^{-1} of anionic Congo red (Dhanavel et al. 2016).

Ni Polyaniline/petaline/NiO was proved to be an efficient absorbent of Reactive Brilliant Red X-3B (Zhong et al. 2018).

Si This group is represented by traditional adsorbents such as silica, silicates and aluminosilicates. Polyaniline/silica rapidly removed Amido Black 10B (Tanzifi et al. 2018a) or Reactive Orange 16 (Aghajani and Tayebi 2017) from aqueous solutions. Polyaniline base/silica adsorbed 5 mg g^{-1} of methylene blue (Ayad et al. 2012). The highest capacity of polyaniline/mesoporous silicate for Acid Blue 62 adsorption was 55 mg g^{-1} (Torabinejad et al. 2017; Binaeian et al. 2018). Polyaniline/clinoptilolite composite had a higher adsorption capacity of Acid Violet 90, 72 mg g^{-1} (Akti and Okur 2018) and a composite with bentonite adsorbed 202–258 mg g^{-1} of Reactive Red 2 (Tie et al. 2017). Polyaniline/starch/montmorillonite was tested for adsorption of Reactive Blue 194 with 92 mg g^{-1} capacity (Olad et al. 2014).

Ti Titanium oxide is widely used as a photocatalyst but its composites were tested also for adsorption. Titanium dioxide coated with polyaniline adsorbed tartrazine dye (Elsayed and Gobara 2016) or Acid Red G (Wang et al. 2015a). The adsorption capacity of latter dye reached 455 mg g^{-1}. The composite performed better than the individual components alone. Polyaniline/carboxymethylcellulose/titanium(IV) oxide adsorbed Congo red (Tanzifi et al. 2018b).

Zn The polyaniline-coated zinc oxide removed methyl orange from the aqueous medium more efficiently than any of the components alone (Nerkar et al. 2018), displaying again the marked synergistic effect. Polyaniline/poly(ethylene oxide) composite was mixed with zinc oxide/silver nanoparticles and subsequently used in the removal of brilliant green with maximum 95 mg g^{-1} capacity (Gouthaman et al. 2018, 2019).The composite with zinc oxide and seaweed was used for the adsorption of methylene blue (Pandimurugan and Thambidurai 2016). Finally, the ternary composite polyaniline/chitosan/zinc oxide adsorbed up to 476 mg g^{-1} of Reactive Orange 16 (Kannusamy and Sivalingam 2013). The adsorption capacity of tartrazine on polyaniline/Zn-Fe double hydroxides reached 488 mg g^{-1} (Sahnoun et al. 2018).

Zr Polyaniline/zirconium(IV) silicophosphate (Gupta et al. 2014) adsorbed methylene blue; a similar phosphoborate (Kaushal et al. 2018) adsorbed both anionic and cationic dyes. The typical capacities were of the order of tens mg g^{-1} (Gupta et al. 2014; Herrera et al. 2018). The composite performed better than neat polyaniline; the non-conducting component alone might have been an efficient adsorbent. On the contrary, adsorption of polyaniline/zirconium dioxide was less efficient compared to polyaniline alone (Agarwal et al. 2016).

Natural polymers Cellulose in various forms has often been used as a support for conducting polymers. Filter paper coated with polyaniline adsorbed well Coomassie Brilliant Blue (Liu et al. 2015). Polyaniline/cellulose (cotton linters) adsorbed 117 mg $g^{-1}$of Acid Red 4 or 56 mg g^{-1} Direct Red 23 (Abbasian et al. 2017a). Cotton textile coated with polyaniline was used for the removal of Acid Red 18 (Gamal and Attia 2019). Other authors used the composite with cellulose (Janaki et al. 2013), bacterial polysaccharide (Janaki et al. 2012a, b), starch (Janaki et al. 2012c; Olad et al. 2014) or chitosan (Janaki et al. 2012d; Abbasian et al. 2017b) for the adsorption of reactive dyes and typical adsorption capacities were 100 mg g^{-1}. Polyaniline/lignocellulose composite had maximum adsorption capacity 312 mg g^{-1} of Reactive Black 5 (Ballav et al. 2015) or as high as 1673 mg g^{-1} for Congo red (Debnath et al. 2015a). The composite was also tested for the adsorption of eosin yellow (Debnath et al. 2015b). Exceptionally high capacities up to 10,560 mg g^{-1} have been observed for adsorption of Acid Red 94 on polyaniline/calcium lignosulfonate composite (Xu et al. 2019c). Such result, however, would need independent verification. The polyaniline/chitosan composite adsorbed both anionic and cationic dyes (Minisy et al. 2019b). Polyaniline containing carboxymethylcellulose/gelatin hydrogel selectively adsorbed acid fuchsin compared with other dyes (Xing et al. 2019).

There was the obvious trend to convert various organic waste products into useful adsorbents for water-pollution treatment (Suba and Rathika 2016), e.g., by in-situ deposition of conducting polymers. Polyaniline-coated kapok fibres adsorbed 41–192 mg g^{-1} of various dyes (Zheng et al. 2012; Mu et al. 2015) and 76 mg g^{-1} of methyl orange (Herrera

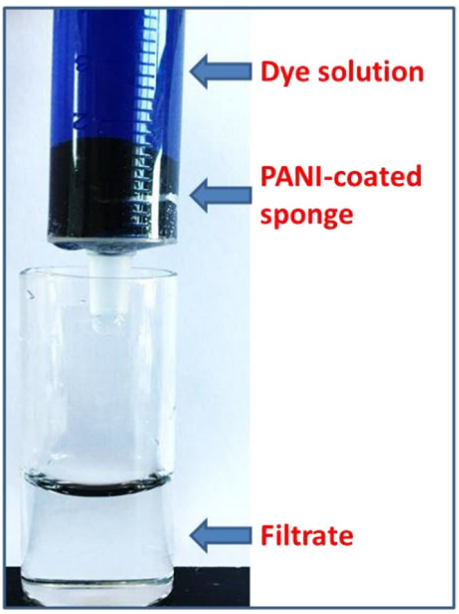

Fig. 20 Dye removal by spontaneous filtration of Reactive Black 5 solution (50 ppm) through polyaniline-coated polyurethane sponge (Wei Lyu, unpublished results)

et al. 2018). Sawdust coated with polyaniline adsorbed Acid Green 25 (Ansari et al. 2011), up to 144 mg g^{-1} Reactive Orange 4 (Baseri et al. 2013), methyl orange (Ansari and Mosayebzadeh 2011) or 213 mg g^{-1} of Acid Red G (Lyu et al. 2018). Peanut-hull waste coated with polyaniline was used as adsorbent of crystal violet (Tahir et al. 2017) and plant leaves for adsorption of diamond green (Kanwal et al. 2018). The biomass of Scenedesmu strain combined with polyaniline proved to be a good adsorbent of Reactive Red 120 with the capacity reaching 753 mg g^{-1} (Maqbool et al. 2019). Polyaniline/seaweed was tested for adsorption of methylene blue (Pandimurugan and Thambidurai 2016). Another natural material, rice husk, modified with polyaniline adsorbed Acid Red 18 (Shabandokht et al. 2016), rice bran was used for adsorption of Acid Orange 7. Polyaniline-coated activated carbon produced from natural organic material removed Direct Red 23 (Gopal et al. 2014) or rhodamine B (Gopal et al. 2016) from the aqueous solution. Polyaniline/xanthan gum composite similarly adsorbed maximum 22 mg g^{-1} of methylene blue (Tanzifi et al. 2019).

Synthetic polymers The composites of conducting polymers with another synthetic polymer have been studied only exceptionally, electrospun polyaniline/polystyrene mats being an example applied for efficient Congo red removal (Gorza et al. 2018) and polyaniline/polyester fabrics for Acid Red 18 separation (Gamal and Attia 2019). Poly(ethylene oxide) was a component in a complex composite used for the adsorption of brilliant green (Gouthaman et al. 2019). Polyaniline deposited on polyamide nanofibres had capacity up to 370 mg g^{-1} for methyl orange adsorption (Zarrini et al. 2017). Polyaniline particles stabilized with poly(*N*-vinylpyrrolidone) removed methyl orange from the aqueous solution completely (Prasad and Joseph 2017); methyl orange was removed selectively from the mixture with methylene blue. An original approach is represented by the filtration of a dye solution through the polyurethane sponge coated with polyaniline (Fig. 20). Polyaniline hydrogel prepared with the assistance of phytic acid removed methylene blue from the aqueous media at the maximum adsorption capacity 71 mg g^{-1} (Yan et al. 2015).

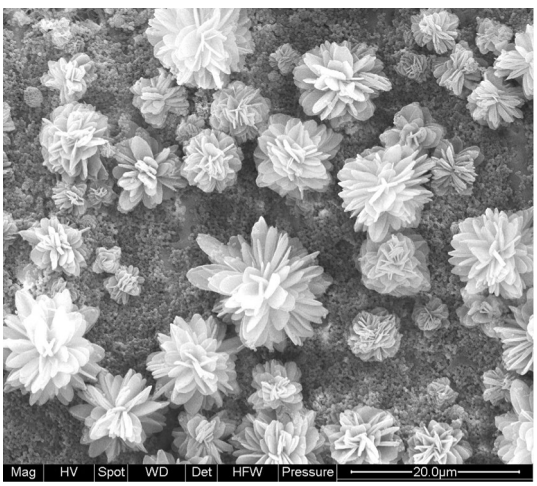

Fig. 21 Flower-like morphology of aniline oligomers (Yanchai Zhao, unpublished results)

Polyaniline-related materials

In addition to polyaniline alone and its composite, related materials are considered: (1) aniline oligomers, (2) polymers of substituted anilines, (3) aniline copolymers, (4) chemically modified polyaniline and (5) carbonized polyanilines. They are all poorly conducting compared with polyaniline but that does not disqualify them for the good position among adsorbents.

The oxidation of aniline under specific conditions yields *aniline oligomers* with a spectacular flower-like (Zhao et al. 2013b) (Fig. 21) or urchin-like morphology (Zhao et al. 2013c). Such oligomers are also able to act as dye adsorbents and 181 mg g^{-1} capacity was reported was for crystal violet (Zhou et al. 2015). The oligomeric oxidation product of *p*-aminodiphenylamine adsorbed anionic dye of anthraquinone type, alizarin red S, as a simple model compound mimicking polyaniline (Liu et al. 2018a). Classical aniline oligomers prepared by the oxidation of aniline under alkaline conditions (Stejskal et al. 2008b) have not been so far tested as adsorbents.

Substituted polyanilines have been used in adsorption experiments only rarely. Poly(*N*-methylaniline)/cellulose and poly(*N*-ethylaniline)/cellulose composites adsorbed anionic azo dyes, Acid Red 4 and Direct Red 23, but less than polyaniline analogue (Abbasian et al. 2017a). Poly(chitosan-*graft*-*N*-metylaniline) adsorbed these dyes at 98 and 112 mg g^{-1} maximum capacity, respectively (Abbasian et al. 2017b). Poly(*o*-methylaniline), poly(*m*-methylaniline) and poly(*N*-methylaniline) prepared similarly in the presence of chitosan were used for the adsorption of Reactive Red 198 (Sayyah et al. 2015).

The oxidation products of phenylenediamine isomers, polyphenylenediamines (Stejskal 2015), represent a promising class of eco-friendly adsorbents due to the similarity of the molecular structure. In contrast to polyaniline, they are non-conducting or their conductivity is low. For simple applications in adsorption, however, this does not seem to be a drawback. *Poly(o-phenylenediamine)*/ferrite composites served for the adsorption of Congo red, as well as for removal of lead(II) and chromium(III) ions (Archana et al. 2016). *Poly(m-phenylenediamine)* alone was reported to have outstanding adsorption capacity up to 470 mg g^{-1} Orange G (Zhang et al. 2012; Meng et al. 2014). Another adsorbent, poly(*m*-phenylenediamine)/graphene oxide/nickel ferrite was tested on Congo red, methyl orange and methyl

Table 5 Dye adsorption on polypyrrole

Colour index	Dye	Type	References
Anionic dyes			
Acid Blue 74	Indigo carmine	ind	Zhou et al. (2017)
Acid Orange 10	Orange G	azo	Zhou et al. (2017)
Acid Orange 52	Methyl orange	azo	Ye et al. (2019b)
Acid Red 1	Acid Red G	azo	Feng et al. (2014)
Acid Red 27	Amaranth	azo	Zhou et al. (2017)
Direct Red 28	Congo red	azo	Chafai et al. (2017a) and Zhou et al. (2017)
Solvent Yellow 14	Sudan Orange G	azo	Ren et al. (2018)
Cationic dyes			
Basic Blue 9	Methylene blue	ptz	Zhou et al. (2017), Maruthapandi et al. (2018) and Yao et al. (2018)
Basic Green 4	Malachite green	tpm	Zhou et al. (2017)

blue (Wang et al. 2017). Poly(*m*-phenylenediamine)/dextrin/graphene oxide composite was found to adsorb methylene blue at 76 mg g^{-1} capacity (Zare et al. 2018b), i.e. much less than polymer alone. *Poly(p-phenylenediamine)* nanocomposite with magnetite adsorbed bromocresol blue, methyl orange (Yang et al. 2014) and Reactive Blue 19 (Liu et al. 2016).

Aniline copolymers are represented by poly(aniline-*co*-anthranilic acid)/magnetite composite which adsorbed both anionic and cationic dyes, methyl red and methylene blue, respectively (Zoromba et al. 2017). The comonomer, anthranilic acid (*o*-aminobenzoic acid), introduced reactive carboxylic groups and ferromagnetic component allows for the easier separation of adsorbent. Simultaneous oxidation of aniline and pyrrole was reported to produce interconnected polyaniline/polypyrrole nanofibres (Bhaumik et al. 2013) but, in fact, they were rather statistical copolymers of aniline and pyrrole (Stejskal et al. 2004b). They nevertheless adsorbed up to 270 mg g^{-1} of Congo red (Bhaumik et al. 2013).

Polyaniline *chemically modified* with diiodomethane, which caused cross-linking of polyaniline chains, was reported to have a high specific surface area 1083 m^2g^{-1} (Sharma et al. 2016). It adsorbed a cationic dye, crystal violet and an anionic dye, methyl orange, to comparable extent, 245 and 220 mg g^{-1}, respectively.

Polyaniline converts to a nitrogen-containing carbon when exposed to ca. 500–600 °C in inert atmosphere (Trchová et al. 2009; Ćirić-Marjanović et al. 2013). Such materials could be used as dye adsorbents but the studies in this direction are so far missing.

Polypyrrole

The adsorption of dyes on polypyrrole alone (Table 5) has been studied only exceptionally within the testing of polypyrrole composites. For example, the adsorption of methylene blue on polypyrrole was 19.3 mg g^{-1} (Maruthapandi et al. 2018) or 11.2 mg g^{-1} (Zhou et al. 2017). Other dyes, such as malachite green, amaranth, Acid Orange 10, Congo red or indigo carmine were adsorbed marginally at 10–20 mg g^{-1} capacity (Zhou et al. 2017). Polypyrrole proved to be a potent adsorbent for Acid Red G, the maximum capacity being 122 mg g^{-1} (Feng et al. 2014) and for Congo red (Chafai et al. 2017a). The highest adsorption capacity, 237 mg g^{-1}, was reported for methyl orange (Ye et al. 2019b). It should be recalled that this dye plays the most important role in the synthesis of polypyrrole nanotubes (vide supra) when methyl orange becomes incorporated into polymer structures.

Polypyrrole composites

On the other hand, the adsorption of dyes on polypyrrole composites has been reported in a number of papers (Table 6). Enhanced adsorption has been typically observed after in situ deposition of polypyrrole on various substrates, and synergistic adsorption effect has been noted (Zeng et al. 2013; Nerkar et al. 2018; Chen et al. 2019b). It seems that more ordered polypyrrole brushes constituting the coating are better adsorbents compared with disordered globular form (Fig. 13).

Depending on the type of the non-conducting substrates the composites may be organized as follows:

Al Alumina coated with polypyrrole adsorbed up to 135 mg g^{-1} of methylene blue (Chen et al. 2016).

C The composite of polypyrrole-coated carbon nanotubes performed better than polypyrrole alone in the adsorption of Sunset Yellow FCF and Congo red (Aliabad and Mahmoodi 2018). Adsorption of Acid Orange 7 on polypyrrole/activated carbon was also investigated (Supriya and Palanisamy 2016). Electropolymerized polypyrrole/graphene oxide

Table 6 Dye adsorption on polypyrrole composites

Colour index	Dye	Type	Composite component	References
Anionic dyes				
Acid Blue 62	Acid Blue 2BR	anq	Silica	Akhbartabar et al. (2017)
			MCM-41 silicate	Binaeian et al. (2018)
Acid Blue 74	Indigo carmine	ind	Lignin, lignosulfonate	Zhou et al. (2017)
Acid Blue 193	Neutral Blue M-TR	azo	Polyester membrane/zeolite	Ghaemi and Safari (2018)
Acid Green 1	Naphthol Green B	–	Attapulgite/iron	Chen et al. (2019a)
Acid Orange 7	Orange II	azo	Activated carbon	Supriya and Palanisamy (2016)
Acid Orange 10	Orange G	azo	Lignin, lignosulfonate	Zhou et al. (2017)
Acid Orange 52	Methyl orange	azo	Halloysite nanotubes	Zhang et al. (2018)
			Silica	Boukoussa et al. (2018)
Acid Red 1	Acid Red G	azo	Graphene oxide	Haque and Wong (2017)
			Magnetite/TiO_2	Feng et al. (2017)
			Titanium dioxide	Li et al. (2012), Wang et al. (2015b) and Li et al. (2019b)
Acid Red 18	Ponceau 4R	azo	Chitosan	Chen et al. (2019b)
			Chitosan/graphene oxide	Salahuddin et al. (2018)
Acid Red 27	Amaranth	azo	Lignin, lignosulfonate	Zhou et al. (2017)
Direct Green 6	Direct Green BG	azo	Activated carbon/plant fruit	Geetha and Palanisamy (2016)
Direct Red 28	Congo red	azo	Ferrite	Aigbe et al. (2018)
			Lignin, lignosulfonate	Zhou et al. (2017)
			Poly(vinylidene fluoride)	Ma et al. (2018)
			Silver nanoparticles	Yihan et al. (2018)
			Zinc ferrite	Karamipour et al. (2016)
			Zinc oxide	Karamipour et al. (2016)
Mordant Red 3	Alizarin Red S	ant	Magnetite	Gholivand et al. (2015)
Mordant Yellow 1	Alizarin Yellow GG	azo	Magnetite	Gholivand et al. (2015)
Reactive Black 5	Remazol Black B	azo	Cellulose/magnetite	Diaz-Flores et al. (2019)
Reactive Blue 4	Reactive Brilliant Blue X-BR	anq	Cellulose/graphene oxide	Ali et al. (2018)
			Polyester membrane/zeolite	Ghaemi and Safari (2018)
Reactive Blue 19	Remazol Brilliant Blue R	azo	Magnetite	Shanehsaz et al. (2015)
Reactive Violet 5	Remazol Brilliant Violet 5R	azo	Sawdust	Supriya and Palanisamy (2017)
Cationic dyes				
Basic Blue 9	Methylene blue	ptz	Alumina	Chen et al. (2016)
			Cellulosic waste	Ovando-Medina et al. (2014)
			Cotton	Ayad et al. (2018a)
			Lignin, lignosulfonate	Zhou et al. (2017)
			Magnetite	Chen et al. (2016) and Yao et al. (2018)
			Magnetite/graphene	Bai et al. (2015)
			Poly(vinylidene fluoride)	Ma et al. (2018)
			Silica	Chen et al. (2016) and Boukoussa et al. (2018)
			Silver nanoparticles	Yihan et al. (2018)
			Titanium dioxide	Li et al. (2013, 2019b)
Basic Green 1	Brilliant green	tpm	Zinc oxide	Zhang et al. (2019c)
Basic Green 4	Malachite green	tpm	Lignin, lignosulfonate	Zhou et al. (2017)
Basic Violet 1	Methyl violet	tpm	Magnetite	Yao et al. (2018)
			Polyester membrane/zeolite	Ghaemi and Safari (2018)
Basic Violet 3	Crystal violet	tpm	Peanut hull	Tahir et al. (2017)
Basic Violet 10	Rhodamine B	dbp	Coffee ground waste	Ovando-Medina et al. (2018)
			Magnetite	Yao et al. (2018)
			Silver nanoparticles	Yihan et al. (2018)

Table 6 (continued)

Colour index	Dye	Type	Composite component	References
Direct Red 28	Congo red	azo	Titanium dioxide	Tanzifi et al. (2016)
Reactive Red 120	Reactive Brilliant Red KE-4B	azo	Cellulose	Ovando-Medina et al. (2015b)

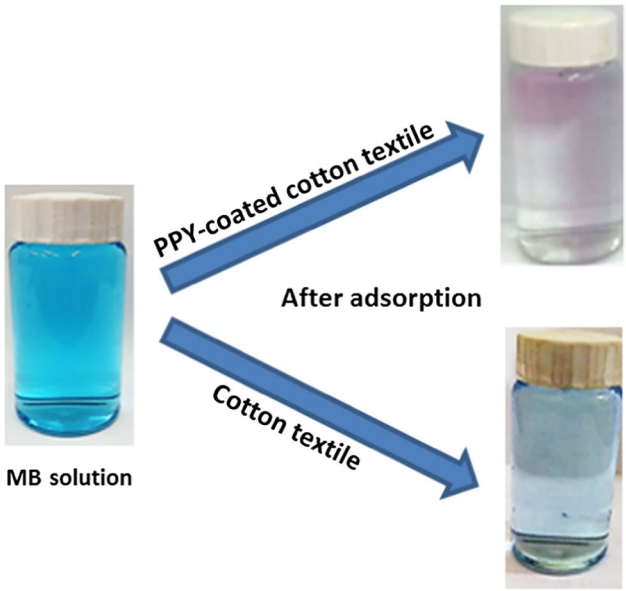

Fig. 22 The colouration of methylene blue solution decreases after the introduction of cotton textile and disappears when the textile was coated with polypyrrole (Ayad et al. 2018a)

allowed for the adsorption of Acid Red 1 and its controlled liberation (Haque and Wong 2017).

Fe The composites containing ferrite or other ferromagnetic particles have been proposed as adsorbents separable by the magnetic field. Adsorptivity of anionic Congo red, 120 mg g^{-1}, was found for polypyrrole/ferrite composite (Karamipour et al. 2016; Aigbe et al. 2018), while polypyrrole/magnetite adsorbed only 23 mg g^{-1} of cationic rhodamine B (Yao et al. 2018), but 116 mg g^{-1} of alizarine (Gholivand et al. 2015). The adsorption capacity of methylene blue, methyl orange or acid fuchsin on polypyrrole/carbon nanotubes/ferrite was 110–140 mg g^{-1} (Li et al. 2017c). Magnetite has also constituted a part of similar polypyrrole composites (Bai et al. 2015; Shanehsaz et al. 2015; Chen et al. 2016; Feng et al. 2017; Diaz-Flores et al. 2019).

Si Silicates have been used as substrates for polypyrrole coating. The high adsorption capacities exceeding 1000 mg g^{-1} were reported only exceptionally, e.g., 1429 mg g^{-1} for Acid Blue 62 on polypyrrole-coated mesoporous silica SBA-15 (Akhbartabar et al. 2017). The adsorption capacity of the same dye on polypyrrole/mesoporous MCM-41 was only 55 mg g^{-1} (Binaeian et al. 2018). Another study announced the adsorption capacity 215 mg g^{-1} for methyl orange on polypyrrole/halloysite (Zhang et al. 2018). Polypyrrole-modified attapulgite clay served for the adsorption of Naphthol Green B (Chen et al. 2019a).

Ti Titanium dioxide coated with polypyrrole was used as an adsorbent of Acid Red G (Li et al. 2012, 2019b) or methylene blue (Li et al. 2013, 2019b), and the adsorption capacities up to 425 and 440 mg g^{-1} were determined, respectively.

Zn Polypyrrole-coated zinc oxide adsorbed brilliant green up to 140 mg g^{-1} (Zhang et al. 2019c) or Congo red (Karamipour et al. 2016).

Natural polymers Polypyrrole deposited in situ on natural polymers ranks among the most studied composites, similarly like polyaniline, cellulose being the polymer of the choice. The conducting polymers deposited on cotton textile represent one of suitable forms of adsorbents (Fan et al. 2017; Ayad et al. 2018a). The sorption capacity for methylene blue was lower for polypyrrole/cotton composite, 6.63 mg g^{-1}, due to reduced amount of polypyrrole (Ayad et al. 2018a) but was more efficient in other experiments (Fan et al. 2017). Cotton alone was an adsorbent but its adsorptivity increased after the coating with polypyrrole (Fig. 22). Cellulosic waste was similarly coated with polypyrrole and the composite adsorbed 68 mg g^{-1} of a dye (Ovando-Medina et al. 2014). A similar material, sawdust coated with polypyrrole, adsorbed Reactive Violet 5 at 10–13 mg g^{-1} capacity (Supriya and Palanisamy 2017). The polypyrrole-coated peanut hull biomass was tested for adsorption of crystal violet (Tahir et al. 2017). Other authors have successfully used chitosan and lignosulfonate as supports for polypyrrole coating (Zhou et al. 2017). The composites were generally better adsorbents than polypyrrole alone. The combination of activated carbon with fruit of gardening plant was tested for adsorption of Direct Green 6 (Geetha and Palanisamy 2016). The polypyrrole/chitosan composites served as model adsorbents of Acid Red 18 (Chen et al. 2019b).

Synthetic polymers Polypyrrole/poly(vinylidene fluoride) adsorption capacity reached 370 mg g^{-1} for cationic methylene blue and 385 mg g^{-1} for anionic Congo red (Ma et al. 2018), again illustrating the independence on the dye type. The filtration of dye solution (50 mg L^{-1}) through polyester membrane coated with polypyrrole completely removed both the anionic and cationic dyes (Ghaemi and Safari 2018). Electrospun polyamide mats coated with polypyrrole served for the adsorption of Basic Orange 2 (Li et al. 2015).

Polypyrrole-related materials

The materials based of substituted polypyrroles have not been so far investigated and this section is limited to carbonized polypyrrole. Polypyrrole nanotubes prepared by standard method using methyl orange template were converted to nitrogen-containing carbon nanotubes by pyrolysis in inert atmosphere (Ćirić-Marjanović et al. 2014; Kopecká et al. 2016; Sapurina et al. 2016; Xin et al. 2017; Kang et al. 2019; Minisy et al. 2019c). Such carbonaceous material has been tested for adsorption of methylene blue, rhodamine B, Congo red and Orange G with adsorption capacities 609, 572, 151 and 122 mg g^{-1}, respectively (Xin et al. 2017).

Photocatalytic decomposition of dyes

In addition to adsorbents, the photocatalytic degradation of dyes in the presence of conducting polymers has often been reported in environmental issues, such as water-pollution treatment. Recent developments in this direction have been reviewed (Lee and Chang 2019) and the synergistic effect between semiconducting inorganic substrates and conducting polymers has been noted. In photocatalytic experiment, the dye removal by adsorption in dark is improved by the subsequent photocatalytic decomposition of adsorbed dye under illumination (Wei et al. 2015; Lakshmi and Rajagopalan 2016; Abukhadra et al. 2018c). The process is based on the catalytic generation of reactive hydroxyl radicals from oxygen, reactive oxygen species, from water molecules during the illumination by visible light or UV-irradiation on heterogeneous substrates, typically on metal oxides (Sushma and Kumar 2017; Abukhadra et al. 2018a; Samai and Bhattacharya 2018; Sobhani-Nasab et al. 2019). The reaction of the active species with organic dyes thus results in the dye modification, degradation or decomposition. Conducting polymers are good absorbents of light in UV–visible region and this fact is probably of importance in the photocatalytic effect supported by these polymers.

From the environmental point of view, the reduction or disappearance of coloration, sometimes called decolorization (Phan et al. 2017), is correctly interpreted as the dye decomposition but that does not mean that the potentially harmful reaction products have been removed. The degradation products have been sometimes identified by liquid chromatography/mass spectrometry (Wei et al. 2015). The degradation of a dye molecule need not be complete, because the destruction even of a single bond only in dye molecule may result in the loss of conjugation and conversion to a colourless compound. It should also be noted that the reverse process illustrated by the photocatalytic oxidative coupling of molecules may take place in the presence of conducting polymers (Kong et al. 2019a). The chemistry of the photocatalytic processes thus offers stimulating field of future studies.

The coating of various metal oxides that are active in photocatalysis of dye decomposition (Janaki et al. 2012d) is expected to improve the adsorption of dyes that is a prerequisite for the subsequent catalytic performance. In addition, the electroactivity of conducting polymers enables them to participate in electron transfers between the dyes and a catalyst that is necessary for the degradation reaction. Such role of conducting polymers to act in electron and proton transfers is also well known in corrosion protection of metals (Yang et al. 2015; Kohl et al. 2017; Sazou and Deshpande 2017; Umoren and Solomon 2019).

Polyaniline

Polyaniline alone was active in photocatalysis of dyes as a photosensitizer (Table 7). The synergistic photocatalytic effect was clearly demonstrated also for the composites,

Table 7 Photocatalytic decomposition of dyes on polyaniline

Colour index	Dye	Type	References
Anionic dyes			
Acid Blue 92	Anazolene	azo	Pirkarami et al. (2013)
Acid Orange 2	Acid Orange 2	azo	Pirkarami et al. (2013)
Acid Orange 7	Orange II	azo	An et al. (2018)
Acid Orange 52	Methyl orange	azo	Salavati and Kohestani (2013), Zhang et al. (2014) and Chatterjee et al. (2019)
Acid Red 88	Acid Red A	azo	Pirkarami et al. (2013)
Reactive Red 2	Reactive Brilliant Red X-3B	azo	Tang et al. (2019a)
Cationic dyes			
Basic Blue 9	Methylene blue	thz	Salavati and Kohestani (2013) and Vidya and Balamurugan (2019a)
Basic Green 4	Malachite green	tpm	Chatterjee et al. (2019)
Basic Red 2	Safranin	phz	Abukhadra et al. (2018a)
Basic Violet 10	Rhodamine B	dbp	Salavati and Kohestani (2013) and Zeng et al. 2016; Chatterjee et al. (2019)

Table 8 Photocatalytic decomposition of dye on polyaniline composites

Colour index	Dye	Type	Composite component	References
Anionic dyes				
Acid Blue 25	Acid Brilliant Blue R	anq	Manganese dioxide	Gemeay et al. (2012)
		anq	Zinc oxide	Gilja et al. (2018)
Acid Blue 74	Indigo carmine	ind	Ferrite	Bashir et al. (2019)
Acid Blue 90	Brilliant blue	tpm	Titanium dioxide	Ansari et al. (2015)
Acid Green 5	Light Green SF	tpm	Heulandite zeolite	Abukhadra et al. (2018c)
Acid Orange 7	Orange II	azo	Ferrite	Pant et al. (2018)
Acid Orange 10	Orange G	azo	Titanium dioxide/chitosan	Mahanta et al. (2011b)
Acid Orange 52	Methyl orange	azo	Bismuth oxychloride	Wang et al. (2013b, 2019d)
			Bismuth oxyiodide/zinc oxide/magnetite	Habibi-Yangjeh and Shekofteh-Gohari (2019)
			Bismuth selenide	Chatterjee et al. (2019)
			Carbon nitride	Zhang et al. (2014)
			Graphene/wolframate	Biswas et al. (2019)
			Ferrite	Arshadnia et al. (2017), Kim et al. (2017) and Jung et al. (2019)
			Ferrite/bismuth oxychloride	Tanwar and Mandal (2019)
			Magnesium indium sulfide	Jing et al. (2019)
			Magnetite	Wang et al. (2015b)
			Ruthenium/titanium dioxide	Mousli et al. (2019)
			Silver phosphate/Ni ferrite	Chen et al. (2019b)
			Titanium dioxide/graphene	Mohammadi et al. (2019)
			Titanium dioxide/poly(vinyl alcohol)	Song et al. (2019)
			Titanium dioxide	Guo et al. (2014), Bahrudin et al. (2018b, 2019) Sun et al. (2019a)
			Tungstophosphoric acid	Salavati and Kohestani (2013)
			Zinc oxide	Saravanan et al. (2016)
Acid Yellow 3	Quinoline yellow	–	Titanium dioxide	Salem et al. (2009)
Acid Red 73	Brilliant Crocein MMO	azo	Titanium dioxide	Vaez et al. (2018) and Mohammadi et al. (2019)
Acid Red 87	Eosin Y	dbp	Thulium titanate	Sobhani-Nasab et al. (2019)
Acid Red 94	Rose bengal	dbp	Graphene	Ameen et al. (2012)
Direct Red 28	Congo red	azo	Graphene oxide	Mitra et al. (2019)
			Iron	Tanwar et al. (2017)
			Titanium dioxide	Guo et al. (2014)
			Zinc oxide	Poorarjmand et al. (2019)
Food Red 17	Allura red	azo	Titanium dioxide	Salem et al. (2009)
Reactive Black 5	Remazol Black B	azo	Titanium dioxide	Subramaniam et al. (2019)
Reactive Blue 19	Remazol Brilliant Blue 19	anq	Titanium dioxide/polyimide	Ding et al. (2019)
Reactive Orange 16	Remazol Brilliant Orange 3R	azo	Chitosan/zinc oxide	Kannusamy and Sivalingam (2013) and Pandiselvi and Thambidurai (2013)
			Nickel/cellulose	Ahmad et al. (2019)
Reactive Red 4	Brilliant Red 7BH	azo	Titanium dioxide	Razak et al. (2014)
Reactive Red 45	Cibacron Brilliant Red 3B-P	azo	Titanium dioxide	Gilja et al. (2017)
Reactive Red 241	Reactive Red M-3BE	azo	Titanium dioxide/polyimide	Ding et al. (2019)
Reactive Yellow 15	Remazol Yellow	azo	Tin dioxide/biotemplate	Karpuraranjith and Thambidurai (2016)
			Tin dioxide/diatomite	Akti (2018)
Cationic dyes				
Acid Black 1	Naphtol blue black	azo	Titanium dioxide	Debnath et al. (2015c)
Acid Red 87	Eosin yellow	dbp	Titanium dioxide	Debnath et al. (2015c)

Table 8 (continued)

Colour index	Dye	Type	Composite component	References
Basic Blue 9	Methylene blue	thz	Bismuth oxyiodide/zinc oxide/magnetite	Habibi-Yangjeh and Shekofteh-Gohari (2019)
			Bismuth phosphate	Yu et al. (2018)
			Bismuth vanadate/graphene oxide/titanium dioxide	Zhao et al. (2019a)
			Carbon nitride	Wu et al. (2019)
			Iron(III) oxide	Ossoss et al. (2019)
			Ferrite	Arshadnia et al. (2017) and Mesdaghi et al. (2019)
			Molybdenum disulfide	Saha et al. (2019)
			Nickel(II) oxide	Vidya and Balamurugan (2019a)
			Silicon carbide	Koysuren (2019)
			Strontium stannate	Faisal et al. (2019)
			Tin dioxide/biotemplate	Karpuraranjith and Thambidurai (2016)
			Titanium dioxide	Min et al. (2007), Min et al. (2008), Wang et al. (2010), Radoičić et al. (2013), Ansari et al. (2015), Reddy et al. (2016), Deng et al. (2017), Radoičić et al. (2017) and Koysuren and Koysuren (2019)
			Titanium dioxide/carbon dots	Feizpoor et al. (2018)
			Titanium dioxide/polyimide	Ding et al. (2019)
			Titanium dioxide/poly(vinyl alcohol)	Song et al. (2019)
			Tungstophosphoric acid	Salavati and Kohestani (2013)
			Zinc oxide	Ovando-Medina et al. (2015b) and Saravanan et al. (2016)
			Zinc selenide	Shirmardi et al. (2018)
Basic Green 4	Malachite green	tpm	Bismuth selenide	Chatterjee et al. (2019)
			Graphene oxide	Mitra et al. (2019)
			Graphene oxide/MnV_{13}	Zhang and Ma (2019)
Basic Red 1	Rhodamine 6G	dbp	Zinc sulfide	Allahveran and Mehrizad (2017)
Basic Red 2	Safranin	phz	Bentonite/nickelIII] oxide	Abukhadra et al. (2018b)
			Heulandite/nickelIII] oxide	Abukhadra et al. (2018a)

Table 8 (continued)

Colour index	Dye	Type	Composite component	References
Basic Violet 10	Rhodamine B	dbp	Bismuth molybdate	Feng et al. (2019)
			Bismuth oxybromide	Hao et al. (2017)
			Bismuth oxychloride	Tang et al. (2019b) and Wang et al. (2019d)
			Bismuth oxide	Wang et al. (2019c)
			Bismuth oxyiodide	Yan et al. (2018)
			Bismuth oxyiodine/zinc oxide/magnetite	Habibi-Yangjeh and Shekofteh-Gohari (2019)
			Bismuth selenide	Chatterjee et al. (2019)
			Bismuth vanadate	Shang et al. (2009)
			Bismuth wolframate	Wang et al. (2014) and Zhao et al. (2019b)
			Cadmium sulfide/pectin	Alipour and Lakouarj (2019)
			Cerium dioxide	Samai and Bhattacharya (2018) and Shah et al. (2018)
			Ferrite	Zeng et al. (2016)
			Graphene oxide	Mitra et al. (2019)
			Silver iodide/sulfonated polystyrene	Liu et al. (2019)
			Silver phosphate/Ni ferrite	Chen et al. (2019b)
			Thulium titanate	Sobhani-Nasab et al. (2019)
			Titanium dioxide	Radoičić et al. (2013), Reddy et al. (2016), Deng et al. (2017) and Radoičić et al. (2017)
			Titanium dioxide/carbon dots	Feizpoor et al. (2018)
			Titanium dioxide/chitosan	Mahanta et al. (2011b)
			Titanium dioxide/cotton	Yu et al. (2019)
			Tungstophosphoric acid	Salavati and Kohestani (2013)
			Zinc oxide/charcoal	Selvin et al. (2018)
			Zirconium dioxide	Carević et al. (2018) and Shah et al. (2018)
Basic Violet 14	Fuchsin	tpm	Titanium dioxide/carbon dots	Feizpoor et al. (2018)

polyaniline-coated bismuth selenide (Chatterjee et al. 2019), carbon nitride (Zhang et al. 2014), manganese ferrite (Zeng et al. 2016), nickel oxide (Vidya and Balamurugan 2019a) or titanium dioxide (An et al. 2018; Sun et al. 2019a) when the photocatalytic activity of composites was higher compared with the performance of any component alone.

Polyaniline composites

The photocatalytic degradation of selected dyes with polyaniline-coated inorganic materials has recently been reviewed (Chatterjee et al. 2019). A typical photocatalyst is represented by a photoactive inorganic compound modified at the surface with a conducting polymer, which takes over the role of a photosensitizer (Table 8). Two or even three inorganic components appear simultaneously in some studies (Amer et al. 2019b; Ma et al. 2019; Zhao et al. 2019a).

The recent survey of the literature provided the following examples, which are listed below according to the nature of inorganic component:

Ag Sulfonated polystyrene microspheres were coated with polyaniline and combined with silver iodide to produce a photocatalyst for the degradation of rhodamine B (Liu et al. 2019). A ternary composite polyaniline/silver phosphate/nickel ferrite served for the photocatalytic removal of rhodamine B and methyl orange (Chen et al. 2019c).

Bi Bismuth vanadate (Shang et al. 2009), bismuth molybdate (Feng et al. 2019), bismuth wolframate (Wang et al. 2014; Zhao et al. 2019b), bismuth oxide (Wang et al. 2019c), bismuth oxychloride (Wang et al. 2013b; Tang et al. 2019b; Tanwar and Mandal 2019; Wang et al. 2019d), bismuth oxybromide (Hao et al. 2017; Liu and Cai 2019) and bismuth oxyiodide (Yan et al. 2018; Habibi-Yangjeh and Shekofteh-Gohari 2019; Wang et al. 2019c) coated with polyaniline have been applied for the photodegradation of methylene blue, methyl orange or rhodamine B under visible light. The composites often contained additional components. The composite with bismuth selenide was photocatalytically active in the decomposition of methyl orange, rhodamine B, or malachite green (Chatterjee et al. 2019). Another composite with bismuth phosphate was similarly used for the decomposition of methylene blue (Yu et al. 2018).

C Among carbonaceous materials, graphene coated with polyaniline performed well in the photocatalytic degradation of rose bengal (Ameen et al. 2012) or in the combination with complex wolframate in decomposition of methyl orange (Biswas et al. 2019). The composite comprising polyaniline and graphene oxide along with two additional inorganic components catalysed the decomposition of methylene blue (Zhao et al. 2019a) or malachite green (Zhang and Ma 2019). Carbon nitride coated with polyaniline displayed marked photocatalytic effect in the decomposition of both methyl orange and methylene blue, the efficiency of the former dye being higher (Zhang et al. 2014). Silicon carbide (Koysuren 2019) and silicon nitride (Wu et al. 2019) coated with polyaniline were similarly been used for the degradation of methylene blue.

Cd Cadmium sulfide dispersed on polyaniline stabilized with hydrolyzed pectin was used for the photocatalytic degradation of rhodamine B (Alipour and Lakouarj 2019).

Ce Cerium(IV) dioxide coated with polyaniline was employed in photocatalytic UV-light degradation of rhodamine B (Samai and Bhattacharya 2018) and of methylene blue under visible light irradiation (Vidya and Balamurugan 2019b).

Fe The composite of polyaniline with NiZn ferrite was used as a photocatalyst for the degradation of methyl orange (Chen et al. 2019c; Tanwar and Mandal 2019), Orange II (Pant et al. 2018) and rhodamine B (Chen et al. 2019c). An analogous composite with MgZn ferrite was applied for decolorization of methylene blue and methyl orange solutions (Arshadnia et al. 2017). Polyaniline/CoMn ferrite was another photocatalyst for degradation of methyl orange (Jung et al. 2019). The incorporation of ferromagnetic components, such as iron (Das et al. 2017; Tanwar et al. 2017), ferrite (Zeng et al. 2016; Arshadnia et al. 2017; Kim et al. 2017; Abukhadra et al. 2018a; Aigbe et al. 2018; Bashir et al. 2019; Chen et al. 2019c; Mesdaghi et al. 2019) or magnetite (Habibi-Yangjeh and Shekofteh-Gohari 2019), allowed for the separation of the catalyst by applying magnetic field. Iron ions improved the adsorption capacity of polyaniline/titanium dioxide with respect to photodegradation of methylene blue (Koysuren and Koysuren 2019).

Mg Polyaniline/magnesium indium sulfide was active in the photodegradation of methyl orange and photoreduction of chromium(VI) ions (Jing et al. 2019).

Mn Polyaniline-coated manganese dioxide was used as catalyst for the degradation of Acid Blue 25 by hydrogen peroxide (Gemeay et al. 2012), which increased in the presence of UV-light.

Mo Molybdenum disulfide coated with polyaniline by in-situ polymerization of aniline was tested in the degradation of methylene blue (Saha et al. 2019).

Ni The decomposition of Reactive Orange 16 using polyaniline composite with nickel nanoparticles has recently been illustrated (Ahmad et al. 2019) but the nickel oxides have been used more often. For example, polyaniline/nickel(II) oxide catalysed the photodecomposition of methylene blue (Vidya and Balamurugan 2019a). It was demonstrated that ternary polyaniline/heulandite/nickel oxide composite catalysed the oxidative degradation of not only safranin but also of other dyes, such as Congo red, crystal violet, methyl orange, methylene violet or malachite green, alone or in mixtures (Abukhadra et al. 2018a). Safranin was also photocatalytically removed using polyaniline/bentonite/nickel(III) oxide composite (Abukhadra et al. 2018b).

Ru A polyaniline-coated mixed ruthenium/titanium dioxide catalysed the degradation of methyl orange both in dark and in simulated sunlight (Mousli et al. 2019). This means that the composite was active not only as a photocatalyst but also as a degradation catalyst. The explanation based on a dye adsorption could also be considered in this case.

Si While silicon compounds have been found to be good adsorbents, they have not practically been used in the photocatalytic experiments. A mixture of polyaniline with heulandite was applied in the photocatalyzed decomposition of Light Green SF (Abukhadra et al. 2018c).

Sn The composite polyaniline/tin dioxide/biotemplate has been used to catalyse the photodegradation of Reactive Yellow 15 (Karpuraranjith and Thambidurai 2016) similarly like analogous composite with diatomite (Akti 2018). Polyaniline/strontium stannate proved to be a good photocatalyst of methylene blue decomposition (Faisal et al. 2019).

Ti Titanium dioxide is the key substrate in the photocatalytic experiments due to its ability to absorb light in UV-region. After coating with polyaniline, which extended light absorption to visible region, the composite has been used for the degradation of Acid Blue 90 (Ansari et al. 2015), Acid Red 73 (Vaez et al. 2018), allura red (Salem et al. 2009), Congo red (Guo et al. 2014; Mousli et al. 2019), eosin yellow (Debnath et al. 2015c), methylene blue (Min et al. 2007, 2008; Wang et al. 2010; Radoičić et al. 2013; Jeong et al.

2014; Reddy et al. 2016; Radoičić et al. 2017; Song et al. 2019; Zhao et al. 2019a), methyl orange (Guo et al. 2014; Mohammadi et al. 2019; Song et al. 2019; Sun et al. 2019a), naphtol blue black (Debnath et al. 2015c), Orange II (An et al. 2018), quinoline yellow (Salem et al. 2009), Reactive Black 5 (Subramaniam et al. 2019), Reactive Red 4 (Razak et al. 2014), Reactive Red 45 (Gilja et al. 2017), or rhodamine B (Radoičić et al. 2013; Ansari et al. 2015; Reddy et al. 2016; Deng et al. 2017; Radoičić et al. 2017). The combination with graphene or carbon dots (Feizpoor et al. 2018; Mohammadi et al. 2019) still improved the photocatalytic properties. The mixture of titanium dioxide with a polyaniline colloid was active in photodegradation of rhodamine B (Zhou et al. 2019) or methyl orange (Bahrudin et al. 2018b, 2019).

Ta Tantalum nitride modified by chemisorption of polyaniline from tetrahedran solution was more efficient in the photodegradation of rhodamine B than nitride alone (Niu and Xu 2019).

Tm Polyaniline/thulium titanate was used in the sonophotocatalytic decomposition of rhodamine B, eosin Y and phenol red (Sobhani-Nasab et al. 2019).

W Polyaniline prepared in the presence of tungstophosphoric acid catalysed the photodecomposition of four selected dyes better than any of the composite components (Salavati and Kohestani 2013). Complex polyaniline/wolframate/graphene composite catalysed the photodecomposition of methyl orange (Biswas et al. 2019).

Zn Polyaniline/zinc oxide was investigated in the decomposition of Congo red (Poorarjmand et al. 2019), methyl orange (Saravanan et al. 2016) and methylene blue (Saravanan et al. 2016; Sahu et al. 2019). The composite with zinc selenide was also tested in the removal of last dye (Shirmardi et al. 2018), with zinc oxide/chitosan for removal of Reactive Orange 16 (Pandiselvi and Thambidurai 2013; Kannusamy and Sivalingam 2013), and the composite of zinc oxide/activated charcoal for degradation of rhodamine B (Selvin et al. 2018). Polyaniline/zinc sulfide was tested for the photocatalytic decomposition of rhodamine 6G (Allahveran and Mehrizad 2017).

Zr The photocatalytic decomposition of rhodamine B on zirconium dioxide was improved after coating the photocatalyst with polyaniline (Carević et al. 2018; Shah et al. 2018).

Natural polymers Cellulose (Ahmad et al. 2019), chitosan (Pandiselvi and Thambidurai 2013) or pectin (Alipour and Lakouarj 2019) participated in some composites tested in this direction.

Synthetic polymers Modified titanium dioxide on polyaniline-coated polyimide fabric degraded methylene blue, Reactive Blue 19 and Reactive Red 241 (Ding et al. 2019).

Polyaniline-related materials

In addition to the adsorption of dyes, polymers of phenylenediamines (Stejskal 2015) have also been used for the catalytic decomposition of dyes. *Poly(o-phenylenediamine)* deposited on bismuth or lanthan vanadates removed photocatalytically methylene blue from the aqueous media (Sivakumar et al. 2019). Poly(*o*-phenylenediamine)/zinc wolframate/fly ash displayed a photocatalytic activity in the degradation of coloured antibiotics, tetracycline (Ye et al. 2019a). Another composite with cobalt ferrite photocatalyzed the degradation of malachite green (Riaz et al. 2016). Finally, titanium dioxide with polypyrrole shell was active in the decomposition of methylene blue (Wang et al. 2012, 2013c) and Acid Orange 7 (Archana et al. 2016). It should be noted that the products of *o*-phenylenediamine oxidation are rather oligomers than polymers (Stejskal 2015). *Poly(m-phenylenediamine)* deposited on zinc oxide degraded under illumination Acid Red 249 (Peng et al. 2014). The photocatalytic degradation of bromocresol green, bromocresol blue, bromocresol purple, rhodamine B, neutral red, methylene blue, Sudan III, methyl orange and Congo red on *poly(p-phenylenediamine)*/magnetite proved high activity under both UV and visible light while magnetite alone was inactive (Yang et al. 2014).

The *copolymers of aniline* with phenylenediamine are represented by poly(aniline-*co*–*o*-phenylenediamine)/iron(III) oxide composite, which served as a photocatalyst in the decomposition of methylene blue (Ossoss et al. 2019). In another study, titanium dioxide was prepared in the presence of poly(aniline-*co*-pyrrole) and tested in the photocatalysis of rhodamine B and methyl orange (Gao et al. 2019).

In a rare study on *carbonized polyaniline*, carbonized polyaniline/titanium dioxide composite displayed higher photocatalytic activity in the degradation of rhodamine B and methylene blue compared with the parent composite (Radoičić et al. 2017). Finally, the sulfonated polyaniline in the combination with titanium dioxide was used in the photocatalytic depomposition of methylene blue and Acid Blue 90 (Ansari et al. 2015).

Polypyrrole

The number of reports on photocatalytic performance of polypyrrole alone is very limited. The photocatalytic activity of polypyrrole in the degradation of safranin has recently been reported (Mohamed et al. 2018). No degradation was observed with globular polypyrrole, while polypyrrole prepared in the presence of a surfactant, sodium dodecyl sulfate, was active (Yuan et al. 2019). This was explained by different nanostructure of conducting polymer but this might have been also due to the difference in the hydrophilicity of both types.

Table 9 Photocatalytic decomposition of dyes on polypyrrole composites

Colour index	Dye	Type	Composite component	References
Anionic dyes				
Acid Green 1	Naphthol Green B	–	Attapulgite/iron	Chen et al. (2019a)
Acid Orange 52	Methyl orange	azo	Titanium dioxide	Li et al. (2018b)
Acid Violet 7	Acid Fuchsine 6B	azo	Zinc oxide	González-Casamachin et al. (2019)
Reactive Red 45	Cibacron Brilliant Red 3B-P	azo	Titanium dioxide	Krehula et al. (2019)
Cationic dyes				
Basic Blue 9	Methylene blue	thz	Copper complex phosphotungstate	Kong et al. (2019b)
			Strontium carbonate	Marquez-Herrera et al. (2016)
			Titanium dioxide	Castillo-Reyes et al. (2015) and Sangareswari and Sundaram (2017)
			Titanium dioxide/magnetite	Wei et al. (2015) and Amer et al. (2019b)
			Zinc oxide	Ovando-Medina et al. (2015b) and Lakshmi and Rajagopalan (2016)
Basic Green 4	Malachite green	tpm	Silver/bismuth oxybromide	Liu and Cai (2018)
Basic Red 1	Rhodamine 6G	tpm	Sodium iodide	Krishnaswamy et al. (2019)
Basic Red 2	Safranin	phz	Zn-Fe double hydroxide	Mohamed et al. (2018)
Basic Violet 10	Rhodamine B	dbp	Bismuth tungstate/carbon nitride	Jiao et al. (2019)
			Carbon nitride	Hayat et al. (2019)
			Titanium dioxide	Zhou et al. (2019)
			Zinc oxide	Lakshmi and Rajagopalan (2016)
			Zinc oxide/silver	Podasca et al. (2019)

Polypyrrole composites

There were various reports on the photocatalytic performance of polypyrrole-based composites (Table 9), even though they are less numerous compared with polyaniline studies.

The survey of photocatalysts ordered according to the inorganic components is as follows:

Ag The composite polypyrrole/Ag/BiOBr was active in the degradation of malachite green or phenol (Liu and Cai 2018) and polypyrrole/Ag/zinc oxide in removal of rhodamine B (Podasca et al. 2019).

Bi A composite comprising polypyrrole, carbon nitride and bismuth tungstate performed also well in the photocatalytic decomposition of rhodamine B under visible light (Jiao et al. 2019).

C Polypyrrole-coated graphitized carbon nitride was tested in the photocatalytic decomposition of rhodamine B (Hayat et al. 2019).

Fe Polypyrrole-coated magnetite-based particles were used for the degradation of Congo red (Wei et al. 2015) and methylene blue (Amer et al. 2019b). Thanks to the presence of ferromagnetic component, the adsorbent was separable by magnetic field. The incorporation of iron nanoparticles in polypyrrole/attapulgite also reported (Chen et al. 2019a).

Sr Strontium carbonate composite with polypyrrole was tested for the adsorption of methylene blue under visible light (Marquez-Herrera et al. 2016). Attapulgite clay coated with polypyrrole served for the degradation of Naphthol Green G (Chen et al. 2019a).

Ti The coating of titanium dioxide with polypyrrole improved the photocatalytic degradation of methylene blue (Castillo-Reyes et al. 2015; Sangareswari and Sundaram 2017; Amer et al. 2019b), methyl orange (Li et al. 2018b) or Reactive Red 45 (Krehula et al. 2019) even under visible light. The titanium dioxide/silver oxide surface-modified with polypyrrole was similarly active (Kumar 2016).

W Copper-complex phosphotungstate compound of Keggin type with in-situ-deposited polypyrrole photocatalytically degraded methylene blue (Kong et al. 2019b).

Zn Polypyrrole/zinc oxide was used for the photocatalytic decomposition of Acid Blue 25 (Gilja et al. 2018), Acid Violet 7 (González-Casamachin et al. 2019), rhodamine B (Lakshmi and Rajagopalan 2016) and methylene blue (Ovando-Medina et al. 2015b; Lakshmi and Rajagopalan 2016) or in the combination with silver for photocatalytic degradation of rhodamine B (Podasca et al. 2019). Polypyrrole/Zn-Fe layered double-hydroxide was active in the photodegradation of safranin (Mohamed et al. 2018). The composites performed better than any of its

components, i.e. the synergism between conducting polymers and the substrate was observed.

Natural polymers Cellulose coated with polypyrrole adsorbed Reactive Red 120 at the capacity 16–96 mg g^{-1} depending on pH (Ovando-Medina et al. 2015a).

Other methods of dye degradation

In addition to UV–visible light irradiation in photocatalytic degradation of organic dyes, the catalytic effect of conducting polymers was supplemented by other energy sources. The exposure to microwaves was used in a single case for the dye degradation (Riaz et al. 2014). Conducting polymers are good absorbers of microwaves and resulting local heating may promote the dye decomposition. The photocatalytic decomposition of polyaniline-coated electrode was also supplemented by the application of an electric potential (Pirkarami et al. 2013). Sonocatalytic degradation of organic dyes with the help of ultrasonic agitation was also reported (Salavati and Kohestani 2013; Wang et al. 2015b; Das et al. 2017).

Other approaches have oriented on promoting the catalytic effect of conducting polymers by incorporation of noble-metals in reductive degradation of dyes. Cotton fabrics coated with polypyrrole and decorated with silver nanoparticles catalysed the reduction of *p*-nitrophenol to *p*-aminophenol (Ayad et al. 2017, 2018b) with sodium borohydride. The process is mentioned here because *p*-nitrophenol is yellow and converts to a colourless compound, and it can, therefore, be followed by the methods used for the degradation of dyes (Mu and Wang 2015). Wool fabric coated with poly(*o*-anisidine) (=poly(*o*-methoxyaniline)) and decorated with silver particles catalysed the reduction of methylene blue (Erdogan et al. 2019). Polyaniline-supported palladium catalyst efficiently degraded methylene blue, rhodamine B or methyl orange also by sodium borohydride (Roy et al. 2019).

Some studies report the catalytic effect of conducting polymers even in the absence of noble metals. For example, polyaniline was used for the catalytic activation of peroxymonosulfate in the degradation of methyl orange (Sun et al. 2019b). Enzymatic degradation of Reactive Blue 4 by ginger peroxidase immobilized on polypyrrole/cellulose/graphene oxide was also tested (Ali et al. 2018).

Conductivity

The conducting polymers and organic dyes share the conjugated structure of alternating double and single bonds that is reflected in their colour. They have the ionic character, as they are typically salts that dissociate in the presence of water and afford the contribution of ionic conductivity. They differ by the presence of charge carriers, e.g., polarons, in conducting polymers, and their absence in dyes. Since conducting polymers and dyes have been observed to interact, as they manifest themselves in adsorption experiments, it is a relevant question how much such interaction will affect the electric properties of conducting polymers. For instance, we can speculate that molecules of organic dyes may assist the charge transport by providing conjugated bridges between conducting polymer chains supported additionally by π–π interactions of aromatic ring of both moieties. There are virtually no studies that would attempt to address this issue.

One-dimensional morphology of conducting moieties is of benefit when the conductivity is the key parameter in the desired application. The percolation limit, and thus the good conductivity level, is much easier reached with one-dimensional objects that are present in the composite due to the formation of conducting network. For that reason, attention has been paid to the preparation of conducting polymer nanotubes or nanofibres, and this applies especially to polypyrrole. In this direction, the organic dyes play a decisive role in the morphology and conductivity control. Another approach relies on the coating of nanotubular objects, e.g., carbon nanotubes, with conducting polymers (Konyushenko et al. 2006; Zeng et al. 2013; Minisy et al. 2019c).

Polyaniline

The conductivity of "standard" globular polyaniline is 4 S cm^{-1} (Stejskal and Gilbert 2002). There are very few reports of the conductivity for polyaniline prepared in the presence of the dyes, probably because there was no significant effect worth to mention. Exceptionally, the conductivity of polyaniline, 2.2 S cm^{-1}, increased to 15 S cm^{-1} when Sunset Yellow FCF was present in the reaction mixture and

Table 10 Polypyrrole prepared in the presence of various dyes (Sapurina et al. 2017)

Dye	Polymer morphology	Conductivity, S cm^{-1}
Methyl orange	Nanotubes	46.8
Ethyl orange	Globules	22.1
Methylene blue	Fused nanoparticles	5.56
Cresol red	Spheres	1.38
No dye	Globular	1.55
Phthalocyaninosulfonic acid	Fused nanoparticles	0.86
Acid Green 25	Fused nanoparticles	0.854
Indigo carmine	Short nanosticks	0.128
Reactive Black 5	Spheres	0.054
Thymol blue	Hollow spheres	2.28×10^{-3}

0.05 M pyrrole was oxidized with 0.05 M iron(III) chloride. Dye concentration was 0.0025 M divided by number of sulfo groups in the molecule

dropped down at still higher dye concentrations (Shi et al. 2017).

It has been observed that polyaniline/cellulose composite decreased its conductivity when exposed to the aqueous solutions with increasing concentration of methylene blue (Sarkar et al. 2018). Such effect, however, might have been caused by the simple deprotonation of polyaniline in distilled water and insufficient pH control. The exposure of polyaniline salt to the solutions of Orange G led to the decrease in the conductivity from 14.5 to 2 S cm^{-1}. This was explained be the incorporation of the dye (Mahanta et al. 2008) but again a partial deprotonation of polyaniline in dye solutions of low acidity would again be alternative explanation. In the photocatalytic decomposition of dyes, the best composite performance was linked to its highest conductivity (Alipour and Lakouarj 2019). Such correlation may exist but it would involve many other parameters, too.

Polypyrrole

The conductivity of globular polypyrrole is 1–2 S cm^{-1} (Sapurina et al. 2017; Acharya et al. 2018). There are some indications in the case of polypyrrole that the smaller conducting polymer particles (Yuan et al. 2019) or thinner one-dimensional structures (Stejskal and Trchová 2018) have higher conductivity. It is tempting to link the conductivity to specific surface area, but, in fact, this is probably due to the better organization of polymer chains in smaller objects (Li et al. 2017b; Stejskal and Trchová 2018). As dyes, similarly like surfactants (Omastová et al. 2003), affect the polymer morphology especially in the case of polypyrrole, the conductivity enhancement seems to be indeed caused mainly by improved polymer-chain ordering rather than by the direct interaction between conducting polymers and dyes at molecular level.

Generally, however, the presence of dyes affects the morphology and conductivity of pyrrole in unpredictable manner (Table 10). This is in the contrast to polyaniline where the dyes have limited influence on conductivity as the published data and preliminary experiments indicate.

Methyl orange, however, is still the best dye routinely used in the improvement of polypyrrole conductivity. Polypyrrole prepared in the absence of a dye had conductivity 1.5 S cm^{-1}. In the presence methyl orange it increased at first as the dye concentration grew to 86 S cm^{-1} and then started to decrease at higher dye concentration (Li et al. 2017b). The same trend was confirmed in another study (Fig. 6) (Sapurina et al. 2017). This was explained by the improvement of polypyrrole-chain organization during the formation of polypyrrole nanotubes, and later the dye acted only as non-conducting filler (Sapurina et al. 2017). With other dyes, the conductivity was improved only in the case of ethyl orange (Li et al. 2017b; Sapurina et al. 2017), methylene blue (*Sapurina et al. 2017) or alizarin red S (Zang et al. 2018) compared with the synthesis without a dye.

The conductivity enhancement from 0.07 to 1.25–3.3 S cm^{-1} was reported after introduction of tryptan blue to the reaction mixture (Yang et al. 2019). Direct Blue 2 and Direct Violet 1 had the similar effect and the conductivities were 1.05 and 0.58 S cm^{-1}, respectively. Indigo carmine had no significant influence, the conductivity being 0.62–1.91 S cm^{-1} (Li et al. 2016). Nevertheless, such variations in conductivity are regarded as small and close to the experimental error of conductivity determination.

The similar pattern applies also to composites. The conductivity of polypyrrole increased from 12.5 to 25.0 S cm^{-1} with increasing fraction of rhodamine B/attapulgite in the reaction mixture and then decreased at still higher dye concentration (Wang et al. 2013d). It was suggested that the pathways for charge carriers were improved by the presence of the dye. The same trend, however, was observed in the preparation of polypyrrole/molybdenum or tungsten disulfides in the absence of any dye (Acharya et al. 2018; Stejskal et al. 2019) and was explained by the improved polymer-chain organization.

Other applications

The conducting polymers were reported to be active in dye removal in water-pollution treatment, regardless of the dye adsorption or degradation mechanism (Zare et al. 2018a). It is generally agreed that the adsorption of cationic and anionic dyes is comparable (Amer et al. 2018; Kaushal et al. 2018; Boukoussa et al. 2018) and conducting polymers are thus universal dye adsorbents. Other uses involving conducting polymers and dyes and related compounds have ocasionally been proposed and these are briefly reviewed below.

Energy conversion and storage

The interaction between conducting polymer and organic dyes is likely to manifest itself also in electrical properties of composites, although this direction has not received attention so far. The supercapacitors are the most studied energy-storage devices. The introduction of redox-active components represented both by the conducting polymers and organic dyes can promote faradaic reactions and enhance the ionic conductivity (Xu et al. 2018). For example, the capacitance of polyaniline prepared in the presence of Acid Red 27 was reached 423 F g^{-1} (Shi et al. 2018) and with Sunset Yellow FCF 467 F g^{-1} (Shi et al. 2017). Polyaniline prepared in the presence of activated carbon and methyl orange had higher capacitance compared with the composite made in dye absence (Jia et al. 2012).

Polypyrrole nanotubes prepared in the presence of methyl orange always contained a significant fraction of this dye (Alekseeva et al. 2015; Sapurina et al. 2016). They have been used in supercapacitor electrodes after deposition on cotton fabric (Xu et al. 2015; Wang et al. 2019e; Zhang et al. 2019b) or alone (Hryniewicz et al. 2019). In the former case the chemical deposition yielded a material with specific capacitance 64–565 F g^{-1}, in the latter electrochemical synthesis the specific capacitance was 423 F g^{-1}. Polypyrrole nanotubes prepared in the presence of methyl orange and decorated with nickel/cobalt sulfide had specific capacitance as high as 1705 F g^{-1} (Wang et al. 2019f).

The capacitances of polypyrrole/attapulgite improved when polypyrrole was prepared in the presence of rhodamine B (Wang et al. 2013d). The authors proposed that the dye provided pathways to charge carriers. The capacitance of polypyrrole prepared in the presence of trypan blue reached 649 F g^{-1} (Yang et al. 2019). Polypyrrole produced by electropolymerization in the presence of alizarin red and carbon nanotubes had the specific capacitance 274 F g^{-1}. In all cases, the dye present in the synthesis has affected the polymer morphology and the associated specific surface area, and its role is not quite understood. Polypyrrole prepared in the presence of indigo carmine was also used as an anode in all-polymer battery (Sultana et al. 2012a, b). Polypyrrole prepared electrochemically in the presence of cationic thiazine dye, methylene green, served as an electrode in ethanol enzynamic biofuel cell (Bonfin et al. 2019). In all these reports, the role of dyes is not quite obvious.

Removal of drugs and herbicides

Many drugs are coloured and have similar features of molecular structure as organic dyes. For that reason such molecules can be similarly adsorbed by conducting polymers. For example, the adsorption of ciprofloxacin antibiotic on polyaniline/silver/silver molybdate composite was reported (Mondal et al. 2019b). Polypyrrole deposited on plant fibres adsorbed 69–78 mg g^{-1} of three antibiotics from floxacin family from solutions containing initially 100 mg L^{-1} (Duan et al. 2019). Polypyrrole/magnetite/silica composites were used for the extraction of sulfonamides from water (Sukchuay et al. 2015), polypyrrole nanotubes for electrochemically controlled extraction of atrazine, caffeine and progesterone (de Lazzari et al. 2019) and polypyrrole-coated polyamide nanofibres for extraction oxacilin and cloxacilin antibiotics followed by determination by capillary electrophoresis (Li et al. 2019a).

Various composites have been used for the photocatalytic decomposition of drugs. e.g., polyaniline/titanium dioxide composite photocatalysed degradation of metronidazole antibiotic (Asgari et al. 2019) or sulfaquinoxaline sulfonamide (Sandikly et al. 2019). The photocatalytic removal of another antibiotic, tetracycline hydrochloride, on poly(*o*-phenylenediamine)/zinc wolframate/fly-ash cenospheres (Ye et al. 2019a), polypyrrole/fly-ash (Pen and Huang 2019) or polypyrrole/silver phosphate/carbon nanotubes (Lin et al. 2019) was reported. Polypyrrole/zinc oxide supported the photodegradation of diclofenac (Silvestri et al. 2019). On the other hand, drug delivery was modelled using droplets of fluorescent dye, Nile red, dissolved in organic solvent encapsulated in polypyrrole shell (Bartel et al. 2018).

Harmful organic pollutants, such as atrazine herbicide (Wang et al. 2018b) are not dyes but they often share their conjugated molecular structure and could be removed by using conducting polymer composites, such as polyaniline/attapulgite (Wang et al. 2018c). The nicosulfuron herbicide was adsorbed at 5.5–13 mg g^{-1} capacity by polyaniline/BEA zeolite (Jevremović et al. 2019). Various chlorinated pollutants also fall to this category (Hayat et al. 2019).

Sensors

Both polyaniline and polypyrrole are regarded as responsive polymers that change their properties, such as conductivity and colour, in the response to external stimuli, for example pH, temperature, humidity or in the presence of various gases and chemicals or their vapours. This is exploited in the design of sensors (Runsewe et al. 2019) and dyes are occasionally mentioned along with conducting polymers.

Optical pH sensor was based on bromothymol blue immobilized in polyaniline sol–gel (Othman et al. 2017). The blend of polyaniline with non-commercial orange azo dye made the basis of impedance humidity sensor (Chani et al. 2013). The cyclic voltammograms of polyaniline film grown on the electrode were altered after the exposure to the solutions of dyes (Mahanta et al. 2011a). Such effect was proposed to be exploited for the dye detection.

Polypyrrole both in globular and nanotubular forms was used for the sensing of ethanol or *n*-heptane vapours (Kopecká et al. 2016). Methyl orange was used in the preparation of polypyrrole nanotubes and was partly incorporated in them. Polypyrrole prepared in the presence of eriochrome cyanine R provided a sensor for ammonia gas (Tavoli and Alizadeh 2013), and the preparation using tartrazine (Acid Yellow 23) yielded the material for a simultaneous electrochemical sensing of ascorbic acid, uric acid and dopamine (Wang et al. 2019a). Electropolymerization of pyrrole in the presence of Alizarin Red S afforded a potentiometric sensor for silver ions (Rounaghi et al. 2015) and with methyl orange the pH-sensor based on Raman spectra (Czaja et al. 2019). Polypyrrole/bromophenol blue was used as ultrasensitive quartz-microbalance sensor in the ppb-range detection of explosive nitro compounds (Eslami and Alizadeh 2019). Electrospun nanofibres coated with polypyrrole were used

for the micro solid phase extraction in the determination of auramine O, chrysoidine and rhodamine B in the industrial wastewater (Qi et al. 2016). Carbonized polypyrrole was applied for the electrochemical determination of Sunset Yellow FCF (Wang et al. 2019b).

Other polymers, methods and applications

The results of some papers that do not exactly fit to above scheme are briefly enumerated here. For instance, in biomedicine polypyrrole nanotubes prepared in the presence of methyl orange were tested as adsorbents of human influenza viruses (Ivanova et al. 2017). Polypyrrole/methylene blue colloids were employed in photo-induced cancer therapy, when polypyrrole efficiently adsorbed light in near-infrared region and methylene blue acted as a photosensitizer promoting the formation of reactive oxygen species (Phan et al. 2017).

In addition to current conducting polymers, polyaniline and polypyrrole, reviewed above, also polythiophenes appear to be emerging class applicable in water purification (Dutta and Rana 2019). The photocatalytic activity of poly(3-hexylthiophene)/titanium dioxide in decomposition of Orange G (Acid Orange 10) was demonstrated (Mukhta et al. 2007). In another direction, poly(3,4-ethylenedioxythiophene) was prepared by the chemical oxidation of corresponding monomer in the presence of Congo red and tested for electrochemical performance (Bai et al. 2018). The maximum specific capacitance was 206 F g^{-1}. Finally, polysafranin/Triton X-100 was used in the electrochemical selective determination of dopamine (Lavanya et al. 2015).

Polypyrrole nanotubes convert to nitrogen-containing carbon nanotubes by the carbonization in inert atmosphere (Ćirić-Marjanović et al. 2014; Kopecká et al. 2016; Sapurina et al. 2016; Xin et al. 2017; Kang et al. 2019; Minisy et al. 2019c) and can be applied as a new type of nanostructured carbons. They offer some alternative to multiwall carbon nanotubes from the morphology point of view but their structure and properties are different. The preparation of polypyrrole nanotubes involves the presence of organic dye, methyl orange, during the synthesis and for that reason they are mentioned here. Such nanotubes have been used in energy conversion devices (Stejskal and Trchová 2018). Carbonized analogues have also been of interest because of high specific surface areas (Lin et al. 2018), viz. 205 m^2g^{-1} (Xin et al. 2017) and 257 m^2g^{-1} (Ćirić-Marjanović et al. 2014). They were tested in electrodes of lithium (Lin et al. 2018) and flow batteries (Wu et al. 2018), in electrochemical capacitors (Xin et al. 2017) or for electrocatalysis in oxygen reduction reaction (Ćirić-Marjanović et al. 2014; Minisy et al. 2019c). On the other hand, they are also promising dye adsorbents, photocatalysts (Radoicic et al. 2017; Xin et al. 2017) and sensors (Kang et al. 2019).

Concluding remarks on perspectives of conducting polymers

The conducting polymers are not just conducting and their role in environmental issues will probably increase in future. Their *electroactivity*, i.e. their ability to be oxidized or reduced chemically or electrochemically, opens the route to the intelligent adsorbents. It has recently been demonstrated that the hydrophobicity of polypyrrole and, consequently, the adsorption on such materials would be affected by the applied electrical potential and thus controlled (Ren et al. 2018). The electrochemically oxidized or reduced forms of polypyrrole generally differ in the adsorption ability and may be used for dye adsorption and release or in adsorbent recovery (Haque and Wong 2017). The same is expected for polyaniline.

The *chemical reaction* on polyaniline or polypyrrole may also be helpful in the water pollution treatment (Huang et al. 2014; Zare et al. 2018a). In addition to removal of organic dyes and related compounds, conducting polymers are able to reduce noble-metal ions to corresponding metals, viz. silver (Stejskal 2013; Bober et al. 2018b; Maráková et al. 2017; Mahlangu et al. 2019), gold (Mu et al. 2015), platinum and palladium (Sapurina et al. 2016) and thus to separate them from aqueous media, too. There is vast number of papers on the adsorption combined with reduction of harmful chromium (VI) to chromium (III) based on the same principle (Ansari et al. 2017; Ma et al. 2018; Shirmardi et al. 2018; Jing et al. 2019; Mitra et al. 2019). Free halogens, such as bromine (Stejskal et al. 2001) or iodine (Stejskal et al. 2008c) become covalently bound to polyaniline and enable, e.g., to remove radioactive isotopes of iodine (Harijan et al. 2018).

The removal of *heavy-metal cation*s by conducting polymers has recently been reviewed (Zare et al. 2018a). Nitrogen atoms in polyaniline, polypyrrole or related polymers promote the complex formation with heavy-metal cations and thus the purification of water from inorganic cations (Dutta and De 2017, Zare et al. 2018a), such as arsenic (III) (Che et al. 2018; Trung et al. 2018), arsenic (V) (Bhaumik et al. 2014), cadmium (II) (Canoluk and Gursoy 2017), chromium (III) (Beyki et al. 2016; Salehi-Barbarsad et al. 2019), chromium (VI) (Bhaumik et al. 2014; Chigondo et al. 2019), copper (II) (Herrera et al. 2018; Soltani et al. 2019), gallium (III) (Saugo et al. 2018), iron (III) (Salehi-Barbarsad et al. 2019) lead (II) (Beyki et al. 2016; Zare et al. 2018b; Teklu et al. 2019), nickel (II), mercury (II) (Kim et al. 2018; Zhao et al. 2019c), silver (I) (Stejskal 2013; Bober et al. 2018b; Maráková et al. 2017; Mahlangu et al. 2019), strontium (II) (Lu et al. 2018), uranium (VI) (Lei et al. 2018; Saghatchi and Ansari 2018) and zinc (II) (Kumar et al. 2017). The removal

of cobalt and europium radionuclides from environment also falls into this category (Metwally et al. 2019).

Various *inorganic anions* have also been reported to adsorb on conducting polymers, such as chromate (Ansari et al. 2017; Ma et al. 2018; Shirmardi et al. 2018), fluoride (Parashar et al. 2016; Chen et al. 2017b), dichromate (Liu et al. 2018b; Chigondo et al. 2019), nitrate (Garcia-Fernandez et al. 2017) or phosphate (Wang et al. 2017).

The application potential of conducting polymers and their composites in water-pollution treatment is thus much broader compared with classical systems. In addition, conducting polymers have been found to be applicable in wound care and skin tissue engineering (Talikowska et al. 2019). Such polymers with adsorbed organic dyes or structurally related pharmaceuticals can be used in the controlled delivery of disinfectants and antibiotics or to improve the antimicrobial performance. This aspect is also important for the water treatment that requires the *removal of various microorganisms* (Ivanova et al. 2017; Hussein et al. 2019) in addition to current organic and inorganic pollutants.

Conclusions

The progress in the studies of the interaction between conducting polymers and organic dyes has been reviewed. Three research directions can be identified: (1) the effect of dyes on the preparation of polyaniline and polypyrrole, (2) the adsorption of dyes on conducting polymers and (3) the photocatalytic removal of dyes assisted by conducting polymers. The reports appearing in the literature have been organized and discussed according these categories with respect to individual conducting polymers, composite components and dye types.

Organic dyes share some features with surfactants and, consequently, they have similar colloidal properties. They have relatively large hydrophobic part and a hydrophilic moiety, typically represented by an anionic or cationic group. It would probably help to the understanding of their behaviour if the dyes were regarded as "coloured surfactants". The interaction of dyes with produced conducting polymers, however, is more intimate and includes specific π–π interactions of the conjugated molecular structure inherent to both moieties.

The influence of dyes used in the preparation of polyaniline has not been systematically investigated so far and it seems to be marginal when it comes to the morphology and conductivity of this conducting polymer. On the other hand, the preparation of polypyrrole is strongly affected by the presence of dyes. The most frequently used methyl orange converts the globular polypyrrole morphology to nanotubes with the simultaneous increase in conducitivity. The preparation of one-dimensional polypyrroles can be achieved with both anionic and cationic dyes.

Both polyaniline and polypyrrole are polycations in their conducting states. It would be logical to expect preferential interaction with oppositely charged anionic dyes. The most dye-adsorption experiments, however, indicate that both anionic and cationic dyes interact with conducting polymers in similar manner. This means that electrostatic ionic interactions are not decisive. The anionic dyes, such as methyl orange and Congo red, along with cationic methylene blue, have most often been used as model sorbates. The deprotonated conducting-polymer bases adsorbed dyes generally more efficiently than corresponding protonated forms. This is due to the higher hydrophobicity of polymer bases compared with polymer salts. Polyaniline and its composites have been used as adsorbents more frequently than polypyrrole analogues. The papers comparing adsorption performance of polyaniline and polypyrrole are so far missing.

Dye adsorption and photocatalytic dye degradation are usually treated as separate phenomena in the literature but they are clearly related. Efficient photocatalysis requires a dye adsorption to catalyst sites. On the other hand, adsorption studies are often blind to the associated photocatalytic processes. Also in these experiments, the use of methyl orange and methylene blue dominates with significant contribution of papers exploring rhodamine B photodegradation.

Conducting polymers, such as polyaniline and polypyrrole, alone or in the composites are efficient materials for the removal of organic dyes from the environment. They have good application potential because of economic production cost of conducting polymers. In addition to organic dyes they remove noble-metal ions, heavy-metal cations and various anions from the aqueous media. Their application role, e.g., in water-pollution treatment, thus may be much broader. The electrical properties, such as the conductivity and redox electroactivity, are expected to be used in future to control the adsorption/desorption phenomena.

In addition to polyaniline, the attention should be paid in future research to aniline-related materials, such as aniline oligomers, polymers of ring-substituted anilines, aniline copolymers, chemically modified polyanilines and various carbonized analogues. This expectation similarly holds in part also for polypyrrole.

Acknowledgements The author thanks the Czech Science Foundation (19-04859S) for the financial support.

References

Abbasian M, Niroomand P, Jaymand M (2017a) Cellulose/polyaniline derivatives nanocomposites: synthesis and their performance in

removal of anionic dyes from simulated industrial effluents. J Appl Polym Sci 134:45352. https://doi.org/10.1002/app.45352

Abbasian M, Jaymand M, Niroomand P, Farnoudian-Habibi A, Karaj-Abad SG (2017b) Grafting of aniline derivatives onto chitosan and their applications for removal of reactive dyes from industrial effluents. Int J Biol Macromol 95:393–403. https://doi.org/10.1016/j.ijbiomac.2016.11.075

Abukhadra MR, Shaban M, Abd El Samad MA (2018a) Enhanced photocatalytic removal of Safranin-T dye under sunlight within minute time intervals using heulandite/polyaniline@nickel oxide composites a novel photocatalyst. Ecotoxicol Environ Safety 162:261–271. https://doi.org/10.1016/j.ecoenv.2018.06.081

Abukhadra MR, Shaban M, Sayed F, Saad I (2018b) Efficient photocatalytic removal of safranin-O dye pollutants from water under sunlight using synthetic bentonite/polyaniline@Ni_2O_3 photocatalyst of enhanced properties. Environ Sci Pollut Res 25:33264–33276. https://doi.org/10.1007/s11356-018-3270-x

Abukhadra MR, Rabia M, Shaban M, Verpoort F (2018c) Heulandite/polyaniline hybrid composite for efficient removal of acidic dye from water; kinetic, equilibrium studies and statistical optimization. Adv Powder Technol 29:2501–2511. https://doi.org/10.1016/j.apt.2018.06.030

Acharya U, Bober P, Trchová M, Zhigunov A, Stejskal J, Pfleger J (2018) Synergistic conductivity increase in polypyrrole/molybdenum disulfide composite. Polymer 50:130–137. https://doi.org/10.1016/j.polymer.2018.07.004

Agarwal S, Tyagi I, Gupta VK, Golbaz F, Golikand AN, Moradi O (2016) Synthesis and characteristics of polyaniline/zirconium oxide conductive nanocomposite for dye adsorption application. J Mol Liq 218:494–498. https://doi.org/10.1016/j.molliq.2016.02.040

Aghajani K, Tayebi HA (2017) Synthesis of SWBA-15/PAni mesoporous composite for adsorption of reactive dye from aqueous media: RBF and MLP networks predicting models. Fibers Polym 18:465–475. https://doi.org/10.1007/s12221-017-6610-4

Ahmad N, Sultana S, Kumar G, Zuhaib M, Sabir S, Khan MZ (2019) Polyaniline base hybrid bionanocomposites with enhanced visible light photocatalytic activity and antifungal activity. J Environ Chem Eng 7:102804. https://doi.org/10.1016/j.jece.2018.11.048

Ahmed SM, El-Dib FI, El-Gendy NS, Sayed WM, El-Khodary M (2016) A kinetic study for the removal of anionic sulphonated dye from aqueous solution using nano-polyaniline and Baker's yeast. Arab J Chem 9:S1721–S1728. https://doi.org/10.1016/j.arabjc.2012.04.049

Ai LH, Jiang J, Zhang R (2010) Uniform polyaniline microspheres: a novel adsorbent for dye removal from aqueous solution. Synth Met 160:762–767. https://doi.org/10.1016/j.synthmet.2010.01.017

Aigbe UO, Kchenfouch M, Ho WH, Majty A, Vallabhapurapu VS, Hemmaragala NM (2018) Congo red dye removal under influence of rotating magnetic field by polypyrrole nanocomposite. Desalin Water Treat 131:328–342. https://doi.org/10.5004/dwt.2018.23028

Akhbartabar I, Yazdanshenas ME, Tayebi HA, Nasirizadeh N (2017) Physical chemistry studies of acid dye removal from aqueous media by mesoporous nano composite: adsorption isotherm, kinetic and thermodynamic studies. Phys Chem Res 5:659–679. https://doi.org/10.22036/pcr.2017.83378.1371

Akti F (2018) Photocatalytic degradation of remazol yellow using polyaniline–doped tin oxide hybrid photocatalysts with diatomite support. Appl Surf Sci 455:931–939. https://doi.org/10.1016/j.apsusc.2018.06.019

Akti F, Okur M (2018) The removal of Acid Violet 90 from aqueous solutions using PANI and PANI/clinoptiolite composites: isotherms and kinetics. J Polym Environ 26:4233–4242. https://doi.org/10.1007/s10924-018-1297-1

Alekseeva E, Bober P, Trchová M, Šeděnková I, Prokeš J, Stejskal J (2015) The composites of silver with globular or nanotubular polypyrrole: the control of silver content. Synth Met 209:105–111. https://doi.org/10.1016/j.synthmet.2015.07.003

Ali M, Husain Q, Sultana S, Ahmad M (2018) Immobilization of peroxidase on polypyrrole-cellulose-graphene oxide nanocomposite via non-covalent interactions for the degradation of Reactive Blue 4 dye. Chemosphere 202:198–207. https://doi.org/10.1016/j.chemosphere.2018.03.073

Aliabad R, Mahmoodi NO (2018) Synthesis characterization of polypyrrole, polyaniline nanoparticles and their nanocomposite for removal of azo dyes: sunset yellow and Congo red. J Clean Prod 179:235–245. https://doi.org/10.1016/j.jclepro.2018.01.035

Alipour A, Lakouarj MM (2019) Photocatalytic degradation of RB dye by the CdS-decorated nanocomposites based on polyaniline and hydrolyzed pectin: isotherm and kinetic. J Environ Chem Eng 7:102837. https://doi.org/10.1016/j.jece.2018.102837

Allahveran S, Mehrizad A (2017) Polyaniline/ZnS nanocomposite as a novel photocatalyst for removal of Rhodamine 6G from aqueous media: optimization of influential parameters by response surface methodology and kinetic modeling. J Mol Liq 225:339–346. https://doi.org/10.1016/j.molliq.2016.11.051

Almeida AKA, Dias JMM, Santos DP, Nogueira FAR, Navarro M, Tonholo J, Lima DJP, Ribeiro AS (2017) A magenta polypyrrole derivatised with Methyl Red azo dye: synthesis and spectroelectrochemical characterization. Electrochim Acta 240:239–249. https://doi.org/10.1016/j.electacta.2017.04.068

Ameen S, Seo SK, Akhtar MS, Shin HS (2012) Novel graphene/polyaniline nanocomposites and its photocatalytic activity toward the degradation of rose Bengal dye. Chem Eng J 210:220–228. https://doi.org/10.1016/j.cej.2012.08.035

Amer WA, Omran MM, Rehab AF, Ayad MM (2018) Acid green crystal-based in situ synthesis of polyaniline hollow nanotubes for the adsorption of anionic and cationic dyes. RSC Adv 8:22536–22545. https://doi.org/10.1039/c8ra02236d

Amer WA, Omran MM, Ayad MM (2019a) Acid-free synthesis of polyaniline nanotubes for dual removal of organic dyes from aqueous solutions. Colloid Surf A-Physicochem Eng Asp 562:203–212. https://doi.org/10.1016/j.colsurfa.2018.10.081

Amer WA, Al-saida B, Ayad MM (2019b) Rational design of a polypyrrole-based competent bifunctional magnetic nanocatalyst. RSC Adv 9:18245. https://doi.org/10.1039/c9ra02544h

An L, Xu Y, Xu ZH, Chen LL, Yang ZH, Wang GH (2018) Coral-like polyaniline/TiO_2 porous micro-composite material: facile preparation, characterization, and enhanced visible-light photocatalytic activity. Phys Chem Nanoclust Nanomater 92:2265–2269. https://doi.org/10.1134/s00360244118110201

Ansari R, Mosayebzadeh Z (2011) Application of polyaniline as an efficient and novel adsorbent for azo dyes removal from textile wastewaters. Chem Pap 65:1–8. https://doi.org/10.2478/s11696-010-0083

Ansari R, Alaie S, Mohammad-Khan A (2011) Application of polyaniline for removal of Acid Green 25 from aqueous solutions. J Sci Ind Res 70:804–809.

Ansari MO, Khan MM, Ansari SA, Cho MH (2015) Electrically conductive polyaniline sensitized defective-TiO_2 for improved visible light photocatalytic and photoelectrochemical performance: a synergistic effect. New J Chem 39:8381–8388. https://doi.org/10.1039/c5nj01127b

Ansari MO, Kumar R, Ansari SA, Ansari SP, Barakat MA, Alshahries A, Cho MH (2017) Anion selective *p*TSA doped polyaniline@graphene oxide-multiwalled carbon nanotube composite for Cr(VI) and Congo red adsorption. J Colloid Interface Sci 496:407–415. https://doi.org/10.1016/j.jcis.2017.02.034

Archana S, Malarvizhi M, Muthirulan P, Sundaram MM (2016) Superior photocatalytic and antibacterial activities of conducting caramic TiO_2@poly(*o*-phenylenediamine) core–shell nanocomposites. J Mater Sci-Mater Electron 27:12691–12700. https://doi.org/10.1007/s10854-016-5403-7

Arshadnia I, Movahedi M, Rasouli N (2017) $MgFe_2O_4$ and $MgFe_2O_4$/$ZnFe_2O_4$ coated with polyaniline as a magnetically separable photocatalyst for removal of a two dye mixture in aqueous solution. Res Chem Intermed 43:4459–4474. https://doi.org/10.1007/s11164-017-2889-4

Asgari E, Esrafili A, Jafari AJ, Kalantary RR, Farzadkia M (2019) Synthesis of TiO_2/polyaniline photocatalytic nanocomposite and its effects on degradation of metronidazole in aqueous solutions under UV and visible light radiation. Desalin Water Treat 161:228–242. https://doi.org/10.5004/dwt.2019.24291

Ates M (2016) Biomedical application of electroactive polymers in electrochemical sensors: a review. J Adhes Sci Techol 30:1510–1536. https://doi.org/10.1080/01694243.2016.1150662

Ayad MM, Abu El-Nasr A (2010) Adsorption of cationic dye (methylene blue) from water using polyaniline nanotubes base. J Phys Chem C 114:14377–14383. https://doi.org/10.1021/jp103780w

Ayad M, Zaghlol S (2012) Nanostructured crosslinked polyaniline with high surface area: synthesis, characterization and adsorption of organic dye. Chem Eng J 204–206:79–86. https://doi.org/10.1016/j.cej.2012.07.102

Ayad MM, Abu El-Nasr A, Stejskal J (2012) Kinetics and isotherm studies of methylene blue adsorption onto polyaniline nanotubes base/silica composite. J Ind Eng Chem 18:1964–1969. https://doi.org/10.1016/j.jiec.2012.05.012

Ayad M, El-Hefnawy G, Zaghlol S (2013) Facile synthesis of polyaniline nanoparticles: its adsorption behavior. Chem Eng J 217:460–465. https://doi.org/10.1016/j.cej.2012.11.099

Ayad MM, Amer WA, Kotp MG (2017) Magnetic polyaniline-chitosan composites decorated with palladium nanoparticles for enhanced catalytic reduction of 4-nitrophenol. Mol Catal 439:72–80. https://doi.org/10.1016/j.mcat.2017.06.023

Ayad MM, Amer WA, Zaghlol S, Minisy IM, Bober P, Stejskal J (2018a) Polypyrrole-coated cotton textile as adsorbent of methylene blue dye. Chem Pap 72:1605–1618. https://doi.org/10.1007/s11696-018-0442-6

Ayad MM, Amer WA, Saghlol S, Maráková N, Stejskal J (2018b) Polypyrrole-coated cotton fabric decorated with silver nanoparticles for the catalytic removal of *p*-nitrophenol from water. Cellulose 25:7393–7404. https://doi.org/10.1007/s10570-018-2088-5

Babayan V, Kazantseva NE, Moučka R, Stejskal J (2017) Electromagnetic shielding of polypyrrole–sawdust composites: polypyrrole globules and nanotubes. Cellulose 24:3445–3451. https://doi.org/10.1007/s10570-017-1357-z

Bagheri M, Mardani E (2019) Removal of Acid Orange 7 dye from aqueous solutions using polyaniline-modified rice bran: isotherms, kinetics, and thermodynamics. Environ Health Eng Manage J 6:203–213. https://doi.org/10.15171/ehem.2019.23

Bahrudin NN, Nawi MA, Ismail WINW (2018a) Physical and adsorptive characterization of immobilized polyaniline for the removal of methyl orange dye. Korean J Chem Eng 35:1450–1461. https://doi.org/10.1007/s1814-018-0052-6

Bahrudin NN, Nawi MA, Nawawi WI (2018b) Photocatalytic enhancement of immobilized TiO_2-polyaniline bilayer (TiO_2-PBL) system for decolorization of methyl orange dye. Mater Res Bull 106:388–395. https://doi.org/10.1016/j.matresbull.2018.06.023

Bahrudin NN, Nawi MA, Nawawi WI (2019) Enhanced photocatalytic decolorization of methyl orange dye and its mineralization pathway by immobilized TiO_2/polyaniline. Res Chem Intermed 45:2771–2795. https://doi.org/10.1007/s11164-019-03762-y

Bai LZ, Li ZP, Zhang Y, Wang T, Lu RH, Zhou WF, Gao HX, Zhang SB (2015) Synthesis of water-dispersible graphene-modified magnetic polypyrrole nanocomposite and its ability to efficiently adsorb methylene blue from aqueous solution. Chem Eng J 279:757–766. https://doi.org/10.1016/j.cej.2015.05.068

Bai MD, Wang XL, Li BM (2018) Capacitative behavior and material characteristics of congo red doped poly(3,4-ethylene dioxythiophene). Electrochim Acta 283:590–596. https://doi.org/10.1016/j.electacta.2018.07.004

Baker CO, Huang XW, Nelson W, Kaner RB (2017) Polyaniline nanofibers: broadening applications for conducting polymers. Chem Soc Rev 46:1510–1525. https://doi.org/10.1039/c6cs00555a

Ballav N, Debnath S, Pillay K, Maity A (2015) Efficient removal of Reactive Black from aqueous solution using polyaniline coated ligno-cellulose as a potential adsorbent. J Mol Liq 209:387–396. https://doi.org/10.1016/j.molliq.2015.05.051

Bartel M, Wysocka B, Krug P, Kepińska D, Kijewska K, Blanchard GJ, Kaczynska K, Lubelska K, Wiktorska K, Głowala P, Wilczak M, Pisarek M, Twardowski A, Mazur M (2018) Magnetic polymer microcapsules loaded with Nile Red fluorescent. Spectrochim Acta A, Molec Biomolec Spectrosc 195:148–156. https://doi.org/10.1016/j.saa.2018.01.056

Baseri JR, Palanisamy PN, Sivakumar P (2013) Polyaniline nano composite for the adsorption of reactive dye from aqueous solutions: equilibrium and kinetic studies. Asian J Chem 25:4145–4149. https://doi.org/10.14233/ajchem.2013.12685

Bashir A, Hanif F, Yasmeen G, Mabood F, Hussain A, Abbas N, Bin Yousaf A, Aamir M, Manzoor S (2019) Polyaniline based magnesium nanoferrite composites as efficient photocatalysts for the photodegradation of Indigo Carmine in aqueous solutions. Desalin Water Treat 164:268–377. https://doi.org/10.5004/dwt.2019.24394

Beyki MH, Alijani H, Fazli Y (2016) Poly *o*-phenylenediamine-MgAl@$CaFe_2O_4$ nanohybrid for effective removing of lead(II), chromium(III) and anionic azo dye. Process Saf Environ Protect 102:687–699. https://doi.org/10.1016/j.psep.2016.04.027

Bhadra S, Khastgir D, Singha NK, Lee JH (2009) Progress in preparation, processing and applications of polyaniline. Prog Polym Sci 34:783–810. https://doi.org/10.1016/j.progpolymsci.2009.04.003

Bhaumik M, McCrindle R, Maity A (2013) Efficient removal of Congo red from aqueous solutions by adsorption onto interconnected polypyrrole-polyaniline nanofibres. Chem Eng J 228:506–515. https://doi.org/10.1016/j.cej.2013.05.026

Bhaumik M, Choi HJ, McCrindle RI, Maity A (2014) Composite nanofibers prepared from metallic iron nanoparticles and polyaniline: high performance for water treatment applications. J Colloid Interface Sci 425:75–82. https://doi.org/10.1016/j.jcis.2014.03.031

Bhaumik M, McCrindle RI, Maity A (2015) Enhanced adsorptive degradation of Congo red in aqueous solutions using polyaniline/Fe^0 composite nanofibers. Chem Eng J 260:716–729. https://doi.org/10.1016/j.cej.2014.09.014

Bhaumik M, McCrindle RI, Maity A, Agarwal S, Gupta VK (2016) Polyaniline nanofibers as highly effective re-usable adsorbent for removal of reactive black5 from aqueous solutions. J Colloid Interface Sci 466:442–451. https://doi.org/10.1016/j.jcis.2015.12.056

Bhowmik KL, Deb K, Bera A, Debnath A, Saha B (2018) Interaction of anionic dyes with polyaniline implanted cellulose: organic π-conjugated macromolecules in environmental applications. J Mol Liq 261:189–198. https://doi.org/10.1016/j.molliq.2018.03.128

Binaeian E, Tayebi HA, Rad AS, Afrashteh S (2018) Adsorption of acid blue on synthesized polymeric nanocomposites, PPy/MCM-41 and PAni/MCM-41: isotherm, thermodynamic and kinetic studies. J Macromol Sci Part A Pure Appl Chem 55:269–279. https://doi.org/10.1080/10601325.2018.1424554

Bingöl D, Veli S, Zor S, Özdemir U (2012) Analysis of adsorption of reactive azo dyes onto $CuCl_2$ doped polyaniline using Box-Behnken design approach. Synth Met 162:1566–1571. https://doi.org/10.1016/j.synthmet.2012.07.011

Biswas MRUD, Cho KY, Jung CH, Oh WC (2019) Novel synthesis of $LaNiSbWO_4$-G-PANI designed as quaternary type composite for high photocatalytic performance of anionic dye and trihydroxy benzoic acid under visible-light. Process Saf Environ Protect 126:348–355. https://doi.org/10.1016/j,psep.2019.04.022

Bober P, Stejskal J, Šeděnková I, Trchová M, Martinková L, Marek J (2015) The deposition of globular polypyrrole and polypyrrole nanotubes on cotton textile. Appl Surf Sci 356:737–741. https://doi.org/10.1016/j.apsusc.2015.08.105

Bober P, Li Y, Acharya U, Panthi Y, Pfleger J, Humpolíček P, Trchová M, Stejskal J (2018a) Acid Blue dyes in polypyrrole synthesis: the control of polymer morphology at nanoscale in the promotion of high conductivity and the reduction of cytotoxicity. Synth Met 237:40–49. https://doi.org/10.1016/j.synthmet.2018.01.010

Bober P, Trchová M, Kovářová J, Acharya U, Hromádková J, Stejskal J (2018b) Reduction of silver ions to silver with polyaniline/poly(vinyl alcohol) cryogels and aerogels. Chem Pap 72:1619–1628. https://doi.org/10.1007/s11696-017-0374-6

Bonfin CS, Franco JH, de Andrade AR (2019) Ethanol bioelectrooxidation in robust poly(methylene green-pyrrole)-mediated enzymatic biofuel cell. J Electroanal Chem 844:43–48. https://doi.org/10.1016/j.jelechem.2019.04.075

Boukoussa B, Hakiki A, Moulai S, Chikh S, Kherroub DE, Bouhajdar I, Guedal D, Messaoudi K, Mokhtar F, Hamacha R (2018) Adsorption behaviours of cationic and anionic dyes from aqueous solution on nanocomposite polypyrrole/SBA-15. J Mater Sci 53:7372–7386. https://doi.org/10.1007/s10853-018-2060-7

Broncová G, Shishkanova TV, Matějka P, Volf R, Král V (2004) Citrate selectivity of poly(neutral red) electropolymerized films. Anal Chim Acta 511:197–205. https://doi.org/10.1016/j.aca.2004.01.052

Broncová G, Shishkanova TV, Kronďák M, Volf R, Král V (2008) Optimalization of poly(neutral red) coated-wire electrode for determination of citrate in soft drinks. Sensors 8:594–606. https://doi.org/10.3390/s8020594

Broncová G, Shishkanova TV, Matějka P, Kubáč D, Král V (2016) Poly(neutral red) in multilayer electrode systems. Chem Listy 110:800–807.

Canoluk C, Gursoy SS (2017) Chemical modification of rose leaf with polypyrrole for the removal of Pb(II) and Cd(II) from aqueous solution. J Macromol Sci A: Pure Appl Chem 54:782–790. https://doi.org/10.1080/10601325.2017.1336722

Carević MV, Abazović ND, Mitrić MN, Ćirić-Marjanović G, Mojović MD, Ahrenkiel SP, Comor MI (2018) Properties of zirconia/polyaniline hybrid nanocomposites and their application as photocatalysts for degradation of model pollutants. Mater Chem Phys 205:130–137. https://doi.org/10.1016/j.matchemphys.2017.11.016

Castillo-Reyes BE, Ovando-Medina VM, Gonzáles-Ortega O, Alonso-Dávila PA, Juaréz-Ramírez I, Martinez-Gutiérrez H, Marquez-Herrera A (2015) TiO_2/polypyrrole nanocomposites photoactive under visible light synthesized by heterophase polymerization in the presence of different surfactants. Res Chem Intermed 41:8211–8231. https://doi.org/10.1007/s11164-014-1886-0

Chafai H, Laabd M, Elbariji S, Bazzaoui M, Albourine A (2017a) Study of congo red adsorption on the polyaniline and polypyrrole. J Disp Sci Technol 38:832–836. https://doi.org/10.1080/01932691.2016.1207185

Chafai H, Laabd M, Elamine M, Albourine A (2017b) Chemical synthesis and characterization of polyaniline: water depollution efficiency and effectiveness. Desalin Water Treat 83:314–320. https://doi.org/10.5004/dwt.2017.21194

Chani MTS, Karimov KS, Khalid FA, Abbas SZ, Bhatty MB (2013) Orange dye–polyaniline composite based impedance humidity sensors. Chin Phys B 22:010701. https://doi.org/10.1088/1674-1056/22/1/010701

Chatterjee MJ, Ahamed ST, Mitra M, Klulsi C, Mondal A, Banerjee D (2019) Visible-light influenced photocatalytic activity of polyaniline-bismuth selenide composites for the degradation of methyl orange, rhodamine B and malachite green dyes. Appl Surf Sci 470:472–483. https://doi.org/10.1016/j.apsusc.2018.11.085

Che XT, Trieu QVV, Tran TQ, Pham TD, VuTQ Tran TH, Mai TA (2018) Possible monitoring and removal of As(III) by an integrated system of electrochemical sensor and nanocomposite materials. J Nanomater 2018:9250463. https://doi.org/10.1155/2018/9250463

Chen S, Zhitomirsky I (2013) Influence of dopants and carbon nanotubes on polypyrrole electropolymerization and capacitive behavior. Mater Lett 98:67–70. https://doi.org/10.1016/j.matlet.2013.01.123

Chen J, Feng JT, Yan W (2016) Influence of metal oxides on the adsorption characteristics of PPy/metal oxides for methylene blue. J Colloid Interface Sci 475:26–35. https://doi.org/10.1016/j.jcis.2016.04.017

Chen XF, Huang Y, Zhang KC, Feng XS, Wang MY (2017a) Synthesis and high-performance of carbonaceous polypyrrole nanotubes coated with SnS_2 nanosheets anode materials for lithium ion batteries. Chem Eng J 330:470–479. https://doi.org/10.1016/j.cej.2017.07.180

Chen J, Shu CJ, Wang N, Feng JT, Ma HY, Yan W (2017b) Adsorbent synthesis of polypyrrole/TiO_2 for effective fluoride removal from aqueous solution for drinking water purification: adsorbent characterization and adsorption mechanism. J Colloid Interface Sci 495:44–52. https://doi.org/10.1016/j.jcis.2017.01.044

Chen Y, Lin ZH, Hao RR, Xu H, Huang CY (2019a) Rapid adsorption and reductive degradation of Naphthol Green B from aqueous solution by Polypyrrole/Attapulgite composites supported nanoscale zero-valent iron. J Hazard Mater 371:8–17. https://doi.org/10.1016/j.jhazmat.2019.02.096

Chen Y, Xu H, Long WC (2019b) Efficient removal of Acid Red 18 from aqueous solution by in situ polymerization of polypyrrole-chitosan composites. J Mol Liq 287:110888. https://doi.org/10.1016/j.molliq.2019.110888

Chen YJ, Zhu PF, Duan M, Li J, Ren ZH, Wang PP (2019c) Fabrication of a magnetically separable and dual Z-scheme PANI/Ag_3PO_4/$NiFe_2O_4$ composite with enhanced visible-light photocatalytic activity for organic pollutant elimination. Appl Surf Sci 486:198–211. https://doi.org/10.1016/j.apsusc.2019.04.232

Chigondo M, Paumo HK, Bhaumik M, Pillay K, Maity A (2019) Magnetic arginine-functionalized polypyrrole with improved and selective chromium(VI) ions removal from water. J Mol Liq 275:778–791. https://doi.org/10.1016/j.molliq.2018.11.032

Chiou NR, Epstein AJ (2005) Polyaniline nanofibers prepared by dilute polymerization. Adv Mater 13:1679–1683. https://doi.org/10.1002/adma.200401000

Chiwunze TE, Palakollu VN, Gill AAS, Kayamba F, Thapliyal NB, Karpoormath R (2019) A highly dispersed multi-walled carbon nanotubes and poly(methyl orange) based electrochemical sensor for the determination of an anti-malarial drug: amodiaquine. Mater Sci Eng C 97:285–292. https://doi.org/10.1016/j.msec.2018.112.018

Ćirić-Marjanović G, Blinova NV, Trchová M, Stejskal J (2007) Chemical oxidative polymerization of safranines. J Phys Chem B 111:2188–2199. https://doi.org/10.1021/jp067407w

Ćirić-Marjanović G, Pašti I, Gavrilov N, Janosević A, Mentus S (2013) Carbonised polyaniline and polypyrrole: towards advanced

nitrogen-containing carbon materials. Chem Pap 67:781–813. https://doi.org/10.2478/s11696-013-0312-1

Ćirić-Marjanović G, Mentus S, Pašti I, Gavrilov N, Krstić J, Travas-Sejdic J, Strover LT, Kopecká J, Morávková Z, Trchová M, Stejskal J (2014) Synthesis, characterization, and electrochemistry of nanotubular polypyrrole and polypyrrole-derived carbon nanotubes. J Phys Chem C 118:14770–14784. https://doi.org/10.1021/jp502862d

Collings PJ, Dickinson AJ, Smith EC (2010) Molecular aggregation and chromonic liquid crystals. Liq Cryst 37:701–710. https://doi.org/10.1080/02678292.2010.481910

Curran SA, Ellis AV, Vijayaraghavan A, Ajayan PM (2004) Functionalization of carbon nanotubes using phenosafranin. J Chem Phys 120:4886–4889. https://doi.org/10.1063/1.1644109

Czaja T, Wójcik K, Grzeszczuk M, Szostak R (2019) Polypyrrole–methyl orange Raman pH sensor. Polymers 11:715. https://doi.org/10.3390/polym11040715

Das R, Bhaumik M, Giri S, Maity A (2017) Sonocatalytic rapid degradation of Congo red dye from aqueous solution using magnetic Fe^0/polyaniline nanofibers. Untrason Sonochem 37:600–613. https://doi.org/10.1016/j.ultsonch.2017.02.022

de Lazzari AC, Soares DP, Sampaio NMFM, Silva BJG, Vidotti M (2019) Polypyrrole nanotubes for electrochemically controlled extraction pf atrazine, caffeine and progesterone. Microchim Acta 186:398. https://doi.org/10.1007/s00604-019-3545-z

Debnath S, Ballav N, Maity A, Pillay K (2015a) Development of polyaniline-lignocellulose composite for optimal adsorption of Congo red. Int J Biol Macromol 75:199–209. https://doi.org/10.1016/j.ijbiomac.2015.01.011

Debnath S, Ballav N, Maity A, Pillay K (2015b) Single stage batch adsorber design for efficient Eosin yellow removal by polyaniline coated ligno-cellulose. Int J Biol Macromol 72:732–739. https://doi.org/10.1016/j.ijbiomac.2014.09.018

Debnath S, Ballav N, Nyoni H, Maity A, Pillay K (2015c) Optimization and mechanism elucidation of the catalytic photodegradation of the dyes Eosin Yellow (EY) and Naphtol blue black by a polyaniline-coated titanium dioxide. Appl Cat B-Environ 163:330–342. https://doi.org/10.1016/j.apcatb.2014.08.011

Deng YC, Tang L, Zeng GM, Dong HR, Yan M, Wang JJ, Hu W, Wang JJ, Zhou YY, Tang J (2017) Enhanced visible light photocatalytic performance of polyaniline modified mesoporous single crystal TiO_2 microsphere. Appl Surf Sci 387:882–893. https://doi.org/10.1016/j.apsusc.2016.07.026

Dhanavel S, Nivethaa EAK, Dhanapal K, Gupta VK, Narayanan V, Stephen A (2016) α-MoO_3/polyaniline composite for effective scavenging of Rhodamine B, Congo red and textile dye effluent. RSC Adv 6:28871–28886. https://doi.org/10.1039/c6ra02576e

Diaz-Flores PE, Guzmán-Alváreez CJ, Ovando-Medina VM, Martínez-Gutiérrez H, González-Ortega O (2019) Synthesis of α-cellulose/magnetite/polypyrrole composite for the removal of reactive black 5 dye from aqueous solutions. Desalin Water Treat 155:350–363. https://doi.org/10.5004/dwt.2019.24013

Ding XD, Wang W, Zhang A, Zhang LS (2019) Efficient visible light degradation of dyes in wastewater by nickel–phosphorus plating–titanium dioxide complex electroless plating fabric. J Mater Res 34:999–1010. https://doi.org/10.1557/jmr.2019.16

Dong JJ, Lin Y, Zong HW, Yang HB (2019a) Hierarchical $LiFe_5O_8$@PPy core-shell nanocomposites as electrode materials for supercapacitors. Appl Surf Sci 470:1043–1052. https://doi.org/10.1016/j.apsusc.2018.11.204

Dong YY, Ma Y, Bai RQ, Zhang Q, Han YQ, Zhong SJ, Zhao YQ, Han L, Li TX (2019b) Exploring the effects of acid fuchsin on microscopic morphology and properties of polypyrrole. J Photopolym Sci Technol 32:51–56

Duan WZ, Li MH, Xiao WL, Wang NF, Niu BH, Zhou L (2019) Enhanced adsorption of three fluoroquinolone antibiotics using polypyrrole functionalized *Calotropis gigantea fiber*. Colloid Surf A-Physicochem Eng Asp 574:178–187. https://doi.org/10.1016/j.colsurfa.2019.04.068

Dubal D, Jagadale A, Chodankar NR, Kim DH, Gomez-Romero P, Holze R (2019) Polypyrrole nanopipes as a promising cathode material for Li-ion batteries and Li-ion capacitors: two-in-one approach. Energy Technol 7:193–200. https://doi.org/10.1002/ente.201800551

Duhan M, Kaur R (2019) Adsorptive removal of methyl orange with polyaniline nanofibers: an unconventional adsorbent for water treatment. Environ Technol. https://doi.org/10.1080/09593330.2019.1593511

Dutta K, De S (2017) Aromatic conjugated polymers for removal of heavy metal ions from wastewater: a short review. Environ Sci Water Res Technol 3:793–805. https://doi.org/10.1039/c7ew00154a

Dutta K, Rana D (2019) Polythiophenes: an emerging class of promising water purifying materials. Eur Polym J 116:370–385. https://doi.org/10.1016/j.eurpolymj.2019.04.033

Elsayed MA, Gobara M (2016) Enhancement removal of tartrazine dye using HCl-doped polyaniline and TiO_2-decorated PANI particles. Mater Res Express 3:085301. https://doi.org/10.1088/2053-1591/3/8/085301

Erdoğan MK, Karakışla M, Saçak M (2019) Morphologically different silver particles decorated conductive poly(*o*-anisidine)/wool fabric composites and investigation of catalytic activity in reduction of methylene blue. Mater Chem Phys 225:72–83. https://doi.org/10.1016/j.matchemphys.2018.12.021

Eslami MR, Alizadeh N (2019) Ultrasensitive and selective QCM sensor for detection of trace amounts of nitroexplosive vapors in ambient air based on polypyrrole–Bromophenol blue nanostruture. Sens Actuator B: Chem 278:55–63. https://doi.org/10.1016/j.snb.2018.09.060

Faisal M, Harraz FA, Ismail AA, Alsaiari MA, Al-Sayari SA (2019) Novel synthesis of polyaniline/$SrSnO_3$ nanocomposites with enhanced photocatalytic activity. Ceram Int 45:20484–20492. https://doi.org/10.1016/j.ceramint.2019.07.027

Fan LL, Wei CZ, Xu Q, Xu J (2017) Polypyrrole-coated cotton fabrics used for removal of methylene blue from aqueous solution. J Textile Inst 108:1847–1852. https://doi.org/10.1080/00405000.2017.1296989

Fedorova S, Stejskal J (2002) Surface and precipitation polymerization of aniline. Langmuir 18:5630–5632. https://doi.org/10.1021/la025665o

Feizpoor S, Habibi-Yangjeh A, Yubuta K (2018) Integration of carbon dots and polyaniline with TiO_2 nanoparticles: substantially enhanced photocatalytic activity to removal various pollutants under visible light. J Photochem Photobiol A-Chem 367:94–104. https://doi.org/10.1016/j.jphotochem.2018.08.017

Feng JT, Yan W, Zhang LZ (2009) Synthesis of polypyrrole micro/nanofibers via a self-assembly process. Microchim Acta 166:261–267. https://doi.org/10.1007/s00604-009-0188-5

Feng JT, Li JJ, Lv W, Xu H, Yang HH, Yan W (2014) Synthesis of polypyrrole nano-fibers with hierarchical structure and its adsorption property of Acid Red G from aqueous solution. Synth Met 191:66–73. https://doi.org/10.1016/j.synthmet.2014.02.013

Feng JT, Sun N, Wu DY, Yang HH, Xu H (2017) Preparation of Fe_3O_4/TiO_2/polypyrrole ternary magnetic composite and using as adsorbent for the removal of Acid Red G. J Polym Environ 25:781–791. https://doi.org/10.1007/s10924-016-0839-7

Feng TT, Yin H, Jiang H, Chai X, Li XL, Li DY, Wu J, Liu XH, Sun B (2019) Design and fabrication of polyaniline/Bi_2MoO_6 nanocomposites for enhanced visible-light-driven photocatalysis. New J Chem 43:9606–9613. https://doi.org/10.1039/c9nj01651a

Galář P, Khun J, Kopecký D, Scholtz V, Trchová M, Fučíková A, Jirešová J, Fišer L (2017) Influence of non-thermal plasma on

structural and electrical properties of globular and nanostructured conductive polymer polypyrrole in water suspension. Sci Rep 7:15068. https://doi.org/10.1038/s41598-017-15184-0

Gamal H, Attia NF (2019) Facile synthesis of textile-based filter for industrial wastewater treatment. Egypt J Chem 62:1419–1426. https://doi.org/10.21608/ejchem.2019.6638.1558

Gao HJ, Cai MH, Liao YW (2019) Enhance photocatalytic properties of TiO_2 using π–π^* conjugate system. J Disp Sci Technol 40:1469–1478. https://doi.org/10.1080/01932691.2018.1518143

Garcia-Fernandez MJ, Sancho-Querol S, Pastor-Bias MM, Sepulveda-Eascribano A (2017) Surfactant-assisted synthesis of conducting polymers. Application to the removal of nitrates from water. J Colloid Interface Sci 494:98–106. https://doi.org/10.1016/j.jcis.2017.01.081

Geetha A, Palanisamy N (2016) Studies oh adsorptive removal of Direct Green 6 using a non-conventional activated carbon and polypyrrole composite. Desalin Water Treat 57:20534–20543. https://doi.org/10.1080/19443994.2015.1107505

Gemeay AHJ, El-sharkawy RG, Mansour IA, Zaki AB (2012) Application of polyaniline/manganese dioxide composites for degradation of acid blue 25 by hydrogen peroxide in aqueous media. Bull Mater Sci 35:585–593. https://doi.org/10.1007/s12034-012-0328-0

Ghaemi N, Safari P (2018) Nanoporous SAPO-34 enhanced thin-film nanocomposite polymeric membrane: simultaneously high water permeation and complete removal of cationic/anionic dyes from water. J Hazard Mater 358:376–388. https://doi.org/10.1016/j.jhazmat.2018.07.017

Ghahramani A, Gheibi M, Eftekhari M (2019) Polyaniline-coated reduced graphene oxide as an efficient adsorbent for the removal of malachite green from water samples. Polym Bull 76:5269–5283. https://doi.org/10.1007/s00289-018-2651-0

Gholivand MB, Yamini Y, Dayeni M, Seidi S (2015) Adsorptive removal of alizarin red-S and alizarin yellow GG from aqueous solutions using polypyrrole-coated magnetic nanoparticles. J Environ Chem Eng 3:529–540. https://doi.org/10.1016/j.jece.2015.01.011

Gilja V, Novaković K, Travas-Sejdic J, Hrnjak-Mirgić Z, Roković MK, Zić M (2017) Stability and synergistic effect of polyaniline/TiO_2 photocatalysts in degradation of azo dye in wastewater. Nanomaterials 7:412. https://doi.org/10.3390/nano7120412

Gilja V, Vrban I, Mandić V, Žic M, Hrnjak-Murgić Z (2018) Preparation of PANI/ZnO composite for efficient photocatalytic degradation of Acid Blue. Polymers 10:940. https://doi.org/10.3390/polym10090940

Girotto EM, Gazotti WA, Tormena CF, De Paoli MA (2002) Photoelectronic and transport properties of polypyrrole doped with dianionic dye. Electrochim Acta 47:1351–1357. https://doi.org/10.1016/s0013-4686%5b01%5d00857-x

González-Casamachin DA, De la Rosa JR, Lucio-Ortiz CJ, De Haro De Rio DA, Martínez-Vargas DX, Flores-Escamilla GA, Guzman NED, Ovando-Medina VM, Moctezuma-Velazquez E (2019) Visible-light photocatalytic degradation of acid violet 7 dye in a continuous annular reactor using ZnO/PPy photocatalyst: synthesis, characterization, mass transfer effect evaluation and kinetic analysis. Chem Eng J 373:325–337. https://doi.org/10.1016/j.cej.2019.09.032

Gopal N, Asaithambi M, Sivakumar P, Sivakumar V (2014) Adsorption studies of a direct dye using polyaniline coated activated carbon prepared from Prosopis juliflora. J Water Process Eng 2:87–95. https://doi.org/10.1016/j.jwpe.2014.05.008

Gopal N, Asaithambi M, Sivakumar P (2016) Continuous fixed bed adsorption studies of Rhodamine-B dye using polymer bound adsorbent. Ind J Chem Technol 23:53–58.

Gorza FDS, Pedro GC, da Silva RJ, Medina Llamas JC, Alcaraz-Espinoza JJ, Chavez-Guajardo AE, de Meloa CP (2018) Electrospun polystyrene-(emeraldine base) mats as high-performance materials for dye removal from aqueous media. J Taiwan Inst Chem Eng 82:300–311. https://doi.org/10.1016/j.jtice.2017.10.034

Gospodinova N, Tomšík E (2015) Hydroge*n*-bonding versus π–π stacking in the design of organic semiconductors: from dyes to oligomers. Prog Polym Sci 43:33–47. https://doi.org/10.1016/j.progpolymsci.2014.10.010

Gouthaman A, Azarudeen RS, Gnanaprakasam A, Sivakumar VM, Thirumarimurungan M (2018) Polymeric composites for the removal of Acid red 52 dye from aqueous solutions: synthesis, characterization, kinetic and isotherm studies. Ecotoxicol Environ Saf 160:42–51. https://doi.org/10.1016/j.ecoenv.2018.05.011

Gouthaman A, Auslin Asir J, Gnanaprakasam A, Sivakumar VM, Thirumarimurugan M, Riswan Ahmed MA, Azarudeen RS (2019) Enhanced dye removal using polymeric nanocomposite through incorporation of Ag doped ZnO nanoparticles: synthesis and characterization. J Hazard Mater 373:493–503. https://doi.org/10.1016/j.jhazmat.2019.03.105

Gouveia-Caridade C, Romeiro A, Brett CMA (2013) Electrochemical and morphological characterization of polyphenazine films on copper. Appl Surf Sci 285:380–388. https://doi.org/10.1016/j.apsusc.2013.08.064

Grądzka E, Makowska P, Winkler K (2018) Chemically formed conducting polyazulene: from micro- to nanostructures. Synth Met 246:115–121. https://doi.org/10.1016/j.synthmet.2018.10.002

Guo X, Fei GT, Su H, Zhang LD (2011) Synthesis of polyaniline micro/nanospheres by a copper(II)-catalyzed self-assembly method with superior adsorption capacity of organic dye from aqueous solution. J Mater Chem 21:8618–8625. https://doi.org/10.1039/c0jm04489j

Guo N, Liang YM, Lan S, Liu L, Zhang JJ, Ji GJ, Gan SC (2014) Microscale hierarchical three-dimensional flowerlike TiO_2/PANI composite: synthesis, characterization, and its remarkable photocatalytic activity on organic dyes under UV-light and sunlight irradiation. J Phys Chem C 118:18343–18355. https://doi.org/10.1021/jp5044927

Guo WL, Hao FF, Yue XX, Liu ZH, Zhang QY, Li XH, Wei J (2016) Rhodamine B removal using polyaniline-supported zero-valent iron powder in the presence of dissolved oxygen. Environ Prog Sustain Energy 35:48–55. https://doi.org/10.1002/ep.12185

Gupta VK, Pathania D, Kothiyal NC, Sharma G (2014) Polyaniline zirconium(IV) silicophosphate nanocomposite for remediation of methylene blue dye from waste water. J Mol Liq 190:139–145. https://doi.org/10.1016/j.molliq.2013.10.027

Habibi-Yangjeh A, Shekofteh-Gohari M (2019) Synthesis of magnetically recoverable visible-light-induced photocataysts by combination of Fe_3O_4/ZnO with BiOI and polyaniline. Prog Nat Sci: Mater Int 29:145–155. https://doi.org/10.1016/j.pnsc.2019.03.003

Hamzehloo M, Farahani BKA, Rostamian R (2019) Adsorption behaviour of Reactive Black dye 5 by magnetically separable nanoadsorbent. Phys Chem Res 7:475–490. https://doi.org/10.22036/pcr.2019.186198.1639

Hao XY, Gong JY, Ren LZ, Zhang D, Xiao X, Jiang YX, Zhang F, Tong ZW (2017) Preparation of polyaniline modified BiOBr with enhanced photocatalytic activities. Funct Mater Lett 10:1750040. https://doi.org/10.1142/s1793604717500400

Haque MM, Wong DKY (2017) Improved dye entrapment-liberation performance at electrochemically synthesized polypyrrole-reduced graphene oxide nanocomposite films. J Appl Electrochem 47:777–788. https://doi.org/10.1007/s10800-017-1079-9

Harijan DKL, Chandra V, Yoon T, Kim KS (2018) Radioactive iodine capture and storage from water using magnetite nanoparticles encapsulated in polypyrrole. J Hazard Mater 344:576–584. https://doi.org/10.1016/j.jhazmat.2017.10.065

Harrison WJ, Mateer DL, Tiddy JT (1996) Liquid-crystalline J-aggregates formed by aqueous ionic cyanine dyes. J Phys Chem 100:2310–2321. https://doi.org/10.1021/jp952532l

Hasan M, Rashid MM, Hossain MM, Al Mesfer MK, Arshad M, Danish M, Lee M, El Jery A, Kumar N (2019) Fabrication of polyaniline/activated carbon composite and its testing for methyl orange removal: optimization, equilibrium, isotherm and kinetic study. Polym Test 77:105909. https://doi.org/10.1016/j.polymertesting.2019.105909

Hayat A, Raziq F, Khan M, Ullah I, Rahman MU, Khan WU, Khan J, Ahmad A (2019) Visible-light enhanced photocatalytic performance of polypyrrole/g-C_3N_4 composites for water splitting to evolve H_2 and pollutants degradation. J Photochem Photobiol A: Chem 379:88–98. https://doi.org/10.1016/j.jphotochem.2019.05.011

Herrera MU, Futalan CM, Gapusan R, Balela MDL (2018) Removal of methyl orange dye and copper(II) ions from aqueous solution using polyaniline-coated kapok (Ceiba pentandra) fibers. Water Sci Technol 78:1137–1147. https://doi.org/10.2166/wst.2018.385

Hryniewicz BM, Lima RV, Wolfart F, Vidotti M (2019) Influence of pH on the electrochemical synthesis of polypyrrole nanotubes and the supercapacitative performance evaluation. Electrochim Acta 393:447–457. https://doi.org/10.1016/j.electacta.2018.09.200

Hu XQ, Lu Y, Liu JH (2004) Synthesis of polypyrrole microtubes with actinomorphic morphology in the presence of a β-cyclodextrin derivative-methyl orange inclusion complex. Macromol Rapid Commun 25:1117–1120. https://doi.org/10.1002/marc.200400067

Hu SC, Zhou Y, Zhang LL, Liu SJ, Cui K, Lu YY, Li KN, Li XD (2018) Effect of indigo carmine concentration on the morphology and microwave adsorbing behavior of PPy prepared by template synthesis method. J Mater Sci 53:3016–3026. https://doi.org/10.1007/s10853-017-1702-5

Huang YS, Li JX, Chen XP, Wang XK (2014) Applications of conjugated polymer based composites in wastewater purification. RSC Adv 4:62160–62178. https://doi.org/10.1039/c4ra11496e

Huang LB, Xu W, Hao JH (2017) Energy device applications of synthesized 1D polymer nanomaterials. Small 13:1701820. https://doi.org/10.1002/smll.201701820

Humpolíček P, Radaskiewicz KA, Capáková Z, Pacherník J, Bober P, Kašpárková V, Rejmontová P, Lehocký M, Ponížil P, Stejskal J (2018) Polyaniline cryogels: biocompatibility of novel conducting macroporous material. Sci Rep 8:135. https://doi.org/10.1038/s41598-017-18290-1

Hussein MA, El-Shishtawy RM, Alamry KA, Asiri M, Mohamed SA (2019) Efficient water disinfection using hybrid polyaniline/graphene/carbon nanotube nanocomposites. Environ Technol 40:2813–2824. https://doi.org/10.1080/09593330.2018.1466921

Inzelt G (2017) Recent advances in the field of conducting polymers. J Solid State Electrochem 21:1965–1975. https://doi.org/10.1007/s10008-017-3611-6

Ivanova VT, Garina EO, Burtseva EI, Kirillova ES, Ivanova MV, Stejskal J, Sapurina IYu (2017) Conducting polymers as sorbents of influenza viruses. Chem Pap 71:495–503. https://doi.org/10.1007/s11696-016-0068-5

Jain R, Jadon N, Pawaiya A (2017) Polypyrrole based next generation electrochemical sensors and biosensors: a review. Trends Anal Chem 97:363–373. https://doi.org/10.1016/j.trac.2017.10.009

Janaki V, Vijayaraghavan K, Ramasamy AK, Lee KJ, Oh BT, Kamala-Kannan S (2012a) Competitive adsorption of Reactive Orange 16 and Reactive Brilliant Blue R on polyaniline/bacterial extracellular polysaccharides composite – a novel eco-friendly polymer. J Hazard Mater 241–2:110–117. https://doi.org/10.1016/j.jhazmat.2012.09.019

Janaki V, Oh BT, Vijayaraghavan K, Kim JW, Kim SA, Ramasamy AK, Kamala-Kannan S (2012b) Application of bacterial extracellular polysaccharides/polyaniline composite for the treatment of Remazol effluent. Carbohydr Polym 88:1002–1008. https://doi.org/10.1016/j.carbpol.2012.01.045

Janaki V, Vijayaraghavan K, Oh BT, Lee KJ, Muthuchelian K, Ramasamy AK (2012c) Starch/polyaniline nanocomposite for enhanced removal of reactive dyes from synthetic effluent. Carbohydr Polym 90:1437–1444. https://doi.org/10.1016/j.carbpol.2012.07.012

Janaki V, Oh BT, Shanthi K, Lee KJ, Ramasamy AM, Kamala-Kannan S (2012d) Polyaniline/chitosan composite: an eco friendly polymer for enhanced removal of dyes from aqueous solution. Synth Met 162:974–980. https://doi.org/10.1016/j.synthmet.2012.04.015

Janaki V, Vijayaraghavan K, Oh BT, Ramasamy AK, Kamala-Kannan S (2013) Synthesis, characterization and application of cellulose/polyaniline nanocomposite for the treatment of simulated textile effluent. Cellulose 20:1153–1166. https://doi.org/10.1007/s10570-013-9910-x

Jangid NK, Chauhan NPS, Punjabi PB (2014) Novel-dye-substituted polyanilines: conducting and antimicrobial properties. Polym Bull 71:2611–2630. https://doi.org/10.1007/s00289-014-1210-6

Jangid NK, Chauhan NPS, Punjabi PB (2015) Preparation and characterization of polyanilines bearing Rhodamine 6-G and Azure B as pendant groups. J Macromol Sci A: Pure Appl Chem 52:95–104. https://doi.org/10.1080/190601325.2015.980714

Javadian H, Angaji MT, Naushad M (2014) Synthesis and characterization of polyaniline/γ-alumina nanocomposite: a comparative study of the adsorption of three different anionic dyes. J Ind Eng Chem 20:3890–3900. https://doi.org/10.1016/j.jiec.2013.12.095

Jeong WH, Amna T, Ha YM, Hassan MS, Kim HC, Khil MS (2014) Novel PANI nanotube@TiO_2 composite as efficient chemical and biological disinfectant. Chem Eng J 246:204–210. https://doi.org/10.1016/j.cej.2014.02.054

Jevremović A, Bober P, Mičušík M, Kuliček J, Acharya U, Pfleger J, Milojević-Rakić M, Krajišnik D, Trchová M, Stejskal J, Ćirić-Marjanović G (2019) Synthesis and characterization of polyaniline/BEA zeolite composites and their application in nicosulfuron adsorption. Micropor Mesopor Mater 287:234–245. https://doi.org/10.1016/j.micromeso.2019.06.006

Jia YJ, Jiang JC, Sun K, Dai TY (2012) Enhancement of capacitance performance of activated carbon–polyaniline composites by introducing methyl orange. Electrochim Acta 71:213–218. https://doi.org/10.1016/j.electacta.2012.03.150

Jiang Y, Niu TC, Wang ZH, Tan WS, Liu F, Kong Y (2018) Electrochemical polymerization of alizarin and the electrochemical properties of poly(alizarin). Ionics 24:1391–1397. https://doi.org/10.1007/s11581-017-2288-2

Jiao Z, Tang Y, Zhao PD, Li S, Sun TC, Cui SC, Cheng LL (2019) Synthesis of *Z*-scheme g-C_3H_4/PPy/Bi_2WO_6 composite with enhanced visible-light photocatalytic performance. Mater Res Bull 113:241–249. https://doi.org/10.1016/j.materresbull.2019.02.016

Jing LQ, Xu YG, Xie M, Liu J, Deng JJ, Huang LY, Xu H, Li HM (2019) Three dimensional polyaniline $MgIn_2S_4$ nanoflower photocatalysts accelerated interfacial charge transfer for the photoreduction of Cr(VI), photodegradation of organic pollution and photocatalytic H_2 production. Chem Eng J 360:1601–1612. https://doi.org/10.1016/j.cej.2018.10.214

Joulazadeh M, Navarchian AH (2015) Polypyrrole nanotubes versus nanofibers: a proposed mechanism for predicting the final morphology. Synth Met 199:37–44. https://doi.org/10.1016/j.synthmet.2014.10.036

Jung HR, Kim KN, Lee WJ (2019) Heterostructured $Co_{0.5}Mn_{0.5}Fe_2O_4$-polyaniline nanofibers: highly efficient photocatalysis for photodegradation of methyl orange. Korean J Chem Eng 36:807–815. https://doi.org/10.1007/s11814-019-0258-2

Kang ZP, Zhang YHPJ, Zhu ZG (2019) A shriveled rectangular carbon tube with the concave surface for high-performance enzymatic glucose/O_2 biofuel cells. Biosens Bioelectron 132:76–83. https://doi.org/10.1016/j.bios.2019.02.044

Kannusamy P, Sivalingam T (2013) Synthesis of porous chitosan-polyaniline/ZnO hybrid composite and application for removal of reactive orange 16 dye. Colloid Surf B-Biointerfaces 108:229–238. https://doi.org/10.1016/j.colsurfb.2013.02.015

Kanwal F, Rehman R, Bakhsh IQ (2018) Batch wise sorptive amputation of diamond green dye from aqueous medium by novel polyaniline-Alstonia scholaris leaves composite in ecofriendly way. J Clean Prod 196:350–357. https://doi.org/10.1016/j.jclepro.2018.06.056

Karabiberoglu SU, Dursun Z (2017) Over-oxidized poly(phenol red) film modified glassy carbon electrode for anodic stripping voltammetric determination of ultra-trace antimony(III). Electroanalysis 29:1069–1080. https://doi.org/10.1002/elan.201600629

Karamipour A, Rasouli N, Movahedi M, Salavati H (2016) A kinetic study on adsorption of Congo red from aqueous solution by ZnO-$ZnFe_2O_4$-polypyrrole magnetic nanocomposite. Phys Chem Res 4:291–301.

Karpuraranjith M, Thambidurai S (2016) Biotemplate SnO_2 particles intercalated PANI matrix: enhanced photo catalytic activity for degradation of MB and RY-15 dye. Polym Degrad Stab 133:108–118. https://doi.org/10.1016/j.polydegradstab.2016.08.006

Karri RR, Tanzifi M, Yaraki MT, Sahu JN (2018) Optimization and modeling of methyl orange adsorption on polyaniline nanoadsorbent through response surface methodology and differential evolution embedded neural network. J Environ Manag 223:517–529. https://doi.org/10.1016/j.jenvman.2018.06.027

Kaushal S, Badru R, Kumar S, Kaur H, Singh P (2018) Efficient removal of cationic and anionic dyes from their binary mixtures by organic-inorganic hybrid material. Inorg Organometal Polym Mater 28:968–977. https://doi.org/10.1007/s10904-018-0817-8

Kharazi P, Rahimi R, Rabbani M (2019) Copper ferrite-polyaniline nanocomposite: structural, thermal, magnetic and dye adsorption properties. Solid State Sci 93:95–100. https://doi.org/10.1016/j.solidstatesciences.2019.05.007

Khatoon H, Ahmad S (2017) A review on conducting polymer reinforced polyurethane composites. J Ind Eng Chem 53:1–12. https://doi.org/10.1016/j.jiec.2017.03.036

Kim KN, Jung HR, Lee WJ (2017) Magnetically separable hollow $MnFe_2O_4$-polyaniline composite nanofibers: highly enhanced visible light photodegradation of methyl orange. Sci Adv Mater 9:1993–1997. https://doi.org/10.1166/sam.2017.3201

Kim Y, Lin Z, Jeon I, Van Voorhis T, Swager TM (2018) Polyaniline nanofiber electrode for reversible capture and release of mercury(II) from water. J Am Chem Soc 140:14413–14420. https://doi.org/10.1021/jacs.8b09119

Kohl M, Kalendová A, Schmidtová E (2017) Enhancing corrosion resistance of zinc-filled protective coatings using conductive polymers. Chem Pap 71:409–421. https://doi.org/10.1007/s11696-016-0054-y

Kong P, Liu P, Tan H, Pei LJ, Wang J, Zhu PQ, Gu XM, Zheng ZF, Li Z (2019a) Conjugated HCl-doped polyaniline for photocatalytic oxidative coupling of amines under visible light. Catal Sci Technol 9:753–761. https://doi.org/10.1039/c8cy02280a

Kong FM, Li SX, Liu CJ, Yang Y, Tan ZL (2019b) Synergistic effect of POMPCs and PPy for enhancing visible-light photocatalytic activity and high quantum yields. J Cluster Sci 30:553–559. https://doi.org/10.1007/s10876-019-01506-x

Konyushenko EN, Stejskal J, Trchová M, Hradil J, Kovářová J, Prokeš J, Cieslar M, Hwang JY, Chen KH, Sapurina I (2006) Multi-wall carbon nanotubes coated with polyaniline. Polymer 47:5715–5723. https://doi.org/10.1016/j.polymer.05.059

Kopecká J, Kopecký D, Vrňata M, Fitl P, Stejskal J, Trchová M, Bober P, Morávková Z, Prokeš J, Sapurina I (2014) Polypyrrole nanotubes: mechanism of formation. RSC Adv 4:1551–1558. https://doi.org/10.1039/c3ra45841e

Kopecká J, Mrlík M, Olejník R, Kopecký D, Vrňata M, Prokeš J, Bober P, Morávková Z, Trchová M, Stejskal J (2016) Polypyrrole nanotubes and their carbonized analogs: synthesis, characterization, gas sensing properties. Sensors 16:1917. https://doi.org/10.3390/s16111917

Kopecký D, Varga M, Prokeš J, Vrňata M, Trchová M, Kopecká J, Václavík M (2017) Optimization routes for high conductivity of polypyrrole nanotubes prepared in the presence of methyl orange. Synth Met 230:89–96. https://doi.org/10.1016/j.synthmet.2017.06.004

Koysuren O (2019) Improving ultraviolet light photocatalytic activity of polyaniline/silicon carbide composites by Fe-doping. J Appl Polym Sci 136:48524. https://doi.org/10.1002/app.48524

Koysuren O, Koysuren NH (2019) Photocatalytic activity of polyaniline/Fe-doped TiO_2 composites by in situ polymerization method. J Macromol Sci Part A Pure Appl Chem 56:267–276. https://doi.org/10.1080/10601325.2019.1565548

Krehula LK, Stjepanovic J, Perlog M, Krehula S, Gilja V, Travas-Sejdic J, Hrnjak-Murgic Z (2019) Conducting polymer polypyrrole and titanium dioxide nanocomposites for photocatalysis of RR45 dye under visible light. Polym Bull 76:1697–1715. https://doi.org/10.1007/s00289-018-2463-2

Krishnaswamy S, Ragupathi V, Raman Panigrahi P, Nagarajan GS (2019) Study of optical and electrical property of NaI-doped polypyrrole thin film with excellent photocatalytic property at visible light. Polym Bull 76:5213–5231. https://doi.org/10.1007/s00289-018-2650-1

Kumar R (2016) Mixed phase lamellar titania-titanate anchored with Ag_2O and polypyrrole for enhanced adsorption and photocatalytic activity. J Colloid Interface Sci 477:83–93. https://doi.org/10.1016/j.jcis.1016.05.039

Kumar R, Ansari MO, Parveen N, Barakat MA, Cho MH (2015) Simple route for the generation of differently functionalized PVC@graphene–polyaniline fiber bundles for the removal of Congo red from wastewater. RSC Adv 5:61486–61494. https://doi.org/10.1039/c5ra10378a

Kumar R, Ansari MO, Parveen N, Oves M, Barakat MA, Alshahri A, Khan MY, Cho MH (2016) Facile route to a conducting ternary polyaniline@TiO_2/GN nanocomposite for environmentally benign applications: photocatalytic degradation of pollutants and biological activity. RSC Adv 6:111308–111317. https://doi.org/10.1039/c6ra24079h

Kumar R, Oves M, Almeelbi T, Al-Makishah NH, Barakat MA (2017) Hybrid chitosan/polyaniline-polypyrrole biomaterial for enhanced adsorption and antimicrobial activity. J Colloid Interface Sci 490:488–496. https://doi.org/10.1016/j.jcis.2016.11.082

Kumar R, Ansari SA, Barakat MA, Aljaafari A, Cho MH (2018) A polyaniline@MoS_2-based organic–inorganic nanohybrid for the removal of Congo red: adsorption kinetic, thermodynamic and isotherm studies. New J Chem 42:18802–18809. https://doi.org/10.1039/c8nj02803f

Lakshmi PV, Rajagopalan V (2016) A new synthetic nanocomposite for dye degradation in dark and light. Sci Rep 6:38606. https://doi.org/10.1038/srep38606

Lavanya M, Reddy YVM, Kiranmai S, Venu M, Madhavi G (2015) Selective determination of dopamine in presence of ascorbic acid by using Triton X-100 poly(safranin) modified carbon paste electrode. Anal Bioanal Electrochem 7:555–568.

Le TA, Tran NQ, Hong Y, Lee H (2019) Intertwined titanium carbide MXene within a 3 D Tangled polypyrrole nanowires matrix for enhanced supercapacitor performances. Chem Eur J 25:1037–1043. https://doi.org/10.1002/chem.201804291

Lee SL, Chang CJ (2019) Recent developments about conductive polymer based composite photocatalysts. Polymers 11:206. https://doi.org/10.3390/polym11020206

Lee JW, Lee HI, Park SJ (2018) Facile synthesis of petroleum-based activated carbons/tubular polypyrrole composites with enhanced electrochemical performance as supercapacitor electrode materials. Electrochim Acta 263:447–453. https://doi.org/10.1016/j.elecacta.2018.01.071

Lei H, Pan N, Wang QX, Zou H (2018) Facile synthesis of phytic acid impregnated polyaniline for enhanced U(VI) adsorption. J Chem Eng Data 63:3989–3997. https://doi.org/10.1021/acs.jced.8b00688

Li D, Huang JX, Kaner RB (2009) Polyaniline nanofibers: a unique polymer nanostructure for versatile applications. Acc Chem Res 42:135–142. https://doi.org/10.1021/ar800080n

Li JJ, Feng JT, Yan W (2012) Synthesis of polypyrrole-modified TiO_2 composite adsorbent and its adsorption performance on Acid Red G. J Appl Polym Sci 128:3231–3239. https://doi.org/10.1002/app38525

Li JJ, Feng JT, Yan W (2013) Excellent adsorption desorption characteristics of polypyrrole/TiO_2 composite for Methylene Blue. Appl Surf Sci 279:400–408. https://doi.org/10.1016/j.apsusc.2013.04.127

Li XQ, Qi FF, Zhou L, He L, Xu Q (2015) *p*-Toluene sulfonate and polypyrrole modified Nylon 6 nanofibers mat for solid phase extraction of Basic Orange II. Chin J Anal Chem 43:1594–1599.

Li YB, Jiang YM, Hu SC, Zhang XD, Zhai J, Han HC, Xiao D, Liu PF (2016) Control of morphology and electromagnetic properties of polypyrrole synthesized by the template method. High Perform Polym 28:225–230. https://doi.org/10.1177/0954008315577822

Li DL, Yang YG, Li CZ, Liu YF (2017a) A mechanistic study on decontamination of methyl orange dyes from aqueous phase by mesoporous pulp waste and polyaniline. Environ Res 154:139–144. https://doi.org/10.1016/j.envres.2016.12.027

Li Y, Bober P, Trchová M, Stejskal J (2017b) Polypyrrole prepared in the presence of methyl orange and ethyl orange: nanotubes versus globules. A comparison study on the improvement of conductivity. J Mater Chem C 5:4236–4245. https://doi.org/10.1039/c7tc00206h

Li XL, Lu HJ, Zhang Y, He F (2017c) Efficient removal of organic pollutants from aqueous media using newly synthesized polypyrrole/CNTs-$CoFe_2O_4$ magnetic nanocomposites. Chem Eng J 316:893–902. https://doi.org/10.1016/j.cdej.2017.02.037

Li J, Wu Z, Duan QY, Alsaedi A, Hayat T, Chen CL (2018a) Decoration of ZIF-8 on polypyrrole nanotubes for highly efficient and selective capture of U(VI). J Clean Prod 204:896–905. https://doi.org/10.1016/j.jclepro.2018.09.050

Li XQ, Wang JD, Hu ZM, Li MJ, Ogino K (2018b) In situ polypyrrole polymerization enhances the photocatalytic activity of nanofibrous TiO_2/SiO_2 membranes. Chin Chem Lett 29:166–170. https://doi.org/10.1016/j.cclet.2017.05.020

Li XH, Miao JJ, Yin ZD, Xu XD, Shi HM (2019a) Polypyrrole-modified Nylon 6 nanofibers as adsorbent for the extraction of two β-lactam antibiotics in water followed by determination with capillary electrophoresis. Molecules 24:2198. https://doi.org/10.3390/molecules24122198

Li JJ, Feng JT, Yan W (2019b) Enhanced adsorption performance of PPy/TiO_2 prepared on surface of TiO_2 without calcination. SN Appl Sci 1:617. https://doi.org/10.1007/s42452-019-0628-8

Lin J, Xu XL, Wang J, Zhang BF, Li D, Wang C, Jin YL, Zhu JB (2018) Nitrogen-doped hierarchically porous carbonaceous nanotubes for lithium ion batteries. Chem Eng J 352:964–971. https://doi.org/10.1016/j.cej.2018.06.057

Lin Y, Wu X, Han Y, Yang CP, Ma Y, Du C, Teng Q, Liu HY, Zhong YY (2019) Spatial separation of photogenerated carriers and enhanced photocatalytic performance on Ag_3PO_4 catalysts via coupling with PPy and MWCNT. Appl Catal B-Environ 258:UNSP117969. https://doi.org/10.1016/j.apcatb.2019.117969

Liu XQ, Cai L (2018) Novel indirect *Z*-scheme photocatalyst of Ag nanoparticles and polymer polypyrrole co-modified BiOBr for photocatalytic decomposition of organic pollutants. Appl Surf Sci 445:242–254. https://doi.org/10.1016/j.apsusc.2018.03.178

Liu XQ, Cai L (2019) A novel double Z-scheme BiOBr-GO-polyaniline photocatalyst: study on the excellent photocatalytic performance and photocatalytic mechanism. Appl Surf Sci 483:875–887. https://doi.org/10.1016/j.apsusc.2019.03.273

Liu JL, Liu P (2019) Synthesis and electrochemical properties of various dimensional poly(1,5-diaminoanthraquinone) nanostructures: nanoparticles, nanotubes and nanoribbons. J Colloid Interface Sci 542:1–7. https://doi.org/10.1016/j.jcis.2019.01.120

Liu WW, Li XQ, Li MJ, Li YG, Ge MQ (2015) Preparation of polyaniline/filter paper composite for removal of Coomassie Brilliant Blue. Polym Polym Compos 23:191–197. https://doi.org/10.1177/096739111502300310

Liu YX, Yan MY, Geng YY, Huang J (2016) Laccase immobilization on poly(*p*-phenylenediamine)/Fe_3O_4 nanocomposite for Reactive Blue 19 dye removal. Appl Sci 6:232. https://doi.org/10.3390/app60890232

Liu YP, Li JJ, Zhu JW, Lyu W, Xu H, Feng JT, Yan W (2018a) The adsorption property and mechanism of phenyl/amine end-capped tetraaniline for alizarin red S. Colloid Polym Sci 296:1777–1786. https://doi.org/10.1007/s00396-018-4401-0

Liu WK, Yang L, Xu SH, Chen Y, Liu BH, Li Z, Jiang CL (2018b) Efficient removal of hexavalent chromium from water by an adsorption–reduction mechanism with sandwiched nanocomposites. RSC Adv 8:15087–15093. https://doi.org/10.1039/c8ra01805g

Liu XT, Zhu HC, Wu JJ, Wang F, Wei FY (2019) The improved photocatalytic capacity derived from AgI-modified mesoporous PANI spherical shell with open pores. Res Chem Intermed 45:2587–2603. https://doi.org/10.1007/s11164-019-03753-z

Loguercio LF, Demingos P, de Mattos Manica L, Griep JB, Santos MJL, Ferreira J (2016) Simple one-step method to synthesize polypyrrole-indigo carmine-silver nanocomposite. J Chem 2016:5284259. https://doi.org/10.1155/2016/5284259

Long YZ, Li MM, Gu CZ, Wan MX, Duvail JL, Liu ZW, Fan ZY (2011) Recent advances in synthesis, physical properties and applications of conducting polymer nanotubes and nanofibers. Prog Polym Sci 36:1415–1442. https://doi.org/10.1016/j.progpolymsci.2011.04.001

Lu TT, Zhu YF, Wang WB, Qi YX, Wang AQ (2018) Polyaniline-functionalized porous adsorbent for Sr^{2+} adsorption. J Radioanal Nuclear Chem 317:907–917. https://doi.org/10.1007/s10967-018-5935-9

Luguercio LF, Alves CC, Thesing A, Ferreira J (2015) Enhanced electrochromic properties of a polypyrrole–indigo carmine–gold nanoparticles composite. Phys Chem Chem Phys 17:1234–1240. https://doi.org/10.1039/c4cp04262j

Lyu W, Yu MT, Feng JT, Yan W (2018) Highly crystalline polyaniline nanofibers coating with low-cost biomass for easy separation and high efficient removal of anionic dye ARG from aqueous solution. Appl Surf Sci 458:413–424. https://doi.org/10.1016/japsusc.2018.07.074

Lyu W, Yu MT, Feng JT, Yan W (2019) Facile synthesis of coral-like hierarchical polyaniline micro/nanostructures with enhanced supercapacitance and adsorption performance. Polymer 162:130–138. https://doi.org/10.1016/j.polymer.2018.12.037

Ma FF, Zhang D, Zhang N, Huang T, Wang Y (2018) Polydopamine-assisted deposition of polypyrrole on electrospun poly(vinylidene fluoride) nanofibers for bidirectional removal of cation and anion dyes. Chem Eng J 354:432–444. https://doi.org/10.1016/j.cej.2018.08.948

Ma ML, Yang YY, Li WT, Ma Y, Tong ZY, Huang WB, Chen L, Wu GL, Wang HL, Lyu P (2019) Synthesis of yolk-shell structure Fe_3O_4/P(MAA-MBAA)-PPy/Au/void/TiO_2 magnetic microspheres as visible light active photocatalyst for degradation of organic pollutants. J Alloys Compd 810:151807. https://doi.org/10.1016/j.jallcom.2019.151807

MacDiarmid AG (2001) "Synthetic metals": a novel role for organic polymers (Nobel lecture). Angew Chem-Int Ed 40:2581–2590. https://doi.org/10.1002/1521-3773(20010716)40:14%3c2581:aid-anie2581%3e3.0.co;2-2

Mahanta D, Madras G, Radhakrishnan S, Patil S (2008) Adsorption of sulfonated dyes by polyaniline emeraldine salt and its kinetics. J Phys Chem B 112:10153–10157. https://doi.org/10.1021/jp803903x

Mahanta D, Munichandraiah N, Radhakrishnan S, Madras G, Patil S (2011a) Polyaniline modified electrodes for detection of dyes. Synth Met 161:659–664. https://doi.org/10.1016/j.synthmet.2011.01.005

Mahanta D, Manna U, Madras G, Patil S (2011b) Multilayer self-assembly of TiO_2 nanoparticles and polyaniline-grafted chitosan copolymer (CPANI) for photocatalysis. ACS Appl Mater Interfaces 3:84–92. https://doi.org/10.1021/am1009265

Mahlangu T, Das R, Abia LK, Onyango M, Ray SS, Maity A (2019) Thiol-modified magnetic polypyrrole nanocomposite: an effective adsorbent for the adsorption of silver ions from aqueous solution and subsequent water disinfection by silver-laden nanocomposite. Chem Eng J 360:423–434. https://doi.org/10.1016/j.cej.2018.11.231

Mahto TK, Chowdhuri AR, Sahu SK (2014) Polyaniline-functionalized magnetic nanoparticles for the removal of toxic dye from wastewater. J Appl Polym Sci 131:40840. https://doi.org/10.1002/app.40840

Mahto TK, Chandra S, Haldar C, Sahu SK (2015) Kinetic and thermodynamic study of polyaniline functionalized magnetic mesoporous silica for magnetic field guided dye adsorption. RSC Adv 5:47909–47919. https://doi.org/10.1039/c5ra08284f

Majumdar S, Baishya A, Mahanta D (2019) Kinetic and equilibrium modeling of anionic dye adsorption on polyaniline emeraldine salt: batch and fixed bed column studies. Fiber Polym 20:1226–1235. https://doi.org/10.1007/s12221-019-8355-8

Mao H, Cao ZQ, Guo X, Dyn DY, Liu DL, Wu SY, Zhang Y, Song XM (2019) Ultrathin NiS/$Ni(OH)_2$ nanosheets filled within ammonium polyacrylate-functionalized polypyrrole nanotubes as an unique nanoconfined system for nonenzymatic glucose sensors. ACS Appl Mater Interfaces 11:10153–10162. https://doi.org/10.1021/acsami.8b20726

Maqbool M, Bhatti HN, Sadaf S, Zahid M, Shahid M (2019) A robust approach towards green synthesis of polyaniline-*Scenedesmus* biocomposite for wastewater treatment applications. Mater Res Exp 6:055308. https://doi.org/10.1088/2053-1591/ab025d

Maráková N, Humpolíček P, Kašpárková V, Capáková Z, Martinková L, Bober P, Trchová M, Stejskal J (2017) Antimicrobial activity and cytotoxicity of cotton fabric coated with conducting polymers, polyaniline or polypyrrole, and with deposited silver nanoparticles. Appl Surf Sci 356:169–176. https://doi.org/10.1016/j.apsusc.2016.11.024

Marquez-Herrera A, Ovando-Medina VM, Castillo-Reyes BE, Zapata-Torresa M, Mendelez-Lira M, González-Castaneda J (2016) Facile synthesis pf $SrCO_3$-$Sr(OH)_2$/PPy nanocomposite with enhanced photocatalytic activity under visible light. Materials 9:30. https://doi.org/10.3390/ma9010030

Maruthapandi M, Kumar VB, Luong JHT, Gedanken A (2018) Kinetics, isotherm, and thermodynamic studies on methylene blue adsorption on polyaniline and polypyrrole macro–nanoparticles synthesized by *C*-dot-initiated polymerization. ACS Omega 3:7196–7203. https://doi.org/10.1021/acsomega.8b00478

Megha R, Ravikiran YT, Vijaya Kumari SC, Raj Prakash HG, Ramana CVV, Thomas S (2019) Enhancement in alternating current conductivity of HCl doped polyaniline by modified titania. Compos Interfaces 26:309–324. https://doi.org/10.1080/09276440.2018.1499352

Meng Y, Zhang LY, Chai LY, Yu WT, Wang T, Wang HY (2014) Facile and large-scale synthesis of poly(*m*-phenylenediamine) nanobelts with high surface area and superior dye adsorption ability. RSC Adv 4:45244–45250. https://doi.org/10.1039/c4ra06553k

Meng OF, Cai KF, Chen YX, Chen LD (2017) Research progress on conducting polymer based supercapacitor electrode materials. Nano Energy 36:268–285. https://doi.org/10.1016/j.nanoen.2017.04.040

Mesdaghi S, Yousefi M, Sadr MH, Mahdavian A (2019) The effect of PANI and MWCNT on magnetic and photocatalytic properties of substituted barium hexaferrite nanocomposites. Mater Chem Phys 236:121786. https://doi.org/10.1016/j.matchemphys.2019.121786

Metwally SS, Hassan HS, Sam NM (2019) Impact of environmental conditions on the sorption behavior of ^{60}C and $^{152+154}Eu$ radionuclides onto polyaniline/zirconium aluminate composite. J Mol Liq 287:110941. https://doi.org/10.1016/j.molliq.2019.110941

Min SX, Wang F, Han YQ (2007) An investigation on synthesis and photocatalytic activity of polyaniline sensitized nanocrystalline TiO_2 composites. J Mater Sci 42:9966–9972. https://doi.org/10.1007/s10853-007-2074-z

Min SX, Wang F, Feng L, Tong YC, Yang ZR (2008) Synthesis and photocatalytic activity of TiO_2/conjugated polymer complex nanoparticles. Chin Chem Lett 19:742–746. https://doi.org/10.1016/j.cclet.2008.03.016

Minisy IM, Bober P, Acharya U, Trchová M, Hromádková J, Pfleger J, Stejskal J (2019a) Cationic dyes as morphology-guiding agents for one-dimensional polypyrrole with improved conductivity. Polymer 174:11–17. https://doi.org/10.1016/j.polymer.2019.04.045

Minisy IM, Salahuddin NA, Ayad MM (2019b) Chitosan/polyaniline hybrid for removal of cationic and anionic dyes from aqueous solutions. J Appl Polym Sci 136:47056. https://doi.org/10.1002/app.47056

Minisy IM, Gavrilov N, Acharya U, Morávková Z, Unterweger C, Mičušík M, Filippov SK, Kredatusová J, Pašti IA, Breitenbach S, Ćirić-Marjanović G, Stejskal J, Bober P (2019c) Tailoring of carbonized polypyrrole nanotubes core by different polypyrrole shells for oxygen reduction reaction selectivity modification. J Colloid Interface Sci 551:184–194. https://doi.org/10.1016/j.jcis.2019.04.064

Mitra M, Ahamed ST, Ghosh A, Mondal A, Kargupta K, Ganguly S, Banerjee D (2019) Polyaniline/reduced graphene oxide composite-enhanced visible-light-driven photocatalytic activity for the degradation of organic dyes. ACS Omega 4:1623–1635. https://doi.org/10.1021/acsomega.8b02941

Mohamed F, Abukhadra MR, Shaban M (2018) Removal of safranin dye from water using polypyrrole nanofiber/Zn-Fe layered double hydroxide nanocomposite (PPyNF/Zn-Fe LDH) of enhanced adsorption and photocatalytic properties. Sci Total Environ 640–1:352–363. https://doi.org/10.1016/j.scitotenv.2018.05.316

Mohammadi R, Massoumi B, Galandar F (2019) Polyaniline-TiO_2/graphene nanocomposite: an efficient catalyst for the removal of anionic dyes. Desalin Water Treat 142:321–330. https://doi.org/10.5004/dwt.2019.23525

Mondal S, Rana U, Das P, Malik S (2019a) Network of polyaniline nanotubes for wastewater treatment and oil/water separation. Appl Polym Mater 1:1624–1633. https://doi.org/10.1021/acsapm.9b00199

Mondal P, Satra J, Ghorui UK, Saha N, Srivastava DN, Adhikary B (2019b) Facile fabrication of novel hetero-structured

organic-inorganic high-performance nanocatalyst: a smart system for enhanced catalytic activity toward ciprofloxacin degradation and oxygen reduction. ACS Appl Nano Mater 1:6015–16026. https://doi.org/10.1021/acsanm.8b00937

Mousli F, Chaouchi A, Jouini M, Maurel F, Kadri A, Chehimi MM (2019) Polyaniline-grafted RuO_2/TiO_2 heterostructure for the catalysed degradation of methyl orange in darkness. Catalysts 9:578. https://doi.org/10.3390/catal9070578

Mu B, Wang AQ (2015) One-pot fabrication of multifunctional superparamagnetic attapulgite/Fe_3O_4/polyaniline nanocomposites served as an adsorbent and catalyst support. J Mater Chem A 3:281–289. https://doi.org/10.1039/c4ta05367b

Mu B, Zheng Y, Wang AQ (2015) Facile fabrication of polyaniline/kapok fiber composites via a semidry method and application in adsorption and catalyst support. Cellulose 22:615–624. https://doi.org/10.1007/s10570-014-0506-x

Mu B, Tang J, Zhang L, Wang AQ (2016) Preparation, characterization and application on dye adsorption of a well-defined two-dimensional superparamagnetic clay/polyaniline/Fe_3O_4 nanocomposite. Appl Clay Sci 132:7–16. https://doi.org/10.1016/j.clay.2016.06.005

Mu B, Tang J, Zhang L, Wang AQ (2017) Facile fabrication of superparamagnetic graphene/polyaniline/Fe_3O_4 nanocomposites for fast magnetic separation and efficient removal of dye. Sci Rep 7:5347. https://doi.org/10.1038/s41598-017-05755-6

Muhammad A, Shah AUA, Bilal S, Rahman G (2019a) Basic Blue dye adsorption from water using polyaniline/magnetite (Fe_3O_4) composites: kinetic and thetmodynamic aspects. Materials 12:1764. https://doi.org/10.3390/ma12111764

Muhammad A, Shah AUA, Bilal S (2019b) Comparative study of the adsorption of Acid Blue 40 on polyaniline, magnetic oxide and their composites: synthesis, characterization and application. Materials 12:2854. https://doi.org/10.3390/ma12182854

Mukhta B, Mahanta D, Patil S, Madras G (2007) Synthesis and photocatalytic activity of poly(3-hexylthiophene)/TiO_2 composites. J Solid State Comun 180:2986–2989. https://doi.org/10.1016/j.jssc.2007.07.017

Nair SS, Mishra SK, Kumar D (2019) Recent progress in conductive polymeric materials for biomedical applications. Polym Adv Technol 2019:1–22. https://doi.org/10.1002/pat.4725

Nasar A, Mashkoor F (2019) Application of polyaniline-based adsorbents for dye removal from water and wastewater – a review. Environ Sci Pollution Res 26:5333–5356. https://doi.org/10.1007/s11356-018-3990-y

Nerkar NV, Kondawar SB, Brahme SK, Kim YH (2018) Polyaniline/ZnO nanocomposites for the removal of methyl orange dye from waste water. Int J Mod Phys B 32:1840085. https://doi.org/10.1142/s0217979218400854

Niu B, Xu ZM (2019) A stable Ta_3N_5@PANI core-shell photocatalyst: shell thickness effect, high-efficient photocatalytic performance and enhanced mechanism. J Catal. 371:175–184. https://doi.org/10.1016/j.jcat.2019.01.025

Olad A, Azhar FF, Shargh M, Jharfi S (2014) Application of response surface methodology for modeling of reactive dye removal from solution using starch-montmorillonite/polyaniline nanocomposite. Polym Eng Sci 54:1595–1607. https://doi.org/10.1002/pen.23697

Omastová M, Mičušík M (2012) Polypyrrole coating of inorganic and organic materials by chemical oxidative polymerisation. Chem Pap 66:392–414. https://doi.org/10.2478/s11696-011-0120-4

Omastová M, Trchová M, Kovářová J, Stejskal J (2003) Synthesis and structural study of polypyrroles prepared in the presence of surfactants. Synth Met 138:447–455. https://doi.org/10.1016/s0379-6779(02)00498-8

Ossoss KM, Hassan MER, Al-Hussaini AS (2019) Novel Fe_2O_3@PANI-*o*-PDA core-shell nanocomposites for photocatalytic degradation of aromatic dyes. J Polym Res 26:199. https://doi.org/10.1007/s10965-019-1856-8

Othman N, Noor UM, Herman SH (2017) Effect of the deposited layer, withdrawal speed and coated length on immobilised bromothymol blue in polyaniline sol gel pH sensing sensitivity. Pertanika J Sci Technol 25:205–214.

Ovando-Medina VM, Díaz-Florés PE, Martínez-Gutierréz H, Moreno Ruíz LA, Antonio-Carmona ID, Hernandéz-Ordoñez M (2014) Composite of cellulosic agricultural waste coated with semiconducting polypyrrole as a potential dye remover. Polym Compos 35:186–193. https://doi.org/10.1002/pc.22649

Ovando-Medina VM, Vizcaino-Mercado J, Gonzáles-Ortega O, de la Garza JAR, Martinez Gutiérrez H (2015a) Synthesis of α-cellulose/polypyrrole composite for the removal of Reactive Red dye from aqueous solution: kinetics and equilibrium modeling. Polym Compos 36:312–321. https://doi.org/10.1002/pc.22945

Ovando-Medina VM, López RG, Castillo-Reyes BE, Alonso-Dávila PA, Martínez-Gutiérerrez HM, González-Ortega O, Farias-Cepeda L (2015b) Composite of acicular rod-like ZnO nanoparticles and semiconducting polypyrrole photoactive under visible light irradiation for methylene blue dye degradation. Colloid Polym Sci 293:3459–3469. https://doi.org/10.1007/s00396-015-3717-2

Ovando-Medina VM, Dávila-Guzmán NE, Perez N, Déctor A (2018) A semi-conducting polypyrrole/coffee grounds waste composite for rhodamine B dye adsorption. Iran Polym J 27:171–181. https://doi.org/10.1007/s13726-018-0598-5

Pandimurugan R, Thambidurai S (2016) Synthesis of seaweed-ZnO-PANI hybrid composite for adsorption of methylene blue dye. J Environ Chem Eng 4:1332–1347. https://doi.org/10.1016/j.jece.2016.01.030

Pant A, Tanwar R, Kaur B, Mandal UK (2018) A magnetically recyclable photocatalyst with commendable dye degradation activity at ambient conditions. Sci Rep 8:14700. https://doi.org/10.1038/s41598-018-32911-3

Parashar K, Ballav N, Debnath S, Pillay K, Maity A (2016) Rapid and efficient removal of fluoride ions from aqueous solution using a polypyrrole coated hydrous tin oxide nanocomposite. J Colloid Interface Sci 476:103–118. https://doi.org/10.1016/j.jcis.2016.05.013

Park JW, Park SJ, Kwon OS, Lee C, Jang J (2014) Polypyrrole nanotube embedded reduced graphene oxide transducer for field-effect transistor-type H_2O_2 biosensor. Anal Chem 86:1822–1828. https://doi.org/10.1021/ac403770x

Patil MR, Shrivastava VS (2016) Adsorptive removal of methylene blue from aqueous solution of polyaniline-nickel ferrite nanocomposite: a kinetic approach. Desalin Water Treat 57:5879–5887. https://doi.org/10.1080/19443994.2015.1004594

Patra BN, Majhi D (2015) Removal of anionic dyes from water by potash alum doped polyaniline: investigation of kinetics and thermodynamic parameters of adsorption. J Phys Chem B 119:8154–8164. https://doi.org/10.18021/acs.jpcb.5b00535

Pauliukaite R, Brett CMA (2008) Poly(neutral red): electrosynthesis, characterization, and application as a redox mediator. Electroanalysis 20:1275–1285. https://doi.org/10.1002/elan.200804217

Pauliukaite R, Selskiene A, Malinauskas A, Brett CMA (2009) Electrosynthesis and characterisation of poly(safranine T) electroactive polymer films. Thin Solid Films 517:5435–5441. https://doi.org/10.1016/j.tsf.2009.01.092

Pei FB, Wang P, Ma EH, Yu HX, Gao CX, Yin HH, Li YY, Liu Q, Dong YH (2018) A sandwich-type amperometric immunosensor fabricated by Au@Pd ND/Fe^{2+}-CS/PPy NTs and Au NPs/NH_2-GS to detect CEA sensitively via two detection methods. Biosens Bioelectron 122:231–238. https://doi.org/10.1016/j.bios.2018.09.065

Pei FB, Wang P, Ma EH, Yang QS, Yu HX, Liu J, Yin HH, Li YY, Liu Q, Dong YH (2019) A sensitive label-free immunosensor for alpha fetoprotein detection using platinum nanodendrites loaded on functional MoS_2 hybridized polypyrrole nanotubes as signal amplifier. J Electroanal Chem 835:197–204. https://doi.org/10.1016/j.jelechem.2019.01.037

Pen JY, Huang G (2019) Selective photocatalytic degradation of tetracycline by metal-free heterojunction surface imprinted photocatalyst base on magnetic fly ash. Inorg Chem Commun 106:202–209. https://doi.org/10.1016/j.inoche.2019.06.012

Peng YG, Ji JL, Zhang YL, Wan HX, Chen DJ (2014) Preparation of poly(*m*-phenylenediamine)/ZnO composites and their photocatalytic activities for degradation of CI Acid Red 249 under UV and visible light irradiations. Environ Prog Sustain Energy 33:123–130. https://doi.org/10.1002/ep.11764

Phan TTV, Bharathiraja S, Nguyen VT, Moorthy MS, Manivasagan P, Lee KD, Oh J (2017) Polypyrrole–methylene blue nanoparticles as a single multifunctional nanoplatform for near-infrared photo-induced therapy and photoacoustic imaging. RSC Adv 7:35027–35037. https://doi.org/10.1039/c7ra02140b

Pirkarami A, Olya ME, Limaee NY (2013) Decolorization of azo dyes by photo electro adsorption process using polyaniline coated electrode. Prog Org Coat 76:682–688. https://doi.org/10.1016/j.porgcoat.2012.12.014

Podasca VE, Buruiana TB, Buruiana EC (2019) Photocatalytic degradation of Rhodamine B dye by polymeric films containing ZnO, Ag nanoparticles and polypyrrole. J Photochem Photobiol A: Chem 371:188–195. https://doi.org/10.1016/j.jphotochem.2018.11.016

Ponprapakaran K, Subramani RH, Baskaran R, Anbarasan R (2017) Synthesis, characterization, catalytic activity and solar cell study of poly (aniline-*co*-thymol blue)/metal oxide nanocomposites. Synth Met 232:144–151. https://doi.org/10.1016/j.synthmet.2017.07.018

Poorarjmand S, Razi MK, Mahjoub AR, Khosravi M (2019) Improving photocatalytic properties of $Zn_{0.95}Ni_{0.04}Co_{0.01}O$ modified by PANI. J Nanoanalysis 6:129–137. https://doi.org/10.22034/jna.2019.667136

Prasad AR, Joseph A (2017) Synthesis, characterization and investigation of methyl orange dye removal from aqueous solutions using waterborne poly vinyl pyrrolidone (PVP) stabilized poly aniline (PANI) core–shell nanoparticles. RSC Adv 7:20960–20968. https://doi.org/10.1039/c7ra01790a

Prokeš J, Varga M, Vrňata M, Valtera S, Stejskal J, Kopecký D (2019) Nanotubular polypyrrole: reversibility of protonation/deprotonation cycles and long-term stability. Eur Polym J 115:290–297. https://doi.org/10.1016/j.eurpolymj.2018.03.037

Qi FF, Qian LL, Liu JJ, Li XQ, Lu LG, Xu Q (2016) A high throughput mat-based micro-solid extraction for the determination of cationic dyes in wastewater. J Chromatogr A 1460:24–32. https://doi.org/10.1016/j.chroma.2016.07.020

Radoičić M, Šaponjić Z, Janković IA, Ćirić-Marjanović G, Ahrenkiel P, Comora MI (2013) Improvments to the photocatalytic efficiency of polyaniline modified TiO_2. Appl Catal B: Environ 136:133–139. https://doi.org/10.1016/j.apcatb.2013.01.007

Radoičić M, Ćirić-Marjanović G, Spasojević V, Ahrenkiel P, Mitrić M, Novaković T, Šaponjić Z (2017) Superior photocatalytic properties of carbonized PANI/TiO_2 nanocomposites. Appl Catal B: Environ 217:155–166. https://doi.org/10.1016/j.apcatb.2017.05.023

Rafiqi FA, Majid K (2017) Sequestration of methylene blue (MB) dyes from aqueous solution using polyaniline and polyaniline-nitroprusside composite. J Mater Sci 52:6506–6524. https://doi.org/10.1007/s10853-017-0886-z

Rakić A, Bajuk-Bogdanović D, Mojović M, Ćirić-Marjanović G, Milojević-Rakić M, Mentus S, Marjanović B, Trchová M, Stejskal J (2011) Oxidation of aniline in dopant-free template-free dilute reaction media. Mater Chem Phys 127:501–510. https://doi.org/10.1016/j.matchemphys.2011.02.047

Rasmussen SC (2018) Revisiting history of synthetic polymers: critiques and new insights. Ambix 65:356–372. https://doi.org/10.1080/0002690.2018.1512775

Razak S, Nawi MA, Haitham K (2014) Fabrication, characterization and application of a reusable immobilized TiO_2-PANI photocatalyst plate for the removal of reactive red 4 dye. Appl Surf Sci 319:90–98. https://doi.org/10.1016/j.apsusc.2014.07.049

Reddy KR, Karthik KV, Prasad SBB, Soni SK, Jeong HM, Raghu AV (2016) Enhanced photocatalytic activity of nanostructure titanium dioxide/polyaniline hybrid photocatalysts. Polyhedron 120:169–174. https://doi.org/10.1016/j.poly.2016.08.029

Ren L, Li K, Chen XF (2009) Soft template method to synthesize polyaniline microtubes doped with methyl orange. Polym Bull 63:15–21. https://doi.org/10.1007/s00289-009-0076-5

Ren YY, Lin Z, Mao XW, Tian WD, Voorhis TV, Hatton TA (2018) Superhydrophobic, surfactant-doped, conducting polymers for electrochemically reversible adsorption of organic contaminants. Adv Funct Mater 28:1801466. https://doi.org/10.1002/adfm.201801466

Riaz U, Ashraf SM, Aqib M (2014) Macrowave-assisted degradation of acid orange using a conjugated polymer, polyaniline, as catalyst. Arab J Chem 7:79–86. https://doi.org/10.1016/j.arabjc.2013.07.001

Riaz U, Ashraf SNM, Raza R, Kohli K, Kashyap J (2016) Sonochemical facile synthesis of self-assembled poly(*o*-phenylenediamine)/cobalt ferrite nanohybrid with enhanced photocatalytic activity. Ind Eng Chem Res 55(22):6300–6309

Riede A, Helmstedt M, Sapurina I, Stejskal J (2002) In situ polymerized polyaniline films 4. Film formation in dispersion polymerization of aniline. J Colloid Interface Sci 248:413–418. https://doi.org/10.1006/jcis.2001.8197

Rounaghi GH, Razavipanah I, Vakili-Zarch MH, Ghanei-Motlagh M, Salavati MR (2015) Electrochemical synthesis of Alizarin Red S doped polypyrrole and its applications in designing a novel silver (I) potentiometric and voltammetric sensor. J Mol Liq 211:210–216. https://doi.org/10.1016/j.molliq.2015.06.066

Roy M, Mondal A, Mondal A, Das A, Mukherjee D (2019) Polyaniline supported palladium catalyzed reductive degradation dyes under mild condition. Curr Green Chem 6:69–75. https://doi.org/10.2174/2213346106666190130101109

Rudajevová A, Varga M, Prokeš J, Kopecká J, Stejskal J (2015) Thermal properties of conducting polypyrrole nanotubes. Acta Phys Polonica A 128:730–736. https://doi.org/10.12693/aphyspola.128.730

Runsewe D, Betancourt T, Irvin JA (2019) Biomedical application of electroactive polymers in electrochemical sensors: a review. Materials 12:2629. https://doi.org/10.3390/ma12162629

Saghatchi H, Ansari R (2018) Application of magnetic polyaniline nanocomposite for separation of uranyl ions from aqueous solutions. Separ Sci Technol 53:2486–2499. https://doi.org/10.1080/01496395.2018.1459701

Saha S, Chaudhary N, Mittal H, Gupta G, Khanuja M (2019) Inorganic–organic nanohybrid of MoS_2-PANI for advance photocatalytic application. Int Nano Lett 9:127–139. https://doi.org/10.1007/s40089-019-0267-5

Sahnoun S, Boutahala M, Finqueneisel G, Zimny T (2018) Adsorption studies of an azo dye using polyaniline coated calcinated layered hydroxides. Desalin Water Treat 129:255–265. https://doi.org/10.5004/dwt.2018.22794

Sahu K, Rahamn KH, Kar AK (2019) Synergic effect of polyaniline and ZnO to enhance the photocatalytic activity of their nanocomposite. Mater Res Express 9:095304. https://doi.org/10.1088/2053-1591/ab2c5f

Salahuddin N, El-Daly H, El Sharkawy RG, Nasr BT (2018) Synthesis and efficacy of PPy/CS/GO nanocomposites for adsorption of ponceau 4R dye. Polymer 146:291–303. https://doi.org/10.1016/j.polymer.2018.04.053

Salavati H, Kohestani T (2013) Preparation, characterization and photochemical degradation of dyes under UV light irradiation by inorganic–organic nanocomposite. Mater Sci Semiconduct Process 16:1904–1911. https://doi.org/10.1016/j.mssp.2013.07.014

Salehi-Barbarsad F, Derikvand E, Razaz M, Yousefi R, Shirmardi A (2019) Heavy metal removal by using ZnO/organic and ZnO/inorganic nanocomposite heterostructures. Int J Environ Anal Chem. https://doi.org/10.1080/03067319.2019.1639685

Salem MA (2010) The role of polyaniline salts in the removal of direct blue 78 from aqueous solution: a kinetic study. React Funct Polym 70:707–714. https://doi.org/10.1016/j.reactfunctpolym.2010.07.001

Salem et al (2009) Salem MA, Al-Ghonemiy AF, Zaki AB (2009) Photocatalytic degradation of Allura red and Quinoline yellow with polyaniline/TiO_2 nanocomposite. Appl Catal B: Environ 91:59–66. https://doi.org/10.1016/j.apcatb.2008.05.027

Salem MA, Elsharkawy RG, Hablas MF (2016) Adsorption of brilliant green dye by polyaniline/silver nanocomposite: kinetic, equilibrium, and thermodynamic studies. Eur Polym J 75:577–590. https://doi.org/10.1016/j.eurpolymj.2015.12.027

Samai B, Bhattacharya SC (2018) Conducting polymer supported cerium oxide nanoparticle: enhanced photocatalytic activity for waste water treatment. Mater Chem Phys 220:171–181. https://doi.org/10.1016/j.matchemphys.2018.08.50

Sananmuang R, Chaiyasith WC, Wongjan K (2017) Adsorption of Reactive Dyes Red 195, Blue 222, and Yellow 145 in solution with polyaniline-chitosan membrane using batch reactor. Key Eng Mater 751:713–718. https://doi.org/10.4028/www.scientific.net/KEM.751.713

Sandikly N, Kassir M, El Jamal M, Takache H, Arnoux P, Mohk S, Al Iskandarani M, Roques-Carmes T (2019) Comparison of the toxicity of waters containing initially sulfaquinoxaline after photocatalytic treatment by TiO_2 and polyaniline TiO_2. Environ Technol https://doi.org/10.1080/09593330.2019.1630485

Sangareswari M, Sundaram MM (2017) Development of efficiency improved polymer-modified TiO_2 for the photocatalytic degradation of an organic dye from waste water environment. Appl Water Sci 7:1781–1790. https://doi.org/10.1007/s13201-015-0351-6

Sapurina I, Stejskal J (2008) The mechanism of the oxidative polymerization of aniline and the formation of supramolecular polyaniline structures. Polym Int 57:1295–1325. https://doi.org/10.1002/pi.2476

Sapurina I, Riede A, Stejskal J (2001) In-situ polymerized polyaniline films 3. Film formation. Synth Met 123:503–507. https://doi.org/10.1016/s0379-6779(01)00349-6

Sapurina I, Osadchev AYu, Volchek BZ, Trchová M, Riede A, Stejskal J (2002) In-situ polymerized polyaniline films 5. Brush like chain ordering. Synth Met 129:29–37. https://doi.org/10.19016/S0379-6779(02)00036-X

Sapurina I, Stejskal J, Šeděnková I, Trchová M, Kovářová J, Hromádková J, Kopecká J, Cieslar M, Abu El-Nasr A, Ayad MM (2016) Catalytic activity of polypyrrole nanotubes decorated with noble-metal nanoparticles and their conversion to carbonized analogues. Synth Met 214:14–22. https://doi.org/10.1016/j.synthmet.2016.01.009

Sapurina I, Li Y, Alekseeva E, Bober P, Trchová M, Morávková Z, Stejskal J (2017) Polypyrrole nanotubes: the tuning of morphology and conductivity. Polymer 113:247–258. https://doi.org/10.1016/j.polymer.2017.02.064

Saravanan R, Sacari E, Gracia F, Khan MM, Mosquera E, Gupta VK (2016) Conducting PANI stimulated ZnO system for visible light photocatalytic degradation of coloured dyes. J Mol Liq 221:1029–1033. https://doi.org/10.1016/j.molliq.2016.06.074

Sarkar K, Deb K, Debnath A, Bera A, Debnath A, Saha B (2018) Polaron localization in polyaniline through methylene blue dye interaction for tuned charge transport and optical properties. Colloid Polym Sci 296:1927–1934. https://doi.org/10.1007/s00396-018-4419-3

Saugo M, Brugnoni LI, Flamani DO, Saidman SB (2018) Immobilization of antibacterial metallic cations (Ga^{31}, Zn^{2+} and Co^{2+}) in a polypyrrole coating formed on Nitinol. Mater Sci Eng C 86:62–69. https://doi.org/10.1016/j.msec.2018.01.009

Sayyah SM, Essawy AA, El-Nggar AM (2015) Kinetic studies and grafting mechanism for methyl aniline derivatives onto chitosan: highly adsorptive copolymers for dye removal fro aqueous solutions. React Funct Polym 96:50–60. https://doi.org/10.1016/j.reactfunctpolym.2015.07.005

Sazou D, Deshpande PP (2017) Conducting polyaniline nanocomposite-based paints for corrosion protection of steel. Chem Pap 71:459–487. https://doi.org/10.1007/s11696-016-0044-0

Selvin SSP, Kumar AG, Sarala L, Rajaram R, Sathiyan A, Merlin JP, Lydia IS (2018) Photocatalytic degradation of rhodamine B using zinc oxide activated charcoal polyaniline nanocomposite and its survival assessment using aquatic animal model. ACS Sustain Chem Eng 6:258–267. https://doi.org/10.1021/acssuschemeng.7b02335

Shabandokht M, Binaeian E, Tayebi HA (2016) Adsorption of food dye Acid red 18 onto polyaniline-modified rice husk composite: isotherm and kinetic analysis. Desalin Water Treat 57:27638–27650. https://doi.org/10.1080/19443994.2016.1172982

Shah A, Akhlaq S, Sayed M, Bilal S, Ali N (2018) Synthesis and characterization of polyaniline-zirconium dioxide and polyaniline-cerium dioxide composites with enhanced photocatalytic degradation of rhodamine B dye. Chem Pap 72:2523–2538. https://doi.org/10.1007/s11696-018-0494-7

Shahriman MS, Zain NNM, Mohamad S, Manan NSA, Yaman SM, Asman S, Raoov M (2018) Polyaniline modified magnetic nanoparticles coated with dicationic ionic liquid for effective removal of rhodamine B (RB) from aqueous solution. RSC Adv 8:33180–33192. https://doi.org/10.1039/c8ra06687f

Shanehsaz M, Seidi S, Ghorbani Y, Shoja SMR (2015) Polypyrrole-coated magnetic nanoparticles as an efficient adsorbent for RB19 synthetic textile dye: removal and kinetic study. Spectrochim Acta A 149:481–486. https://doi.org/10.1016/j.saa.2015.04.114

Shang M, Wang WZ, Sun SM, Ren J, Zhou L, Zhang L (2009) Efficient visible light-induced photocatalytic degradation of contaminant by spindle-like PANI/$BiVO_4$. J Phys Chem C 113:20228–20233. https://doi.org/10.1021/jp9067729

Sharma G, Naushad M, Kumar A, Devi S, Khan MR (2015) Lanthanum/cadmium/polyaniline bimetallic nanocomposite for the photodegradation of organic pollutant. Iran Polym J 24:1003–1013. https://doi.org/10.1007/s13726-015-0388-2

Sharma V, Rekha P, Mohanty P (2016) Nanoporous hypercrosslinked polyaniline: an efficient adsorbent for the adsorptive removal of cationic and anionic dyes. J Mol Liq 222:1091–1100. https://doi.org/10.1016/j.molliq.2016.07.130

Shen JJ, Shahid S, Amura I, Sarihan A, Tian M (2018) Enhanced adsorption of cationic and anionic dyes from aqueous solutions by polyacid doped polyaniline. Synth Met 245:151–159. https://doi.org/10.1016/j.synthmet.2018.08.015

Shi MW, Zhang YY, Bai MD, Li BM (2017) Facile fabrication of polyaniline with coral-like nanostructure as electrode material for supercapacitors. Synth Met 233:74–78. https://doi.org/10.1016/j.synthmet.2017.09.007

Shi MW, Bai MD, Li BM (2018) Acid Red 27-crosslinked polyaniline with nanofiber structure as electrode material for supercapacitors.

Mater Lett 212:259–262. https://doi.org/10.1016/j.matlet.2017.10.107
Shirmardi A, Teridi MAT, Azimi HR, Basirun WJ, Jamali-Sheini F, Yousefi R (2018) Enhanced photocatalytic performance of ZnSe/PANI nanocomposites for degradation of organic and inorganic pollutants. Appl Surf Sci 462:730–738. https://doi.org/10.1016/j.appsusc.2018.06.252
Silvestri S, Ferreira CD, Oliveira V, Varejão JMTB, Labrincha JA, Tobaldi DM (2019) Synthesis of PPy-ZnO composite used as photocatalyst for the degradation of diclofenac under simulated solar irradiation. J Photochem Photobiol A: Chem 375:261–269. https://doi.org/10.1016/j.jphotochem.2019.02.034
Singh NB, Agarwal S, Rachna KM (2019) Methylene blue dye removal from water by nickel ferrite polyaniline nanocomposite. J Sci Ind Res 78:118–121. http://nopr.niscair.res.in/handle/123456789/45760
Sivakumar V, Suresh R, Giribabu K, Narayanan V (2019) Characterization and visible light driven photocatalytic activity of (M = Bi, La) MVO_4@poly(*o*-phenylenediamine) nanocomposite. Mater Sci Eng B 240:41–48. https://doi.org/10.1016/j.mseb.2019.01.011
Škodová J, Kopecký D, Vrňata M, Varga M, Prokeš J, Cieslar M, Bober P, Stejskal J (2013) Polypyrrole–silver composites prepared by the reduction of silver ions with polypyrrole nanotubes. Polym Chem 4:3610–3616. https://doi.org/10.1039/c3py00250k
Sobhani-Nasab A, Behpour M, Rahimi-Nasrabadi M, Ahmadi F, Pourmasoud S, Sedighi F (2019) Preparation, characterization and investigation of sonophotocatalytic activity of thulium titanate/polyaniline nanocomposites in degradation of dyes. Ultrason Sonochem 50:46–55. https://doi.org/10.1016/j.ultsonch.2018.08.021
Soltani H, Belmokhtar A, Zeggai FZ, Benyoucef A, Bousalem S, Bachari K (2019) Copper(II) removal from aqueous solutions by PANI-clay hybrid material: fabrication, characterization, adsorption, kinetics study. J Inorg Organomet Polym Mater 29:841–851. https://doi.org/10.1007/ss10904-018-01058-z
Song XF, Qin JT, Li TT, Liu G, Xia XX, Li YS, Liu Y (2019) Efficient construction and enriched adsorption-photocatalytic activity of PVA/PANI/TiO_2 recyclable hydrogel by electron beam radiation. J Appl Polym Sci 136:48516. https://doi.org/10.1002/app.48516
Sousa MM, Melo MJ, Parola AJ, Morris PJT, Rzepa HS, de Melo JSS (2008) A study in mauve: unveiling Perkin's dye in historic samples. Chem Eur J 14:8507–8513. https://doi.org/10.1002/chem.200800718
Spiridon MCS, Aissou K, Mumtaz M, Brochon C, Cloutet E, Fleury G, Hadziioannou G (2018) Surface relief gratings formed by microphase-separated disperse red 1 acrylate-containing diblock copolymers. Polymer 137:378–384. https://doi.org/10.1016/j.polymer.2018.01.032
Stejskal J (2001) Colloidal dispersions of conducting polymers. J Polym Mater 18:225–258 **(WOS: 000171631800001)**
Stejskal J (2013) Conducting polymer–silver composites. Chem Pap 67:814–848. https://doi.org/10.2478/s11696-012-0304-6
Stejskal J (2015) Polymers of phenylenediamines. Prog Polym Sci 41:1–31. https://doi.org/10.1016/j.progpolymsci.2014.10.007
Stejskal J (2017) Conducting polymer hydrogels. Chem Pap 71:269–291. https://doi.org/10.1007/s11696-016-0072-9
Stejskal J (2018) Strategies towards the control of one-dimensional polypyrrole morphology and conductivity. Polym Int 67:1461–1465. https://doi.org/10.1002/pi.5654
Stejskal J, Bober P (2018) Conducting polymer colloids, hydrogels, and cryogels: common start ro various destinations. Colloid Polym Sci 296:989–994. https://doi.org/10.1007/s00396-018-4303-1
Stejskal J, Gilbert RG (2002) Polyaniline. Preparation of a conducting polymer (IUPAC technical report). Pure Appl Chem 74:857–867. https://doi.org/10.1351/pac200274050857
Stejskal J, Sapurina I (2005) Polyaniline: thin films and colloidal dispersions. Pure Appl Chem 77:815–826. https://doi.org/10.1351/pac200577050815
Stejskal J, Trchová M (2018) Conducting polypyrrole nanotubes: a review. Chem Pap 72:1563–1595. https://doi.org/10.1007/s11696-018-0394x
Stejskal J, Sapurina I, Prokeš J, Zemek J (1999) In-situ polymerized polyaniline films. Synth Met 105:195–202. https://doi.org/10.1016/s379-6779(99)00105-8
Stejskal J, Trchová M, Prokeš J, Sapurina I (2001) Brominated polyaniline. Chem Mater 13:4083–4086. https://doi.org/10.1021/cm011059n
Stejskal J, Hlavatá D, Holler P, Trchová M, Prokeš J, Sapurina I (2004a) Polyaniline prepared in the presence of various acids: a conductivity study. Polym Int 53:294–300. https://doi.org/10.1002/pi.1406
Stejskal J, Trchová M, Ananieva IA, Janča J, Prokeš J, Fedorova S, Sapurina I (2004b) Poly(aniline-*co*-pyrrole): powders, films and colloids. Thermophoretic mobility of colloidal particles. Synth Met 146:29–36. https://doi.org/10.1016/j.synthmet.2004.06.013
Stejskal J, Prokeš J, Trchová M (2008a) Reprotonation of polyaniline: a route to various conducting polymer materials. React Funct Polym 68:1355–1361. https://doi.org/10.1016/j.reactfunctpolym.2008.06.012
Stejskal J, Sapurina I, Trchová M, Konyushenko EN (2008b) Oxidation of aniline: polyaniline granules, nanotubes, and oligoaniline microspheres. Macromolecules 41:3530–3536. https://doi.org/10.1021/ma702601q
Stejskal J, Trchová M, Blinova NV, Konyushenko EN, Reynaud S, Prokeš J (2008c) The reaction of polyaniline with iodine. Polymer 49:180–185. https://doi.org/10.1016/j.polymer.2007.11.023
Stejskal J, Sapurina I, Trchová M (2010) Polyaniline nanostructures and the role of aniline oligomers in their formation. Prog Polym Sci 35:1420–1481. https://doi.org/10.1016/j.progpolymsci.2010.07.006
Stejskal J, Sapurina I, Trchová M, Šeděnková I, Kovářová J, Kopecká J, Prokeš J (2015) Coaxial conducting polymer nanotubes: polypyrrole nanotubes coated with polyaniline or poly(*p*-phenylenediamine) and products of their carbonization. Chem Pap 69:1341–1349. https://doi.org/10.1515/chempap-2015-0152
Stejskal J, Trchová M, Bober P, Morávková Z, Kopecký D, Vrňata M, Prokeš J, Varga M, Watzlová E (2016) Polypyrrole salts and bases: superior conductivity of nanotubes and their stability towards the loss of conductivity by deprotonation. RSC Adv 6:88382–88391. https://doi.org/10.1039/c6ra19461c
Stejskal J, Bober P, Trchová M, Kovalcik A, Hodan J, Htromádková J, Prokeš J (2017) Polyaniline cryogels supported with poly(vinyl alcohol): soft and conducting. Macromolecules 50:972–978. https://doi.org/10.1021/acs.macromol.6b02526
Stejskal J, Acharya U, Bober P, Hajná M, Trchová M, Mičušík M, Omastová M, Pašti I, Gavrilov N (2019) Surface modification of tungsten disulfide with polypyrrole for enhancement of the conductivity and its impact on hydrogen evolution reaction. Appl Surf Sci 492:497–503. https://doi.org/10.1016/j.apsusc.2019.06.175
Stoikov DI, Porfirjeva AV, Shurpik DN, Stoikov II, Evtyugin GA (2019) Electrochemical DNA sensors on the basis of electropolymerized thionine and Azure B with addition of pillar[5]arene as an electron transfer mediator. Russ Chem Bull 68:431–437. https://doi.org/10.1007/s11172-019-2404-8
Suba V, Rathika G (2016) Novel adsorbents for the removal of dyes and metals from aqueous solution—a review. J Adv Phys 5:277–294. https://doi.org/10.1166/jap.2016.1269

Subramaniam MN, Goh PS, Lau WJ, Ismail AF, Gursoy M, Karaman M (2019) Synthesis of Titania nanotubes/polyaniline via rotating bed-plasma enhanced chemical vapor deposition for enhanced visible light degradation. Appl Surf Sci 484:740–750. https://doi.org/10.1016/j.apsusc.2019.04.118

Sukchuay T, Kanatharana P, Wannapob R, Thavarungkul P, Bunkoed O (2015) Polypyrrole/silica/magnetite nanoparticles as a sorbent for the extraction of sulfonamides from water samples. J Sep Sci 38:3921–3927. https://doi.org/10.1002/jssc.201500766

Sultana I, Rahman MM, Wang JZ, Wang CY, Wallace GG (2012a) All-polymer battery system based on polypyrrole (PPy)/para (toluene sulfonic acid) (*p*TS) and polypyrrole (PPy)/indigo carmine (IC) free standing films. Electrochim Acta 83:209–215. https://doi.org/10.1016/j.electacta.2012.08.043

Sultana I, Rahman MM, Wang JZ, Wang CY, Wallace GG, Liu HK (2012b) Indigo carmine (IC) doped polypyrrole (PPy) as a free-standing polymer electrode for lithium secondary battery application. Solid State Ionics 215:29–35. https://doi.org/10.1016/j.ssi.2012.03.034

Sun XF, Sun QH, Gong QH, Gao TT, Zhou GW (2019a) Double-shell structural polyaniline-derived TiO_2 hollow spheres for enhanced photocatalytic activity. Transit Met Chem 44:555–564. https://doi.org/10.1007/s11243-019-00312-8

Sun BJ, Ma WJ, Wang N, Xu P, Zhang LJ, Wang BN, Zhao HH, Lin KYA, Du YC (2019b) Polyaniline: a new metal-free-catalyst for peroxomonosulfate activation with highly efficient and durable removal of organic pollutants. Environ Sci Technol 53:9771–9780. https://doi.org/10.1021/acs.est.9b03374

Supriya S, Palanisamy PN (2016) Adsorptive removal of acid orange 7 from industrial effluents using activated carbon and conducting polymer composite – a comparative study. Ind J Chem Technol 23:506–512 **(WOS: 000392458700008)**

Supriya S, Palanisamy PN (2017) Preparation, characterization and removal of hazardous reactive violet dye from aqueous solution using activated carbon and electroactive conducting polymer—a comparative study. Desalin Water Treat 78:281–291. https://doi.org/10.5004/dwt.2017.20746

Sushma C, Kumar SG (2017) Advancements in the zinc oxide nanomaterials for efficient photocatalysis. Chem Pap 71:2023–2042. https://doi.org/10.1007/s11696-017-0217-5

Tahir N, Bhatti HN, Iqbal M, Noreen S (2017) Biopolymers composites with peanut hull waste biomass and application for crystal violet adsorption. Int J Biol Macromol 94:210–220. https://doi.org/10.1016/j.ijbiomac.2016.10.013

Talikowska M, Fu XX, Lisak G (2019) Application of conducting polymers to wound care and skin tissue engineering: a review. Biosens Bioelectron 135:50–63. https://doi.org/10.1016/j.bios.2019.04.001

Tang TT, Li K, Dai L, Zhou S, Zhang HB, Jia JP (2019a) Visible-light driven conversion of pollutants into hydrogen and electricity based on a polyaniline dynamic electrode. J Electrochem Soc 166:F399–F405. https://doi.org/10.1149/2.0831906jes

Tang YH, Zhou P, Wang K, Lin F, Lai JP, Chao YG, Li HX, Guo SJ (2019b) BiOCl/ultrathin polyaniline core/shell nanosheets with a sensitization mechanism for efficient visible-light-driven photocatalysis. Sci China Mater 62:95–102. https://doi.org/10.1007/s40843-018-9284-0

Tanwar R, Mandal UK (2019) Photocatalytic activity of $Ni_{0.5}ZnO_{0.5}Fe_2O_4$@polyaniline-decorated BiOCl for azo dye degradation under visible light-integrated role and degradation kinetics interpretation. RSC Adv 9:8977–8993. https://doi.org/10.1039/c9ra00548j

Tanwar R, Kumar S, Mandal UK (2017) Photocatalytic activity of PANI/Fe^0 doped BiOCl under visible light-degradation of Congo red dye. J Photochem Photobiol A-Chem 333:105–116. https://doi.org/10.1016/j.jphotochem.2016.10.022

Tanzifi M, Karimipour M, Mirchenari S (2016) Removal of Congo red anionic dye from aqueous solution using polyaniline/TiO_2 and polypyrrole/TiO_2 nanocomposites: isotherm, kinetic, and thermodynamic studies. Int J Eng, Trans C 29:1659–1669. https://doi.org/10.5829/idosi.ije.2016.29.12c.04

Tanzifi M, Hosseini SH, Kiadehi AD, Olazar M, Karimipour K, Rezaiemehr R, Ali I (2017) Artificial neural network optimization for methyl orange adsorption onto polyaniline nano-adsorbent: kinetic, isotherm and thermodynamic studies. J Mol Liq 244:189–200. https://doi.org/10.1016/j.molliq.2017.08.122

Tanzifi M, Yaraki MT, Kiadehi AD, Hosseini SH, Olazar M, Bharti AK, Agarwal S, Gupta VK, Kazemi A (2018a) Adsorption of Amide Black 10B from aqueous solution using polyaniline/SiO_2 nanocomposite: experimental investigation and artificial neural network modeling. J Colloid Interface Sci 510:246–261. https://doi.org/10.1016/j.jcis.2017.09.055

Tanzifi M, Yaraki MT, Karami M, Karimi S, Kiadehi AD, Karimipour K, Wang SB (2018b) Modelling of dye adsorption from aqueous solution on polyaniline/carboxymethyl cellulose/TiO_2 nanocomposites. J Colloid Interface Sci 519:154–173. https://doi.org/10.1016/j.jcis.2018.02.059

Tanzifi M, Esmizadeh E, Bazgir H, Nazari A, Vahidifar A (2019) Adsorption of methylene blue dye from aqueous solution using polyaniline/xanthan gum nanocomposite: kinetic and isotherm studies. J Polym Compos 7:17–26.

Tavoli F, Alizadeh N (2013) Optical ammonia gas sensor based on nanostructured dye-doped polypyrrole. Sens Actuat B-Chem 176:761–767. https://doi.org/10.1016/j.snb.2012.09.013

Tavoli F, Alizadeh N (2014) In-situ UV-vis spectroelectrochemical study of dye doped nanostructure polypyrrole as electrochromic film. J Electroanal Chem 720–721:128–133. https://doi.org/10.1016/j.jelechem.2014.03.022

Tayebi HA, Dalirandeh Z, Rad AS, Mirabi A, Binaeian E (2016) Synthesis of polyaniline/Fe_3O_4 magnetic nanoparticles for removal of reactive red 198 from textile waste water: kinetic, isotherm, and thermodynamic studies. Desalin Water Treat 57:22551–22563. https://doi.org/10.1080/19943994.2015.113323

Teklu T, Wangatia LM, Alemayehu E (2019) Removal of Pb(II) from aqueous media using adsorption onto polyaniline coated sisal fibers. J Vinyl Additive Technol 25:189–197. https://doi.org/10.1002/vnl.21652

Tie J, Fang X, Wang X, Zhang Y, Gu T, Deng S, Li G, Tang D (2017) Adsorptive removal of a reactive azo dye using polyaniline-intercalated bentonite. Pol J Environ Stud 26(3):1259–1268. https://doi.org/10.15244/pjoes/67554

Torabinejad A, Nasirizadeh N, Yazdanshenas ME, Tayebi HA (2017) Synthesis of conductive polymer-coated mesoporous MCM-41 for textile dye removal from aqueous media. J Nanostruct Chem 7:217–229. https://doi.org/10.1007/s40097-017-0232-7

Trchová M, Stejskal J (2011) Polyaniline: the infrared spectroscopy of conducting polymer nanotubes (IUPAC technical report). Pure Appl Chem 83:1803–1817. https://doi.org/10.1351/pac-rep-10-02-01

Trchová M, Stejskal J (2018) Resonance Raman spectroscopy of conducting polypyrrole nanotubes: disordered surface versus ordered body. J Phys Chem A 122:9298–9306. https://doi.org/10.1021/acs.jpca.8b09794

Trchová M, Šeděnková I, Konyushenko EN, Stejskal J, Holler P, Ćirić-Marjanović G (2006) Evolution of polyaniline nanotubes: the oxidation of aniline in water. J Phys Chem B 110:9461–9468. https://doi.org/10.1021/jp057528g

Trchová M, Konyushenko EN, Stejskal J, Kovářová J, Ćirić-Marjanović G (2009) The conversion of polyaniline nanotubes to nitrogen-containing carbon nanotubes and their comparison with multiwall carbon nanotubes. Polym Degrad Stab 94:929–938. https://doi.org/10.1016/j.polymdegradstab.2009.03.001

Trung VQ, Trang NTH, Thi TM, Vorayuth K, Nghia NM, Tuan MA (2018) Synthesis and properties of Fe_3O_4 polyaniline nanomaterial and its ability of removing arsenic in wastewater. Mater Trans 59:1095–1100. https://doi.org/10.2320/matertrans.md201703

Tuo X, Li BR, Yu XH, Chen CL, Huang ZL, Cao H, Huang YN, Li L (2018) Facile synthesis of magnetic polypyrrole composite nanofibers and their application in Cr(VI) removal. Polym Compos 39:1507–1513. https://doi.org/10.1002/pc.24091

Umoren SA, Solomon MM (2019) Protective polymeric films for industrial substrates: a critical review on past and recent applications with conducting polymers and polymer composites/nanocomposites. Prog Mater Sci 104:380–450. https://doi.org/10.1016/j.prmatsci.2019.04.002

Vaez M, Alijani S, Omidkhah M, Moghaddam AZ (2018) Synthesis, characterization, and optimization of N-TiO_2/PANI nanocomposite for photodegradation of acid dye under visible light. Polym Compos 39:4605–4616. https://doi.org/10.1002/pc.24574

Valtera S, Prokeš J, Kopecká J, Vrňata M, Trchová M, Varga M, Stejskal J, Kopecký D (2017) Dye-stimulated control of conducting polypyrrole morphology. RSC Adv 7:51495–51505. https://doi.org/10.1039/c7ra10027b

Varga M, Kopecká J, Morávková Z, Křivka I, Trchová M, Stejskal J, Prokeš J (2015) Effect of oxidant on electronic transport in polypyrrole nanotubes synthesized in the presence of methyl orange. J Polym Sci, Part B: Polym Phys 53:1147–1159. https://doi.org/10.1002/polb.23755

Varga M, Kopecký D, Kopecká J, Křivka I, Hanuš J, Zhigunov A, Trchová M, Vrňata M, Prokeš J (2017) The ageing of polypyrrole nanotubes synthesized with methyl orange. Eur Polym J 96:176–189. https://doi.org/10.1016/j.eurpolymj.2017.08.052

Vidya J, Balamurugan P (2019a) Photocatalytic degradation of methylene blue using PANi-NiO nanocomposite under visible light irradiation. Mater Res Express 6:0950c8. https://doi.org/10.1088/2053-1591/ab34a3

Vidya J, Balamurugan P (2019b) Photocatalytic degradation of methylene blue using PANi/Ceria nanocomposite under visible light irradiation. Desalin Water Treat 156:349–356. https://doi.org/10.5004/dwt.2019.23934

Vidya J, John Bosco A, Haribaaskar K, Balamurugan P (2019) Polyaniline-$BiVO_4$ nanoconmposite as an efficient adsorbent for the removal of methyl orange from aqueous solution. Mater Sci Semicond Process 103:104645. https://doi.org/10.1016/j.mssp.2019.104645

Wang F, Min SX, Han YQ, Feng L (2010) Visible-light-induced photocatalytic degradation of methylene blue with polyaniline-sensitized TiO_2 composite photocatalysts. Superlattices Microstruct 48:170–180. https://doi.org/10.1016/j.spmi.2010.06.009

Wang YJ, Yang C, Liu P (2011) Acid blue AS doped polypyrrole (PPy/AS) nanomaterials with different morphologies as electrode materials for supercapacitors. Chem Eng J 172:1137–1144. https://doi.org/10.1016/j.cej.2011.06.061

Wang HL, Zhao DY, Jiang WF (2012) Synthesis and photocatalytic activity of poly-*o*-phenylenediamine (PoPD)/TiO_2 composite under VIS-light irradiation. Synth Met 162:296–302. https://doi.org/10.1016/j.synthmet.2011.12.009

Wang YJ, Wang X, Yang C, Mu B, Liu P (2013a) Effect of Acid Blue BRL on morphology and electrochemical properties of polypyrrole materials. Powder Technol 235:901–908. https://doi.org/10.1016/j.powtec.2012.11.049

Wang QZ, Hui J, Li JJ, Cai YX, Yin SQ, Wang FP, Su BT (2013b) Photodegradation of methyl orange with PANI-modified BiOCl photocatalyst under visible light irradiation. Appl Surf Sci 283:577–583. https://doi.org/10.1016/j.apsusc.2013.06.149

Wang HL, Zhao DY, Jiang WF (2013c) VIS-light-induced photocatalytic degradation of methylene blue (MB) dye using PoPD/TiO_2 composite photocatalysts. Desalin Water Treat 51:2826–2835. https://doi.org/10.1080/19443994.2012.750789

Wang YJ, Liu P, Yang C, Mu B, Wang AQ (2013d) Improving capacitance performance of attapulgite/polypyrrole composite by introducing rhodamine B. Electrochim Acta 89:422–428. https://doi.org/10.1016/j.electacta.2012.11.065

Wang WZ, Xu JH, Zhang L, Sun SM (2014) Bi_2WO_4/PANI: an efficient visible-light-induced photocatalytic composite. Catal Today 224:147–153. https://doi.org/10.1016/j.cattod.2013.11.030

Wang N, Li JJ, Feng JT, Yan W (2015a) Synthesis of polyaniline TiO_2 composite with excellent adsorption performance on acid red G. RSC Adv 5:21132–21141. https://doi.org/10.1039/c4ra16910g

Wang Y, Gai LG, Ma WY, Jiang HH, Peng XQ, Zhao LC (2015b) Ultrasound-assisted catalytic degradation of methyl orange with Fe_3O_4/polyaniline in near neutral solution. Ind Eng Chem Res 54:2279–2289. https://doi.org/10.1021/ie504242k

Wang W, Cai K, Wu XF, Shao XH, Yang XJ (2017) A novel poly(*m*-phenylenediamine)/reduced graphene oxide/nickel ferrite magnetic adsorbent with excellent removal ability of dyes and Cr(VI). J Alloys Compd 722:532–543. https://doi.org/10.1016/j.jallcom.2017.06.069

Wang GQ, Liu JQ, Dong WN, Yan C, Zhang W (2018a) Nitrogen/sulfur co-doped porous carbon nanosheets and its electrochemical performance. Acta Phys Sinica 67:238103. https://doi.org/10.7498/aps.67.20181524

Wang HF, Duan MM, Guo Y, Wang CY, Shi ZT, Liu JD, Lv JH (2018b) Graphene oxide edge grafting of polyaniline composite: an efficient adsorbent for methylene blue and methyl orange. Water Sci Technol 77:2751–2760. https://doi.org/10.2166/wst.2018.250

Wang C, Guo ZP, Hong P, Gao J, Guo Y, Gu C (2018c) A novel method of synthesis of polyaniline and its application for catalytic degradation of atrazine in a Fenton-like system. Chemosphere 197:576–584. https://doi.org/10.1016/j.chemosphere.2018.01.050

Wang ML, Cui MZ, Liu WF, Liu XG (2019a) Highly dispersed conductive polypyrrole hydrogels as sensitive sensor for simultaneous determination of ascorbic acid, dopamine and uric acid. J Electroanal Chem 832:174–181. https://doi.org/10.1016/j.jelechem.2018.10.057

Wang ML, Shi HF, Ciu MZ, Liu WF, Liu XG (2019b) Ultrasensitive electrochemical determination of Sunset Yellow in foods using size-tunable nitrogen-doped carbon spheres. J Electrochem Soc 166:B13–B22. https://doi.org/10.1149/2.1151816jes

Wang L, Li X, Tang ZC, Zhou N, Yu ZS, Dong YZ, Li XZ, Wei DG, Dong YL, Li QH, Liu P (2019c) Preparation and photocatalytic performance of Bi_5O_7I/PANI composites. Chin J Inorg Chem 35:271–276. https://doi.org/10.11862/cjic.2019.047

Wang J, Hao XY, Jiang YX, DE Zhang, Ren LZ, Gong JY, Wu XJ, Zhang YY, Tong ZW (2019d) Synthesis, structure, and photocatalytic activity of PANI/BiOCl nanocomposites. Mater Res Exp 6:0850c1. https://doi.org/10.1088/2053-1591/ab1fa5

Wang LC, Zhang CG, Jiao X, Yuan ZH (2019e) Polypyrrole-based hybrid nanostructures grown on textile for wearable supercapacitors. Nano Res 12:1129–1137. https://doi.org/10.1007/s12274-019-2360-5

Wang YZ, Liu YX, Xia K, Zhang Y, Yang JL (2019f) $NiCo_2S_4$ nanoparticles anchoring on polypyrrole nanotubes for high-performance supercapacitor electrodes. J Electroanal Chem 840:242–248. https://doi.org/10.1016/j.jelechem.2019.03.076

Wei M, Dai TY, Lu Y (2010) Controlled fabrication of nanostructured polypyrrole on ion association template: tubes, rods and networks. Synth Met 160:849–854. https://doi.org/10.1016/j.synthmet.2010.01.032

Wei ST, Hu XL, Liu HL, Wang Q, He CY (2015) Rapid degradation of Congo red by molecularly imprinted polypyrrole coated magnetic TiO_2 nanoparticles in dark and at ambient conditions.

J Hazard Mater 294:168–176. https://doi.org/10.1016/j.jhazmat.2015.03.067

Wei WL, Du PC, Liu D, Wang Q, Liu P (2018) Facile one-pot synthesis of well-defined coaxial sulfur/polypyrrole nanocomposites as cathodes for long-cycling lithium–sulfur batteries. Nanoscale 10:13037–13044. https://doi.org/10.1039/c8nr01530a

Wu MC, Zhao TS, Zhang RH, Wei L, Jiang HR (2018) Carbonized tubular polypyrrole with high activity for the Br_2/Br^- redox reaction in zinc-bromine flow batteries. Electrochim Acta 284:569–576. https://doi.org/10.1016/j.electacta.2018.07.192

Wu HH, Chang CW, Lu D, Maeda K, Hu CC (2019) Synergistic effect of hydrochloric and phytic acid doping on polyaniline-coupled g-C_3N_4 nanosheets for photocatalytic Cr(VI) reduction and dye degradation. ACS Appl Mater Interfaces 11:35702–35712. https://doi.org/10.1021/acsami.9b10555

Würthner F, Kaiser TE, Saha-Möller CR (2011) J-Aggregates: from serendipitous discovery to supramolecular engineering of functional dye materials. Angew Chem Int Ed 50:3376–3410. https://doi.org/10.1002/anie.201002307

Xiao DJ, Ma J, Chen CL, Luo QM, Ma J, Zheng LR, Zuo X (2018) Oxygen-doped carbonaceous polypyrrole nanotubes-supported Ag nanoparticle as electrocatalyst for oxygen reduction reaction in alkaline solution. Mater Res Bull 105:184–191. https://doi.org/10.1016/j.matresbull.2018.04.030

Xie HF, Yan M, Zhang Q, Qu HX, Kong JM (2017) Hemin based biomimetic synthesis of PANI@iron oxide and its adsorption of dyes. Desalin Water Treat 67:346–356. https://doi.org/10.5004/dwt.2017.20409

Xin SC, Yang N, Zhao J, Li L, Teng C (2017) Three-dimensional polypyrrole-derived carbon nanotube framework for dye adsorption and electrochemical supercapacitor. Appl Surf Sci 414:218–223. https://doi.org/10.1016/j.apsusc.2017.04.109

Xin SC, Yang N, Gao F, Zhao J, Li L, Teng C (2018) Free-standing and flexible polypyrrole nanotube/reduced graphene oxide hybrid film with promising thermoelectric performance. Mater Chem Phys 212:440–445. https://doi.org/10.1016/j.matchemphys.2018.03.025

Xing JY, Yang B, Shen Y, Wang ZH, Wang F, Shi XF, Zhang ZW (2019) Selective removal of Acid Fuchsin from aqueous solutions by rapid adsorption onto polypyrrole crosslinked cellulose/gelatin hydrogels. J Dispers Sci Technol 40:1591–1599. https://doi.org/10.1080/01932691.2018.1518147

Xu J, Wang DX, Fan LL, Yuan Y, Wei W, Liu R, Gu SJ, Xu WL (2015) Fabric electrodes coated with polypyrrole nanorods for flexible supercapacitor application prepared via self-degraded template. Org Electron 26:292–299. https://doi.org/10.1016/j.orgel.2015.07.054

Xu CM, Wang HY, Deng J, Wang Y (2018) High-performance flexible redox supercapacitors induced by methylene blue with a wide voltage window. Sustain Energy Fuels 2:357–360. https://doi.org/10.1039/c7se00492c

Xu YQ, Gao ZY, Chen W, Wang E, Li Y (2019a) Preparation and application of malachite green molecularly imprinted/gold nanoparticle composite film-modified glassy carbon electrode. Ionics 25:1177–1185. https://doi.org/10.1007/s11581-018-2778-x

Xu H, Zhang YJ, Cheng Y, Tian WG, Zhao ZT, Tang J (2019b) Polyaniline attapulgite supported nanoscale zero-valent iron for the rival removal of azo dyes in aqueous solution. Adsorpt Sci Technol 37:217–235. https://doi.org/10.1177/0263617418822917

Xu WJ, Chen YZ, Kang JX, Li BJ (2019c) Synthesis of polyaniline/lignosulfonate for highly efficient removal of acid red 94 from aqueous solution. Polym Bull 76:4103–4116. https://doi.org/10.1007/s00289-018-2586-5

Xue YP, Lu XF, Xu Y, Bian XJ, Kong LR, Wang C (2010) Controlled fabrication of polypyrrole capsules and nanotubes in the presence of Rhodamine B. Polym Chem 1:1602–1605. https://doi.org/10.1039/c0py00305k

Yan W, Han J (2007) Synthesis and formation mechanism study of rectangular-sectioned polypyrrole micro/nanotubules. Polymer 48:6782–6790. https://doi.org/10.1016/j.polymer.2007.09.026

Yan B, Chen ZH, Cai L, Chen ZM, Fu JW, Xu Q (2015) Fabrication of polyaniline hydrogel: synthesis, characterization and adsorption of methylene blue. Appl Surf Sci 356:39–47. https://doi.org/10.1016/j.apsusc.2015.08.024

Yan C, Zhang Z, Wang W, Ju T, She H, Wang Q (2018) Synthesis and characterization of polyaniline-mofified BiOI: a visible-light-response photocatalysts. J Mater Sci: Mater Electron 29:18343–18351. https://doi.org/10.1007/s10854-018-9948-5

Yang YJ (2016) Facile synthesis of poly(Safranine T)/reduced graphene oxide nanocomposite for supercapacitors with wide potential window in aqueous neutral electrolyte. Fuller Nanotub Carbon Nanostruct 24:243–248. https://doi.org/10.1080/1536383x.2016.1146708

Yang Z, Chen ZH (2019) Thermally doped polypyrrole nanotubes with sulfuric acid for flexible all-solid-state supercapacitors. Nanotechnology 30:245402. https://doi.org/10.1088/1361-6528/ab0be7

Yang XM, Zhu ZX, Dai TY, Lu Y (2005) Facile fabrication of functional polypyrrole nanotubes via a reactive self-degraded template. Macromol Rapid Commun 26:1736–1740. https://doi.org/10.1002/marc.200500514

Yang SW, Ye CC, Song X, He L, Liao F (2014) Theoretical calculation based synthesis of a poly(*p*-phenylenediamine)-Fe_3O_4 composite: a magnetically recyclable photocatalysts with high selectivity for acid dyes. RSC Adv 4:54810–54818. https://doi.org/10.1039/c4ra11138a

Yang CL, Wei HG, Guan LT, Guo J, Wang YR, Yan XR, Zhang X, Wei SY, Guo ZH (2015) Polymer nanocomposites for energy storage, energy saving, and anticorrosion. J Mater Chem A 3:14929–14941. https://doi.org/10.1039/c5ta02707a

Yang CY, Zhang PF, Nautiyal A, Li SH, Liu N, Yin JL, Deng KL, Zhang XY (2019) Tunable three-dimensional nanostructured conductive polymer hydrogels for energy-storage applications. ACS Appl Mater Interfaces 11:4258–4267. https://doi.org/10.1021/acsami.8b19180

Yao TJ, Jia WJ, Tong X, Feng Y, Qi Y, Zhan X, Wu J (2018) One-step preparation on nanobeads-based polypyrrole hydrogel by a reactive template method and their applications in adsorption and catalysis. J Colloid Interface Sci 525:214–221. https://doi.org/10.1016/j.jcis.2018.05.052

Yashas SR, Sandeep S, Shivakumar BP, Swamy NK (2019) A matrix of perovskite micro-seeds and polypyrrole nanotubes tethered laccase/graphite biosensor for sensitive quantification of 2,4-dichlorophenol in wastewater. Anal Meth 11:4511–4519. https://doi.org/10.1039/c9ay01468c

Ye LJ, Zhang T, Shao SW, Yang L, Guan WS (2019a) Synthesis of poly-*o*-phenylenediamine (PoPD)/$znWO_4$ supported on the fly-ash cenospheres with enhanced photocatalytic performance under visible light. Mater Lett 236:370–373. https://doi.org/10.1016/j.matlet.2018.10.137

Ye X, Xu QC, Xu J (2019b) Oxidant-templating fabrication of pure polypyrrole hydrogel beads as a highly efficient dye adsorbent. RSC Adv 9:5895–5900. https://doi.org/10.1039/c9ra00209j

Yihan S, Mingming L, Guo ZG (2018) Ag nanoparticles loading of polypyrrole-coated superwetting mesh for on-demand separation of oil-water mixtures and catalytic reduction of aromatic dyes. J Colloid Interface Sci 527:187–194. https://doi.org/10.1016/j.jcis.2018.05.048

Yu WJ, Cheng Y, Zou T, Liu Y, Wu K, Peng N (2018) Preparation of $BiPO_4$-polyaniline hybrid and its enhanced photocatalytic

performance. Nano 13:1850009. https://doi.org/10.1142/s1793292018500091

Yu J, Pang ZG, Zheng CH, Zhou TC, Zhang J, Zhou HM, Wei QF (2019) Cotton fabric finished by PANI/TiO_2 with multifunctions of conductivity, anti-ultraviolet and photocatalysis activity. Appl Surf Sci 470:84–90. https://doi.org/10.1016/j.apsusc.2018.11.112

Yuan XJ, Floresyona D, Aubert PH, Bui TT, Remita S, Ghosh S, Brisset F, Goubart F, Remita H (2019) Photocatalytic degradation of organic pollutant with polypyrrole nanostructures under UV and visible light. Appl Catal B: Environ 242:284–292. https://doi.org/10.1016/j.apcatb.2018.10.002

Zang LM, Liu QF, Yang C, Chen J, Qiu JH, Song G (2018) Alizarin red: a reactive dye to enhance nanoengineered polypyrrole with high electrochemical energy storage. Polym Bull 75:3311–3323. https://doi.org/10.1007/s00289-017-2211-z

Zare EN, Motahari A, Sillanpää (2018a) Nanoadsorbents based on conducting polymer nanocomposites with main focus on polyaniline and its derivatives for removal of heavy metal ions/dyes: a review. Environ Res 162:173–195. https://doi.org/10.1016/j.envres.2017.12.025

Zare EN, Lakouraj MM, Kasirian N (2018b) Development of effective nano-biosorbent based on poly-*m*-phenylenediamine grafted dextrin for removal of Pb(II) and methylene blue from water. Carbohydr Polym 201:539–548. https://doi.org/10.1016/j.carbpol.2018.08.091

Zarrini K, Rahimi A, Alihosseini F, Fashandi H (2017) Highly efficient dye adsorbent based on polyaniline-coated nylon-6 nanofibers. J Clean Prod 142:3645–3654. https://doi.org/10.1016/j.jclepro.2016.10.103

Zeng Y, Zhao LJ, Wu WD, Lu GX, Xu F, Tong Y, Liu WB, Du JH (2013) Enhanced adsorption of malachite green onto carbon nanotube/polyaniline composites. J Appl Polym Sci 127:2475–2482. https://doi.org/10.1002/app.37947

Zeng S, Yang J, Qiu XY, Liang ZY, Zhang YM (2016) Magnetically recyclable $MnFe_2O_4$/polyaniline composite with enhanced visible light photocatalytic activity for rhodamine B degradation. J Ceram Soc Jpn 124:1152–1156. https://doi.org/10.2109/jcersj2.16056

Zhang CL, Ma RH (2019) Synthesis and photocatalytic activity of MnV_{13}/GO/PANI composite catalysts. J Coord Chem. https://doi.org/10.1080/00958972.2019.1670816

Zhang LY, Wang HY, Yu WT, Su Z, Chai LY, Li JH, Shi Y (2012) Facile and large-scale synthesis of functional poly(*m*-phenylenediamine) nanoparticles by Cu^{2+}-assisted methods with superior ability for dye adsorption. J Mater Chem 22:18244–18251. https://doi.org/10.1039/c2jm32859c

Zhang SW, Zhao LP, Zeng MY, Li JX, Xu JZ, Wang XK (2014) Hierarchical nanocomposites of polyaniline nanorods arrays on graphitic carbon nitride sheets with synergistic effect for photocatalysis. Catal Today 224:114–121. https://doi.org/10.1016/j.cattod.2013.12.008

Zhang J, Liu Y, Guan HJ, Zhao YF, Zhang B (2017) Decoration of nickel hydroxide nanoparticles onto polypyrrole nanotubes with enhanced electrochemical performance for supercapacitors. J Alloys Compd 721:731–740. https://doi.org/10.1016/j.jallcom.2017.06.061

Zhang MM, Chang LL, Yu ZH (2018) Fabrication of halloysite nanotubes/polypyrrole nanocomposites for efficient removal of methyl orange. Desalin Water Treat 110:209–218. https://doi.org/10.5004/dwt.2018.22220

Zhang XJ, Sheng QL, Zheng JB (2019a) Synthesis of palladium nanocubes decorated polypyrrole nanotubes and its application for electrochemical sensing. J Iran Chem Soc 16:1061–1069. https://doi.org/10.1007/s13738-018-01578-y

Zhang CJ, Tian JX, Rao WD, Guo B, Fan LL, Xu WL, Xu J (2019b) Polypyrrole@metal-organic framework (UIO-66)@cotton fabric electrodes for flexible supercapacitors. Cellulose 26:3387–3399. https://doi.org/10.1007/s10570-019-02321-3

Zhang MM, Chang LL, Zhao YY, Yu ZH (2019c) Fabrication of zinc/oxide/polypyrrole nanocomposite for Brilliant Green removal from aqueous phase. Arab J Sci Eng 44:111–121. https://doi.org/10.1007/s13369-018-3258-3

Zhao Y, Chen HL, Li J, Chen CL (2013a) Hierarchical MWCNT/Fe_3O_4/PANI magnetic composite as adsorbent for methyl orange removal. J Colloid Interface Sci 450:189–195. https://doi.org/10.1016/j.jcis.2015.03.015

Zhao YC, Tomšík E, Wang JX, Morávková Z, Zhigunov A, Stejskal J, Trchová M (2013b) Self-assembly of aniline oligomers. Chem Asian J 8:129–137. https://doi.org/10.1002/asia.201200836

Zhao YC, Stejskal J, Wang JX (2013c) Towards directional assembly of hierarchical structures: aniline oligomers as the model precursors. Nanoscale 5:2620–2626. https://doi.org/10.1039/c3nr00145h

Zhao JJ, Biswas MRUD, Oh WC (2019a) A novel $BiVO_4$-GO-TiO_2-PANI composite for upgraded photocatalytic performance under visible light and its non-toxicity. Environ Sci Pollut Res 26:11888–11904. https://doi.org/10.1007/s11356-019-04441-6

Zhao LM, Shao X, Wang M, Zhao H, Ge B, Li WZ (2019b) A novel rose-like polyaniline Bi_2WO_6 nanocomposite: synthesis and its application in photocatalysis. Desalin Water Treat 163:224–232. https://doi.org/10.5004/dwt.2019.24390

Zhao YH, Xia X, Zhang ZZ, Zhu ZM, Guo YF, Qu Z (2019c) Facile synthesis of polypyrrole-functionalized $CoFe_2O_4$@SiO_2 for removal of Hg(II). Nanomaterials 9:455. https://doi.org/10.3390/nano9030455

Zheng Y, Liu Y, Wang AQ (2012) Kapok fiber oriented polyaniline for removal of sulfonated dyes. Ind Eng Chem Res 51:10079–10087. https://doi.org/10.1021/ie300246m

Zhong DJ, Liao XR, Liu YQ, Zhong NB, Xu YL (2018) Enhanced electricity generation performance and dye wastewater degradation of microbial fuel cell by using petaline NiO@polyaniline-carbon felt anode. Bioresour Technol 258:125–134. https://doi.org/10.1016/j.biortech.2018.01.117

Zhou CQ, Li XX, Gong XX, Han J, Guo R (2015) Ethanol-guided synthesis of flower-on-leaf-like aniline oligomers with excellent adsorption properties. New J Chem 39:9257–9264. https://doi.org/10.1039/c5nj01828e

Zhou J, Lü QF, Luo JJ (2017) Efficient removal of organic dyes from aqueous solution by rapid adsorption onto polypyrrole-based composites. J Clean Product 167:739–748. https://doi.org/10.1016/j.jclepro.2017.08.196

Zhou T, Ma L, Gan MY, Wang HH, Hao CX (2019) Sandwich-structured hybrids: a facile electrostatic self-assembly of exfoliated titania nanosheets and polyaniline nanoparticles and its high visible-light photocatalytic performance. J Phys Chem Solids 125:123–130. https://doi.org/10.1016/j.jpcs.2018.10.021

Zoromba MS, Ismail MIM, Bassyouni M, Abdel-Aziz MH, Saleh N, Alshahrie A, Memic A (2017) Fabrication and characterization of poly(aniline-*co*-*o*-anthranilic acid)/magnetite nanocomposites and their application in waste water treatment. Colloid Surf A-Physicochem Eng Asp 520:121–130. https://doi.org/10.1016/j.colsurfa.2017.01.075